

Russian Academy of Sciences

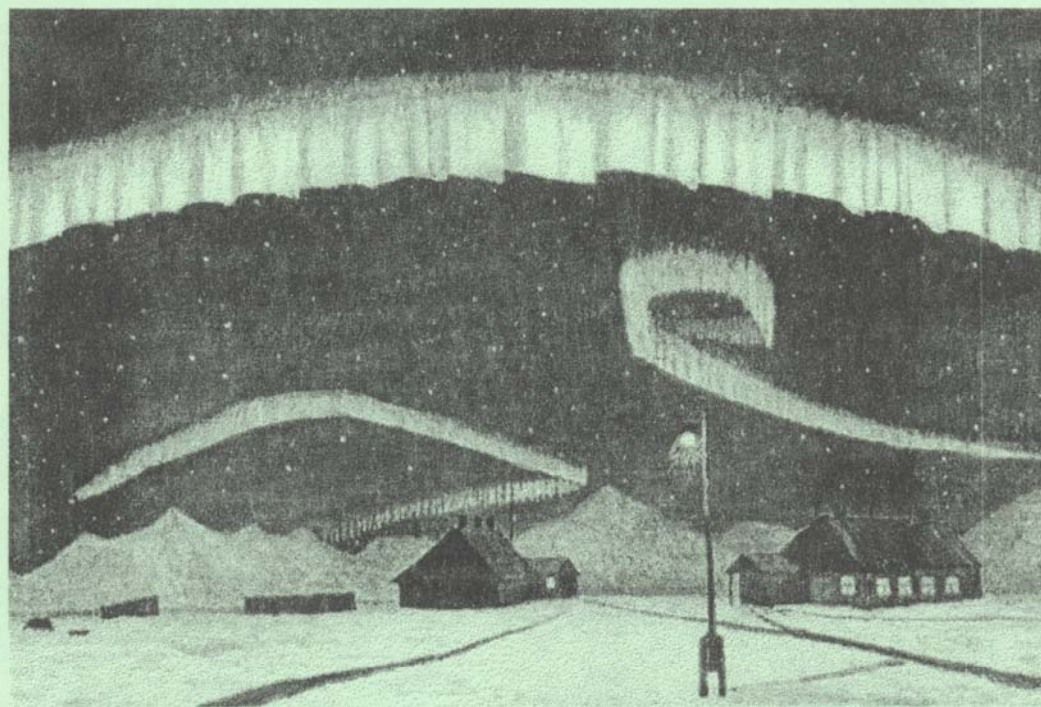
PGI -12-01-128

PHYSICS OF AURORAL PHENOMENA

35th Annual Seminar

28 February – 2 March 2012

Abstracts



Apatity
2012

Russian Academy of Sciences
KOLA SCIENCE CENTER
Polar Geophysical Institute

PGI -12-01-128

PHYSICS OF AURORAL PHENOMENA

35th Annual Seminar

Abstracts

28 February – 2 March 2012

Apatity

2012

The seminar is supported by the
Russian Foundation for Basic Research
grant 12-05-06005 г

The organizing committee:

Alexander Yahnin (chair)
Anatoly Pashin
Yuri Katkalov
Nadezhda Semenova
Alexey Mochalov
Irina Despirak

Addresses:

Apatity department
Fersman str., 14
Apatity, 184209
Murmansk region
Russia

Murmansk department
Khalturina str., 15
Murmansk, 183010
Russia

The editorial board:

A.G. Yahnin
A.A. Mochalov
N.V. Semenova

E-mail: seminar@pgia.ru
<http://pgia.ru/seminar>

© Kola Science Center
Russian Academy of Science, 2012

CONTENTS

SESSION 1. GEOMAGNETIC STORMS AND SUBSTORMS

E.E. Antonova, I.P. Kirpichev, V.V. Vovchenko, M.O. Riazantseva, M.S. Pulinets, I.L. Ovchinnikov, S.S. Znatkova, M.V. Stepanova	Magnetospheric storms and substorms, nature and topology of high latitude current systems	13
L.P. Borovkov	On the aurora intensity variations before the auroral breakup	13
S.A. Chernouss	Priority of Lomonosov in field of auroral research	13
I.A. Chernyaev, V.A. Sergeev, S.V. Dubyagin, Y. Miyashita	Research into the characteristics of plasma injection penetrating to the geostationary orbit	14
I.V. Despirak, A.A. Lubchich, R. Koleva	Substorms associated with the fronts of high-speed streams in the solar wind	14
N.P. Dmitrieva	The vortex aurora structures inside the auroral bulge	15
E. Gordeev, V.A. Sergeev, T.I. Pulkkinen, M. Palmroth	Contribution of magnetotail reconnection to the cross-polar cap potential drop	15
I.B. Ievenko, S.G. Parnikov, V.N. Alexeyev	Observation of the onset of auroral substorm expansion at 56° geomagnetic latitude during a major magnetic storm	16
Yu. Katkalov, Ya. Sakharov, A. Viljanen	EURISGIC data services: Eurisgic.org	16
I.A. Kornilov, T.A Kornilova	Substorm development – current disruption or reconnection?	16
T.A. Kornilova and I.A. Kornilov	Spatio-temporal dynamics of counter-streaming auroras during the substorm active phase	17
T.A. Kornilova and I.A. Kornilov	Substorm development on 11 February 2008 on the basis of THEMIS auroral and spacecraft data	17
J. Kovalevsky	Investigation of elementary geomagnetospheric substorms (EGSSs) associated with B_z -component of interplanetary magnetic field (IMF)	17
B.V. Kozelov, I.V. Golovchanskaya	Signatures of inverse turbulent cascade during auroral intensification	18
T.V. Kozelova, B.V. Kozelov	THEMIS observations of substorm intensification near inner edge of the plasma sheet	18
A. A. Krishtopov, N. P. Dmitrieva	The study of the dynamics of the equatorial region during auroral substorm expansion phase according to Canadian all-sky cameras	19
A.V. Nikolaev, V.A. Sergeev, N.A. Tsyganenko, H. Singer, V. Angelopoulos	Substorm current wedge and Region-2-polarity current loop: magnetic observations on GOES and THEMIS spacecraft chain during substorm expansion phase	19
Yu.V. Platov, S.A. Chernouss, M.V. Uspensky	Observations of rocket exhaust optical phenomena by Finnish and Russian networks	19

A.V. Roldugin, S.V. Pilgaev and V.C. Roldugin	Observations of proton auroras in Spitzbergen	20
Ya. Sakharov, Yu. Katkalov, V. Selivanov, M. Barannik, A. Viljanen	EURISGIC Project: Geomagnetically induced currents in a power grid at the north-west of Russia	20
S.A. Timofeeva, V. A. Sergeev	Investigation of the energetic particle precipitation during the substorm explosive phase	20
V.G. Vorobjev, O.I. Yagodkina, Yu.V. Katkalov, A.S. Kirillov	Global distribution of ionospheric conductivities and auroral luminosity inferred from the Auroral Precipitation Model	20
V.G. Vorobjev, O.I. Yagodkina, Yu.V. Katkalov, A.S. Kirillov	Monitoring of ionospheric and magnetospheric conditions from the Auroral Precipitation Model and dayside aurora observations	21
T.A. Yahnina and A.G. Yahnin	Dynamics of the localized precipitation of energetic protons during geomagnetic storm	21
А.Е. Левитин, Л.И. Громова, С.В Громов, Л.А. Дремухина	Геомагнитная активность в полярной шапке при значительной северной вертикальной компоненте ММП	22
А.А. Шаповалова, Ю.А. Караваев, В.В. Мишин, и В.М. Мишин	Супербуря 06.04.2000: определение скрытых зависимостей магнитного потока долей хвоста от значений динамического давления и электрического поля солнечного ветра	22

SESSION 2. FIELDS, CURRENTS, PARTICLES IN THE MAGNETOSPHERE

N.A. Barkhatov, S.E. Revunov, D.V. Shadrukov	Wavelet component manifestation of Solar Wind parameter disturbances which corresponding to the plasma flows at the dynamics of magnetic disturbance spectrums along the geomagnetic meridian	25
D.V. Chugunin, M.M. Mogilevsky, I.L. Moiseenko, T.V. Romantsova	Ions heating on the polar border of the aurora	25
I.B. Ievenko	Response of the magnetosphere to an impulse of solar wind density at southward IMF in the dynamics of aurorae near the plasmapause	25
I.A. Kornilov, T.A. Kornilova	Fine space-time structure of fields and particle fluxes measured by THEMIS	26
V.A. Ljubchich	Investigation of fractal properties of geophysical data by two-dimensional wavelet analysis	26
M.N. Melnik, O.V. Mingalev, I.V. Golovchanskaya	Numerical modeling of non-linear interactions of small-scale field-aligned current filaments by the macroparticle method	27
O.V. Mingalev, I.V. Mingalev, M.N. Melnik, H.V. Malova, L.M. Zelenyi, A.V. Artemyev	Influence of the external magnetic field component B_y on the thin current sheet configuration	27
M.S. Pulinets, M. Riazantseva, E.E. Antonova, I.P. Kirpichev	Magnetic field parameters near the subsolar magnetopause in accordance with THEMIS data	27
K.Yu. Slivka, N.P. Dmitrieva, and V.S. Semenov	Study of magnetic field intensity in the magnetic barrier near the subsolar point of the Earth's magnetosphere in dependence on IMF	28
M.A. Volkov	The influence of the tailward magnetic field lines on the formation of the currents within the Harang discontinuity	28

A.G. Yahnin and T.A. Yahnina	Mapping the sub-oval proton aurora spots relatively plasmapause	28
T.A. Yahnina, A.G. Yahnin, F. Soraas	Unusual sub-oval proton aurora occurred on 10 and 11 November 2004: Image of plasmapause	29
И.Л. Моисеенко, М.М. Могилевский, Т.В. Романцова, Д.В. Чугунин, Я. Ханаш	Авроральное километровое излучение как индикатор образования каверны Кальверта	29
SESSION 3. WAVES, WAVE-PARTICLE INTERACTION		
V.B. Belakhovsky, A.E. Kozlovsky, V.A. Pilipenko	The morning auroral arcs associated with Pc5 geomagnetic pulsations	33
V.B. Belakhovsky, V.A. Pilipenko	Poloidal geomagnetic Pc5 pulsations and pulsations in the fluxes of energetic particles	33
A.G. Demekhov	Saturation of amplitude of whistler-mode waves generated in a nonuniform magnetic field and possible consequences for the parameters of VLF chorus emissions	34
I.V. Golovchanskaya, O.V. Mingalev, B.V. Kozelov, M.N. Melnik, and I.V. Despirak	Broadband electrostatic noise associated with Alfvénic turbulence in the topside ionosphere	34
N.G. Kleimenova	Geomagnetic pulsations associated with substorm	34
B.V. Kozelov, E.E. Titova, V.E. Yurov, L.P. Borovkov, S.V. Pilgaev	Spatio-temporal features of pulsating aurora: New observations and approaches	35
D.I. Kubyshkina, D.A. Sormakov, V.S. Semenov, V.A. Sergeev	Kink and sausage modes of the flapping oscillations in the magnetotail current sheet	35
J. Manninen, N.G. Kleimenova, O.V. Kozyreva	Temporal change of the VLF hiss polarization: Case study of the event on 12 April 2011	35
D. Pasmanik, M. Hayosh, A. Demekhov, O. Santolík, E. Titova, and M. Parrot	Simultaneous observations of correlated quasi-periodic ELF/VLF wave emissions and energetic-electron precipitation by DEMETER	36
V.C. Roldugin, AV. Roldugin and S.V. Pilgaev	Pc1-2 auroral pulsations	36
N.A. Smirnova, A.A. Isavnin, T.V. Bondareva, A.N. Vasilev, Yu.V. Katkalov	Methods of fractal analysis of the high-latitude ULF emissions to study magnetosphere dynamics and monitor the space weather	37
E. Titova, B. Kozelov, A. Demekhov, O. Santolík, E. Macusova, J.-L. Rauch, J.-G. Trotignon, D. Gurnett, and J. Pickett	Using VLF chorus elements observed by CLUSTER satellites for study of the backward wave oscillator in the magnetosphere	37
E.Н. Федоров, В.А. Пилипенко, Б. Хэйлиг, П. Сатклиф, Х.Л. Люр	Модель поля среднеширотных Pi2 пульсаций на ионосферных высотах	38

SESSION 4. THE SUN, SOLAR WIND, COSMIC RAYS

Yu.V. Balabin, A.V. Germanenko.	Observing of atmospheric hadronic shower on the Barentsburg neutron monitor	41
N.A. Barkhatov, E.A. Revunova, A.E. Levitin	Geomagnetic efficiency of Solar ejection depended on relative orientation of Sun and Earth rotation axes	41
R.O. Bortnikov, V.S. Semenov	Oscillations of a thin flux tube inside polytropic star	42
E.A. Maurchev, Yu.V. Balabin, E.V. Vashenyuk, B.B. Gvozdevsky	Simulation analysis of galactic cosmic ray transport through the atmosphere	42
E.A. Maurchev, A.V. Germanenko, Yu.V. Balabin, E.V. Vashenyuk	Gamma-ray spectrometers developed for problems of radiation monitoring: Comparison of simulations with experimental data	42
E.A. Maurchev, A.V. Germanenko, Yu.V. Balabin, E.V. Vashenyuk	Modeling of ground level X-ray radiation increases during atmosphere precipitations	42
A. I. Podgorny, I. M. Podgorny	MHD simulation of solar flare - determination mechanism of the phenomenon or hypothesis testing	43
I. M. Podgorny, A. I. Podgorny	The active region magnetic field association with solar flares	43
V.A. Uljev, M.I. Tyasto, O.A. Danilova, O.I. Shumilov	The interhemispheric asymmetry of the parameters of midday recovery (MDR) effect during PCA events	43
J.O. Vinnikova, Yu.L. Sasunov, V.S. Semenov	Study of the MHD discontinuities inside the reconnection exhausts in the solar wind	44
N.V. Zolotova, D.I. Ponyavin	Impulses of sunspot activity and surges of magnetic field to the solar poles	44
В.В. Пчелкин	Применение теории распознавания образов для решения задачи отбора требуемых событий в базах данных мировой сети нейтронных мониторов и результатов измерений параметров межпланетной среды на космических аппаратах	44

SESSION 5. IONOSPHERE AND UPPER ATMOSPHERE

O.M. Barkhatova, I.A. Dodonova, N.V. Kosolapova	The display of heliogeophysical disturbance in midlatitude ionospheric activity index (IAI)	47
A.A. Chernyshov, M.M. Mogilevsky, B.V. Kozelov	Application of nonlinear dynamics methods to study the auroral region	47
E.N. Ermakova, A.V. Pershin, T. Bosinger, Q. Zhou	Diurnal dynamics of the broadband spectral maximum in the ULF background noise	48
M.V. Filatov, S.V. Pilgaev, A.V. Larchenko, Yu.V. Fedorenko	A new multichannel analog-to-digital converter synchronizing data with GPS clock	48
A.S. Kirillov	The calculation of rate coefficients for the interaction of vibrationally excited singlet and triplet molecular oxygen in the active medium of chemical oxygen-iodine laser	48

A.S. Kirillov	The study of the influence of intermolecular electron energy transfer processes on vibrational populations of $N_2(a^1\Pi_g)$ and $N_2(A^3\Sigma_u^+)$ molecules in the mixture of N_2 and O_2 molecules	49
M.V. Klimenko, V.V. Klimenko	High- and mid-latitude ionospheric disturbances during geomagnetic storms	49
V.V. Klimenko, M.V. Klimenko, V.G. Vorobjev, O.I. Yagodkina	Various magnetospheric inputs to the GSM TIP model for investigation of ionospheric response to geomagnetic storm events on May 2010	49
S.K. Kondratiev, V.D. Nikolaeva, L.N. Makarova, A.V. Shirochkov, V.N. Morozov	Background ionization calculation in the auroral ionospheric model	50
Yu.N. Korenkov, M.V. Klimenko, V.V. Klimenko, F.S. Bessarab, I.V. Karpov	Modeling of the thermosphere-ionosphere system response to the high-latitude Sudden Stratospheric Warming events	50
B.V. Kozelov, S.V. Pilgaev, L.P. Borovkov, V.E. Yurov	On triangulation by auroral cameras	50
A.V. Larchenko, O.M. Lebed, R. Zubov, M. Shkarbalyuk, M. Filatov and Yu.V. Fedorenko	Calibration of an induction magnetometer and a vertical electric field antenna	51
O.M. Lebed, S.V. Pilgaev, Yu.V. Fedorenko	Velocity of atmospherics along Lovozero – Barentsburg propagation path	51
A.A. Namgaladze, O.V. Zolotov, B.E. Prokhorov	Ionospheric TEC variations before three recent strong earthquakes: A comparative study	51
V.D. Nikolaeva, A.L. Kotikov, T.I. Sergienko, S.K. Kondratiev	Study of fine structure of ionospheric current with the conjugate DMSP and EISCAT measurements	52
A.B. Pashin, A.A. Mochalov	Absorption of high frequency waves in a heated ionosphere region	52
V.C. Roldugin, M.E. Shkarbalyuk	The event of riometer absorption on 5 May 2011 may be caused by auroral protons?	53
Yu.V. Romanovskaya, A.A. Namgaladze	Is the F2-layer Summer Nighttime Anomaly Midlatitudinal or Subauroral: An investigation by means of global numerical modeling	53
I. Shagimuratov, S. Chernouss, Y. Cherniak, I. Ephishov	Ionospheric fluctuations over high latitude using Greenland GPS network and aurora	53
E.D. Tereshchenko, A.E. Sidorenko	Schumann resonance in the vertical magnetic field observed near geological faults	54
V.D. Tereshchenko, S.M. Cherniakov, V.A. Tereshchenko, O.F. Ogloblina	An underwater explosion and its acoustic effects on the D region of the polar ionosphere	54
V.D. Tereshchenko, V.A. Tereshchenko, S.M. Cherniakov, O.F. Ogloblina	Experimental researches of wave disturbances in the polar lower ionosphere during the partial solar eclipse on 1 June 2011	54
E.E. Timofeev, S.L. Shalimov, O.G. Chkhetiani, M.K. Vallinkoski, J. Kangas	Characteristics of the anomalous heat structures within dusty auroral dynamo layer	55

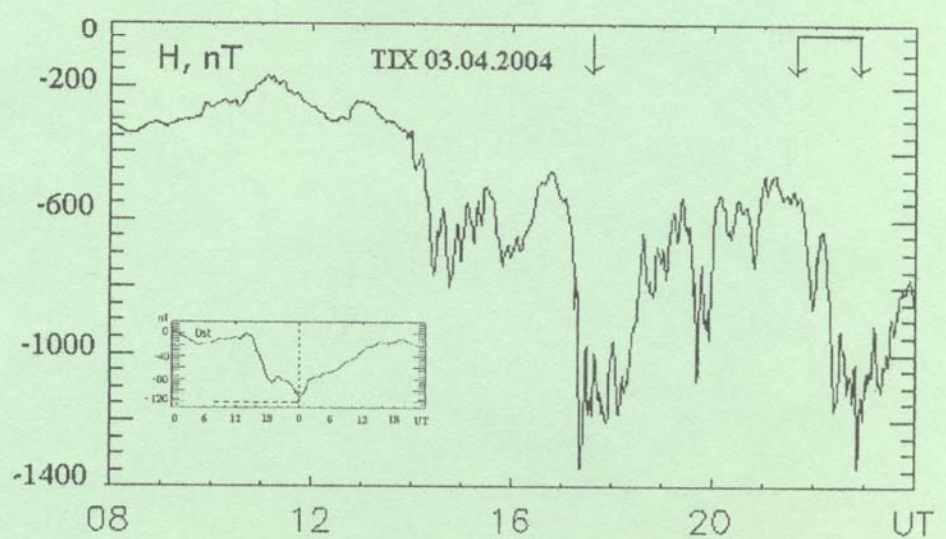
R.A. Zubov, O.M. Lebed, Yu.V. Fedorenko	Numerical study of atmospherics EM field structure near day-night transition	55
K.E. Белоушко	Моделирование взаимосвязи нижней и верхней атмосферы	55
Е.Н. Ермакова, С.В. Поляков, А.В. Першин	Исследование вариаций собственных частот ионосферного альвеновского резонатора на средних широтах	56
А.Ю. Щекотов, Е.Н. Федоров	Наблюдаемые «резонансные» структуры и спектры ИАР	56
А.Ю. Щекотов, Е.Н. Федоров, М. Хаякава	Сейсмо-ионосферная депрессия в окрестности мощных землетрясений	56

SESSION 6. LOW ATMOSPHERE, OZONE

Yu.V. Balabin, E.A. Maurchev	Anisotropy variation of low energy neutron background in the atmosphere	59
V.I. Demin, G.P. Beloglazova, A.M. Zvyagintsev	Total ozone content over the Kola Peninsula: 1973-2011	59
V.I. Demin, A.M. Zvyagintsev	Atmospheric circulations epoch and long-range total ozone variations	59
I.V. Mingalev, G.I. Mingaleva, V.S. Mingalev	A model study of how solar activity affects the global circulation of the middle atmosphere for January conditions	59
L.I. Miroshnichenko, A.S. Kirillov, R. Werner, V. Guineva	The increase of NO _x content in the polar middle atmosphere during intensive solar proton events	60
R. Werner, D. Valev, At. Atanasov, V. Guineva, I. Kostadinov, G. Giovanelli, A. Petritoli, F. Ravegnani, S. Masieri, A. Kirillov	Stratospheric NO ₂ long time trends obtained at the Stara Zagora station and some NDACC stations	60
A.M. Zvyagintsev	Differences between Antarctic and Arctic spring ozone losses	61
Ю.В. Балабин, А.В. Германенко, Б.Б. Гвоздевский, Э.В. Вашенюк	Вариации спектров гамма-излучения во время осадков	61
Ю.В. Балабин, А.В. Германенко, Б.Б. Гвоздевский, Э.В. Вашенюк	Непрерывная регистрация спектров гамма-излучения в широком диапазоне энергий во время атмосферных осадков	61
Ю.В. Балабин, Н.М. Салихов, О.Н. Крякунова, Г.Д. Пак, А.Л. Щепетов, А.В. Германенко, Э.В. Вашенюк	Вариации естественного рентгеновского излучения в приземной атмосфере на различных широтах	62
В.И. Кириллов, А.А. Галахов, М.И. Белоглазов, В.В. Пчелкин, О.И. Ахметов	Исследование амплитудного распределения потока атмосфериков в УНЧ-ОНЧ диапазонах при двухкомпонентной регистрации	62
И.В. Мингалев, Н.М. Астафьева, К.Г. Орлов, В.С. Мингалев, О.В. Мингалев, В.М. Чечеткин	Влияние геометрии течения воздушных масс в области внутритропической зоны конвергенции на процесс формирования циклонических вихрей	62

B.B. Пчелкин	Отражение суточного перемещения долготного максимума глобальной грозовой активности в угловых распределениях шумовых электромагнитных сигналов диапазона частот первого шумановского резонанса	63
B.B. Пчёлкин	Связь сезонных изменений глобальной грозовой активности с сезонными вариациями амплитудных характеристик шумового электромагнитного поля диапазона частот 6-11 Гц	63
SESSION 7. HELIOBIOSPHERE		
E.S. Gorshkov, V.V. Ivanov	On correlation between superweak radiation readings and cosmophysical factors	67
V.V. Ivanov, E.S. Gorshkov	Characteristics of changes in length of subjective minute at different space-and-time conditions	67
R.E. Mihaylov, H.K Belisheva, R.G. Novoseltsev, S.D. Cherney, A.N. Vinogradov	Solar activity and life expectancy of patients in the mental boarding	68
D.A. Petrashova, N.K. Belisheva	Cytogenotoxic effects of the ionizing radiation in the minners buccal cells	69
Н.К. Белишева, Д.А. Петрашова, А.А. Мартынова, В.В. Пожарская, С.В. Пряничников	Физиологическая основа чувствительности организма к гелиогеофизическим агентам	69
Н.К. Белишева, Л.В. Талыкова, Н.А. Мельник	Вклад гелиогеофизических агентов в структуру заболеваемости населения Мурманской области	70
А.А. Мартынова, С.В. Пряничников, Т.Б. Новикова, Н.К. Белишева	Зависимость адаптации детей Заполярья к средним широтам от геомагнитных возмущений	71
Author index		72

Geomagnetic Storms and Substorms



Magnetospheric storms and substorms, nature and topology of high latitude current systems

E.E. Antonova^{1,2}, I. P. Kirpichev^{2,1}, V.V. Vovchenko², M.O. Riazantseva^{1,2}, M.S. Pulinets¹, I.L. Ovchinnikov¹, S.S. Znatkova¹, M.V. Stepanova³

¹ Skobeltsyn Institute of Nuclear Physics, Moscow State University, Moscow, 119991, Russia,
antonova@orearm.msk.ru

² Space Research Institute (IKI) Russian Academy of Science, Moscow, Russia

³ Physics Department, Science Faculty, Universidad de Santiago de Chile, Chile

The magnetospheric substorm is one of the most extensively studied magnetospheric phenomena for the most than 50 latest years. However the mechanism of observed energy explosion and localization of substorm onset continue to be widely discussed. We summarize the results of observations demonstrating the isolated substorm onset at geosentric distances smaller than 10Re and discuss the nature of observed phenomena.

The nighttime region at geocentric distances \sim 7-10Re is ordinarily considered as the near tail region. However the results of observations including latest THEMIS mission clearly demonstrate the existence of surrounding the Earth plasma ring at these geocentric distances. The distribution of plasma pressure in the ring is near to azimuthally symmetric. Daytime compression of magnetic field lines and shift of minimal value of the magnetic field till high latitudes lead to splitting of daytime transverse currents in Z direction. As a result nighttime transverse currents in the surrounding the Earth plasma ring are concentrated near equator, daytime transverse currents are spread along compressed by solar wind field lines forming the cut ring current (CRC) which is the high latitude continuation of the ordinary ring current. CRC is supported by directed to the Earth plasma pressure gradients. It is suggested that isolated substorm onset is localized in CRC.

The role of CRC in the development of magnetic storm and the creation Dst variation is analyzed. We stress that the development of partial ring current, which is one of the well-known features of magnetic storm, in the CRC region helps to eliminate paradox, appeared when it was suggested that tail current can have the considerable role in Dst formation. The contribution CRC in the process of Dst formation during magnetic storms is evaluated for selected magnetic storms with known radial profile of plasma pressure.

On the aurora intensity variations before the auroral breakup

L.P. Borovkov (Polar Geophysical Institute, Apatity, Russia)

Sometimes before the auroral breakup the auroral arc intensity decrease is registered. This phenomenon is known as the auroral fading. In this report the auroral brightness variations, including the fading, related to auroral activations and breakups are discussed on the basis of optical spectral measurements of the OI 636 nm, H α 656 nm and 1PGN2 660 nm emissions in Apatity.

Priority of Lomonosov in field of auroral research

S.A. Chernouss (Polar Geophysical Institute KSC RAS, Apatity)

Last year we have celebrated the 300 anniversary of the birth of Russian Academician Lomonosov. He was encyclopedic scientists, left more than 15 volumes of publications in physics, chemistry, geophysics, geography, philology, and other sciences and arts. Mikhail Vasilyevich Lomonosov (1711-1765) was born and raised in the Arkhangelsk region in pomors family, where his childhood was lucky to repeatedly watch the aurora. Later, when he became interested in their physical nature, it does not rely on other people's descriptions are often far removed from reality, but on his own observations. He was the first, who proposed the electrical nature of the aurora. The main his work on the aurora nature was the "*Oration on aerial phenomena, proceeding from the force of electricity proposed by Mikhail Lomonosov*" , which was reported at the meeting of the Academy of Sciences November 26, 1753. According to Lomonosov, the electric force may be cause for auroras glow which in appearance resembles the glow of the gas discharge. In particular, he wrote "So, it is likely that the northern lights are born from occurring of the electric force in the air. It is confirmed by likeness of the phenomenon appearance and disappearance, movement, color and form, which are shown in the northern lights and the electric light of the third kind". Fundamental task for a long time was to determine the height of the aurora. Lomonosov wrote, "The position of the northern lights above the limits of the atmosphere shows a comparison of dawn with them". In those times and later the scientists were challenged to define what constitutes the aurora - intrinsic luminescence of the atmosphere, or reflected, scattered, or diffracted rays from external light sources. Lomonosov noticed that the stars can be seen

Geomagnetic storms and substorms

through the lights, and on this basis concluded that "All of the northern lights shown that light species may not be vapor or clouds, shining under some lighting. They are almost always have a regular figure, and stars clearly seen through the northern light luminosity". Thus it was shown that aurora is self luminosity phenomena of the atmosphere but not reflected or scattered light of remote source. This discovery of the scientist were subsequently confirmed by spectral measurements just one hundred year later by famous Swedish physicist Angstrom in 1866-67 years. The thought of Lomonosov on relationship of auroral colors with the particular substance was also promising: "By the way if some main colors composed the white color born in the air then no doubt be that the main components separately may seen too". Great interest are pictures and drawings of the aurora taken by Lomonosov. Forty-seven drawings were engraved on 11 copper engraving and stored in the Museum of Lomonosov in St.-Petersburg. We can see the typical forms of auroras on them. One can only wonder at the foresight of genius, who anticipated that knowledge of the nature of the aurora, which have become accessible to us only in the 20 century.

Research into the characteristics of plasma injection penetrating to the geostationary orbit

I.A. Chernyaev¹, V.A. Sergeev¹, S.V. Dubyagin¹, Y. Miyashita²

¹ Institute of Physics, Saint Petersburg State University, Saint Petersburg, Russia.

² Department of Geophysics, Kyoto University, Kyoto, Japan.

Many recent studies show that the bursty bulk flows (BBFs) make the main contribution to the Earthward plasma convection from the magnetosphere plasma sheet. In this study, we identify key characteristics of BBFs and evaluate their plasma and magnetic parameters, using the Geotail satellite located at the center of the plasma sheet at a distance of 8-13 R_E from the Earth. The fact of the penetration into the inner magnetosphere was determined from the geostationary satellites data (LANL). In the plasma bubble model, the motion is caused by the electric polarization due to lowest values for the entropy $S_B = PV$. To estimate the volume of earthward moving plasma tubes we used the formula from the (Wolf et al, JGR, 2006).

On the one hand, we obtained that the BBFs with lowest values of entropy S_B and large amplitudes of dipolization have a better chance to penetrate into the inner magnetosphere, and the penetration depth of the BBFs does not depend on its initial velocity. That is good confirmation of plasma bubble model. On the other hand, the entropy parameter depends on the radial distance. That contradicts the model of a plasma bubble.

We obtained that the depth of penetration also depends on the state of the magnetosphere, as expected. Plasma tube compresses while moving toward the Earth (increasing concentration, plasma pressure and magnetic field). With this motion the total pressure inside the plasma bubble remains equal to the total pressure in the surrounding plasma tubes. The closer the registration point of BBF to the geostationary orbit, the greater the chance to discover the plasma injection into the inner magnetosphere. This is unexpected and interesting result. Thus, this study identifies the key parameters that control the penetration depth of the BBFs and provide some evidence in favor of plasma bubble model.

Substorms associated with the fronts of high-speed streams in the solar wind

I.V. Despirak¹, A.A. Lubchich¹, R. Koleva²

¹ Polar Geophysical Institute, Apatity, 184209, Russia

² Space Research & Technologies Institute, BAS, Sofia, Bulgaria

It is well known that the various structures in the solar wind flow are either related to the solar corona structure or are created along solar wind propagation. Structures created while the solar wind propagates through the Solar system are the regions of compressed plasma at the fronts of recurrent solar wind streams (CIR) and magnetic clouds (Sheath). Auroral disturbances observed by Polar spacecraft during Sheath and CIR events had an unusual form. On one side these disturbances exhibited typical substorm signatures – localized onset, poleward and east-west expansion, but on the other side they had very large longitudinal dimensions and covered a very large area. To examine weather these disturbances represent substorms we considered data from the Geotail spacecraft in the magnetotail. Auroral bulge parameters were obtained by the Ultra Violet Imager onboard Polar; solar wind parameters were taken from the OMNI data base. All auroral disturbances observed by Polar during Sheaths and CIRs for the periods 1997-1998; 2000; October 2001 and December 1996 were studied. Selected are 9 events when Geotail was in the plasma sheet during the auroral bulge formation related to Sheath and CIR. We show that some signatures of a typical substorm were observed in the magnetotail, namely: 1) fast plasma flows associated with a reconnection process (tailward/earthward flows) 2) a sharp decrease of the total pressure following the interval of a

pressure increase. This enables us to consider the auroral disturbances during the fronts of high-speed streams as substorm.

The vortex aurora structures inside the auroral bulge

N.P. Dmitrieva (*St.-Petersburg State University, Physical Department, St.-Petersburg, Russia*)

The main ionospheric manifestation of a substorm is a sudden poleward expansion of the night auroral oval connected with the substorm explosive phase. The dynamics of aurora inside the auroral bulge during the expansive phase is very complex and nonstationary. It is possible, however, to pick out some characteristic features of the aurora dynamics within the auroral bulge region. One of these features is a formation of vortex in aurora where the meridionally elongated structures firstly move equatorward and then turn to the east or to the west. Such structures appear for about 5-10 min after auroral intensification and often are followed by pulsating aurora. We compare the spatio-temporal pattern of auroras with THEMIS satellites magnetic field and plasma observations and suggest that these equatorward drifting auroral structures are connected to the earthward fast plasma flows from the substorm active region.

Contribution of magnetotail reconnection to the cross-polar cap potential drop

E. Gordeev¹, V.A. Sergeev¹, T.I. Pulkkinen², M. Palmroth³

¹ *Saint-Petersburg State University*

² *School of Electrical Engineering, Aalto University, Espoo, Finland*

³ *Finnish Meteorological Institute, Helsinki, Finland*

Since the work of Dungey [1961], the global circulation pattern with two (dayside and nightside) reconnection regions has become a classic concept. However, the contributions of dayside and nightside sources to the cross-polar cap potential (PCP) are not fully understood, particularly, the relative role and specifics of the nightside source are poorly investigated both in quantitative and qualitative terms. To fill this gap, we address the contributions of dayside and nightside sources to the PCP by conducting global MHD simulations with both idealized solar wind input and an observed event input. The dayside source was parameterized by solar wind-based ‘dayside merging potential’ (Φ_d or DPD) $\Phi_d = L_{\text{eff}} V B_t \sin^4(\theta/2)$, whereas to characterize the nightside source we integrated across the tail the dawn-dusk electric field in the plasma sheet to obtain the ‘cross-tail potential’ (Φ_n or NPD). For the idealized run we performed simulations using four MHD codes available at Community Coordinated Modelling Center (CCMC) to show that contribution of the nightside source is a code-independent feature (although there are many differences in the outputs provided by different codes). Particularly, we show that adding a nightside source to the linear fit function for the ionospheric potential (i.e., using the fit function $\Phi_{\text{fit}} = K_d \Phi_d + K_n \Phi_n + \Phi_0$) considerably improves the fitting results both in the idealized events as well as in the simulation of an observed event. According to these simulations the nightside source contribution to the PCP has a fast response time (< 5min) and a modest efficiency (potential transmission factor from tail to the ionosphere is small, $K_n < 0.2$), which is closely linked to the primarily inductive character of strong electric field generated in the plasma sheet. The latter time intervals are marked by strongly enhanced nightside (lobe) reconnection and can be associated with substorm expansion phases. This association is further strengthened by the simulated patterns of precipitation, the R1-type field-aligned substorm current wedge currents and Hall electrojet currents, which are consistent with the known substorm signatures.

Geomagnetic storms and substorms

Observation of the onset of auroral substorm expansion at 56° geomagnetic latitude during a major magnetic storm

I.B. Ievenko, S.G. Parnikov, V.N. Alexeyev (*Yu. G. Shafer Institute of Cosmophysical Research and Aeronomy, Yakutsk, Russia*)

It is known that the first onset of the auroral substorm expansion is connected with the brightness increase and break up of the most equatorial arc. Subsequent substorm intensifications can be manifested in the occurrence and brightening of auroral arcs at higher latitudes. As a result a formation of auroral bulge and a poleward shift of westward electrojet maximum take place. The development of auroral bulge maps the precipitation dynamics of the energetic particles during a magnetospheric substorm.

In this work the research results of auroral substorm during a major magnetic storm on March 20, 2001 (Dst =-150 nT) are submitted. The aurorae were observed at the Yakutsk meridian (130°E; 200°E, geom..) with the scanning and zenith photometers in the 630, 557.7 [OI], 427.8 (N₂⁺) and 486.1 nm (H beta) emissions.

The main development features of the auroral substorm on March 20, 2001. Before the substorm onset the equatorial arc is observed at low geomagnetic latitudes of 55-57°N (the dipole L=3.0-3.3). The intensity maxima of 630.0 and 557.7 nm emissions in the arc are separated in latitude at 1-1.5°. The zenith photometer registers an intense H beta emission in the arc.

The first onset of substorm expansion with the equatorial arc break up and poleward extension of aurorae was registered in the evening sector of MLT. The fast increase of the 427.8, 557.7 and 630.0 nm emission intensity in an arc is accompanied by the decrease of H beta intensity by a factor of ~5. During the substorm intensification there is the increase of the westward electrojet with a maximum at 56-57°N latitude.

In ~ 40 minutes the second intensification of a substorm begins after a short growth phase. It was manifested in the smooth increase of 427.8 nm and H beta emission intensity in the auroral arc when its movement to the former latitude. The explosive intensity increase and poleward shift of aurorae is accompanied by amplification and extension of the westward electrojet up to the latitude of st. Tixie (66°N, geom.).

The aurorae dynamics are compared with the measurements of precipitating flux of electrons and protons aboard DMSP F15, substorm injections at a geosynchronous orbit, variations in the solar wind and IMF and also images of auroral oval from the IMAGE satellite. The results of ground and satellite observations are considered from a position of change of the magnetic field configuration and the energetic particles flux in the inner magnetosphere during the low-latitude substorm.

EURISGIC data services: Eurisgic.org

Yu. Katkalov¹, Ya. Sakharov¹, A. Viljanen²

¹*Polar Geophysical Institute;*

²*Finnish Meteorological Institute*

The eurisgic.org website was developed by Polar Geophysical Institute to provide access to the continuously updated archive of GIC recordings during EURISGIC project. The purpose of eurisgic.org is to provide the information about GIC activity to the Consortium members and public. The public part of services is a near real time view to the present GIC activity at a number of stations via online plots. The restricted part of services is accessible only to EURISGIC Participants and provides access to the data in digital form.

The research leading to these results has received funding from the European Community's Seventh Framework Programme (FP7/2007-2013) under grant agreement no 260330

Substorm development – current disruption or reconnection?

I.A. Kornilov, T.A. Kornilova (*Polar Geophysical Institute, Apatity, Russia. kornilova@pgia.ru*)

Two models of substorm development dominate nowadays - current disruption (CD) and tail reconnection (TR) paradigms. Both models have many experimental proofs, but most of them base on one, maximum 2-3 events case study. We examined all THEMIS ground based and satellite data for about 200 substorms (2007-2011), and now can suppose that both paradigms are valid. Both CD and TR processes take place, often in rather mixed and complicated consequence of events during entire substorm development – from preliminary phase till substorm fading. On the other hand, there are also examples when substorm was initiated by current disruption mechanism only, and, vice

versa, exclusively by reconnection process (transient reconnection). Examples of these three possible cases are presented and discussed in our report.

Spatio-temporal dynamics of counter-streaming auroras during the substorm active phase

T.A. Kornilova and I.A. Kornilov (*Polar Geophysical Institute, Apatity, Russia*)

Auroral forms arising in association with poleward boundary intensifications (PBIs) and reaching the pre-existing growth phase arc, may trigger substorm onset (e.g., Nishimura et al., 2010). As known (Aikio and Kaila, 1996) such auroral forms are observed after breakup onset as well. They may encounter poleward expanding auroras from preceding breakup activations at equatorial boundary of the oval and penetrate through them preserving their entity. On the basis of PGI and Canadian THEMIS all sky camera auroral TV observations with using special effective keogram filtering, studying of counter-streaming auroral activations was carried out. An analysis of the velocities of equatorward moving auroral forms inside the bulge (namely, optical intrusions from auroral poleward boundary and auroral arcs referred to breakup at the equatorial boundary of the auroral oval) for 11 events allows us to suppose that the electron acceleration mechanisms are different for counter-streaming auroras.

Substorm development on 11 February 2008 on the basis of THEMIS auroral and spacecraft data

T.A. Kornilova and I.A. Kornilov (*Polar Geophysical Institute, Apatity, Russia*)

THEMIS data and images from the THEMIS all-sky imager array were used to investigate in detail substorm of 11 February 2008. The THEMIS satellites in situ provided excellent opportunity to examine substorm development in different regions in respect to auroral oval. All-sky data were presented in the form of mosaic pictures allowing us to observe a substorm development over large region of the ionosphere. During the substorm P1 probe footprint was located poleward of the auroral oval, while P2 was situated equatorward of that. Bulge propagation took place very close to the clustered footprints of the P3, P4, P5. Relation between fine structure of auroras and electric and magnetic field variations registered by THEMIS probes during substorm was considered. It was revealed that diffuse luminosity changes occurring out of the auroral oval to a more extent depend on electric field variations but not on that of the magnetic field. Dynamics of active auroras inside and out of the oval closely related with both electric and magnetic fields. Pattern of counter-streaming auroras during expansive phase are clearly seen in the peculiarities of the electric and magnetic fields and particle spectra.

Investigation of elementary geomagnetospheric substorms (EGSSs) associated with B_Z -component of interplanetary magnetic field (IMF)

J. Kovalevsky (*Pushkov Institute of Terrestrial Magnetism, Ionosphere and Radio Wave Propagation of RAS (IZMIRAN), Troitsk, Moscow Region, Russia*)

A system representation of EGSSs as totality interconnected physical processes suggest an integrity of their external manifestation. This offers for EGSSs classification according to some basic process or sets of such processes. The scale classification of 61 EGSSs is realized according to AE and D_{st} indices and B_Z IMF component (in terms of mean values \overline{AE} , \overline{D}_{st} , \overline{B}_Z and theirs standard deviations $\sigma(AE)$, $\sigma(D_{st})$, $\sigma(B_Z)$ in event time) with the aim of separation of EGSSs clusters with rather alike inner (solar wind – magnetosphere couplings (SWMCs)) structures. Three EGSSs clusters types (C1, C2, C3) during moderate and small storms are separated. They are characterized by the following averaged (over the entire cluster events) basic processes peak values - C1: $\overline{B}_Z = -9.0$ nT, $\overline{AE}^{max} = 937$ nT, $\overline{D}_{st}^{min} = -68$ nT; C2: $\overline{B}_Z = -7.3$ nT, $\overline{AE}^{max} = 782$ nT, $\overline{D}_{st}^{min} = -45$ nT; C3: $\overline{B}_Z = -7.6$ nT, $\overline{AE}^{max} = 897$ nT, $\overline{D}_{st}^{min} = -37$ nT. The content physical analysis of the EGSSs for C1-3 is carried out on the base of correlativity clustering of 32 processes characterizing every EGSS. The directly driven processes to the disturbances generation are studied. The EGSSs of every cluster are characterized by common inner SWMCs structures (CP). In turn the CP for all clusters exist: $(AE) + [D_{st}] + [B_Z]$. However the EGSSs of C1, C2 and C3 clusters have different inner structures and hence are characterized by different EGSS physical development of which are

Geomagnetic storms and substorms

impossible to interpret by single known coupling function or parameter (say, B_Z , E_Y and so on). The role of the well-known epsilon-function of Akasofu in such EGSSs development is contradictory. It is found that investigated EGSSs have a near linear relationships $AE(B_Z)$, $\overline{\overline{AE}}(\overline{\overline{F_M}} \equiv \overline{\overline{VB_S}}(\overline{nV^2})^{1/3})$, $\overline{\overline{D_{st}}}(\overline{\overline{V^2B_S}})$, $\overline{\overline{FEM6}}(AE) \equiv \overline{\overline{Q}}(AE)$, where $\overline{\overline{FEM6}} \equiv \overline{\overline{Q}} = dDR / dt + DR / 6$, and that $AE - D_{st}$ relationships are varied over wide limits (from strong to weak). It is argued in favor of hypothesis about connection between physical peculiarities or SWMCs of obtained clusters EGSSs and their “external” characteristics (AE , D_{st} and B_Z). Our results support the idea about multicausality and multivariance of substorms.

Signatures of inverse turbulent cascade during auroral intensification

B.V. Kozelov, I.V. Golovchanskaya (*Polar Geophysical Institute, Apatity, Murmansk region, 184209 Russia*)

By now, different types of scale-free behavior exhibited by auroral variations have been presented from analyzing ground-based and satellite imaging observations. Signatures of spatial and temporal scaling in the magnetosphere-ionosphere system have also been reported for fluctuations of electric and magnetic fields on the auroral field lines. Within the second order statistics, scaling properties of fluctuations can be characterized by scaling index. Using UVI images from the Polar satellite, we show that for auroral structures observed at the beginning of substorm expansion, the scaling index varies from values less than unity to ~ 1.5 , increasing with breakup progress. This feature can be interpreted as a signature of inverse turbulent cascade which develops in the magnetosphere-ionosphere plasma due to non-linear interaction of Alfvénic coherent structures according to the *Chang et al.* [2004] scenario. Observational evidence of small-scale coherent structures is discussed with ground-based observations in Apatity.

THEMIS observations of substorm intensification near inner edge of the plasma sheet

T.V. Kozelova, B.V. Kozelov (*Polar Geophysical Institute, Apatity, Russia*)

The changes of the magnetic field during a substorm in the near-Earth magnetotail follow well established pattern. The magnetic field line stretching are due to an increase in the intensity and/or earthward motion of the cross-tail current sheet during growth phase. An expansion of the plasma sheet and an injection of energetic particles accompany the magnetic field dipolarization during substorm explosive phase.

Kozelova et al [1998] have presented the estimation of equivalent differential equatorial transverse currents dJ associated with magnetic field perturbations during substorm explosive phase using measurements from one satellite (CRRES). Here we show the development of these transverse currents dJ from the THEMIS observations during the substorm intensifications on 6 January 2008 at premidnight sector at $r \sim 5-10$ Re.

Analysis of the current perturbations shows the existence different regimes of the current evolution in the near-Earth plasma sheet. The satellite near the inner edge of the plasma sheet observed slow magnetic field line stretching and the passage across of the Alfvén convective boundary for hot electrons during growth phase. In this time the westward current dJ_W was located tailward of the satellite location and moves earthward. However during sudden rapid local magnetic field line stretching a short-time eastward current dJ_E appears earthward of the satellite location. Simultaneously the auroral arc appeared at the Sodankyla station. This variation may be associated with the quick transition from the region with dipolar field to tail-like field region.

During the ground-based magnetic and auroral activations, the current sheet displays complex space-time distribution including embedded reversals in the current direction within the dipolarization region. The energetic particle injections are observed when the current dJ_E appears tailward of the satellite location. The observed variations of particle fluxes and fields are consistent with the substorm current disruption model [Lui et al., 1988].

The study of the dynamics of the equatorial region during auroral substorm expansion phase according to Canadian all-sky cameras

A.A. Krishtopov, N.P. Dmitrieva (*Institute of Physics, Saint-Petersburg State University, Saint Petersburg, Russia*)

During the substorm explosive phase equatorward motion of the discrete aurora equatorial boundary observed simultaneously with a sharp auroral poleward boundary shift as well as equatorial drift of the individual auroral structures inside auroral bulge area.

In this paper we study the equatorial boundary and auroral structures dynamics after auroral breakup. Using Canadian all-sky cameras data we determine latitude-longitude position of the discrete oval boundary depending on time.

The calculated substorm current wedge size and its longitudinal position were compared with the position of the auroras active region. Extreme position of auroral structure traces and equatorward boundary was compared.

Substorm current wedge and Region-2-polarity current loop: magnetic observations on GOES and THEMIS spacecraft chain during substorm expansion phase

A.V. Nikolaev¹, V.A. Sergeev¹, N.A. Tsyganenko¹, H. Singer², V. Angelopoulos³

¹ *Physical Institute, St-Petersburg State University, St-Petersburg, Russia*

² *Space Weather Prediction Center, NOAA, Boulder, Colorado, USA*

³ *University of California, Los Angeles, USA*

The 3-dimensional current system of magnetic substorm expansion phase is historically recognized as a cartoon-like sketch model SCW which consists of westward electrojet flowing in the auroral bulge which is limited in longitude by downward and upward field-aligned currents (FACs) at the east/west side of the bulge and they in turn are closed in equatorial magnetosphere. We found that substorm current wedge (SCW) magnetic effects quantitatively modeled on geostationary distance sector systematically differ from observed magnetic variations on GOES spacecraft during expansion phase. Testing of single-loop quantitative SCW model showed that systematic mismatch of observed and modeled magnetic variations on geostationary distance depends on (1) concurrent magnetotail configuration, (2) spacecraft location and (3) substorm expansion phase time. This mismatch can be partly attributed to additional Region-2-polarity FACs in the same longitudinal sector as Region-1 SCW loop and associated with earthward flow of plasma which is heat the region of strong quasi-dipole inner magnetospheric field. We analyze magnetic variations on THEMIS and GOES spacecraft radially-distributed in the night side of magnetosphere with a view to evaluate the distance to equatorial termination of Region-2 current loop depending on magnetotail configuration and estimate it's intensity using extended quantitative SCW model.

Observations of rocket exhaust optical phenomena by Finnish and Russian networks

Yu.V. Platov¹, S.A. Chernouss², M.V. Uspensky³

¹ *IZMIRAN, Troitsk, Moscow region, Russia*

² *Polar Geophysical Institute of the KSC RAS, Apatity, Murmansk region, Russia*

³ *Finnish Meteorological Institute, Helsinki, Finland*

The results of research of the optical phenomena connected with rocket exhaust in the upper atmosphere are submitted. The optical signatures in the upper atmosphere accompanying rocket launches made from the Archangelsk region ranges have been registered for many years by ground-based network of all-sky cameras in the northern regions of Russia and Finland as a part of routine auroral recordings. The most intensive, large-scale and dynamical phenomena are caused by separation of rocket stages and shut off solid propellant of rocket engines and physical conditions in the field of a rocket flight. Rocket plumes and large-scale diffuse formations have been captured both by imagers and spectrographs. The dynamic and morphological features of the artificial clouds as a function of the relative quantity of gaseous and dispersed components from the rocket and analysis of accompanied phenomena are presented.

Geomagnetic storms and substorms

Observations of proton auroras in Spitzbergen

A.V. Roldugin, S.V. Pilgaev and V.C. Roldugin (*Polar Geophysical Institute, Apatity, Russia*)

The regular observations of auroral spectra in Barentsburg start on 14 November 2011. Its spectral lines show auroral intensity variation along geomagnetic meridian from north horizon to south one, spectral interval covers from 420 to 780 nm, time resolution is 1 frame per minute. The events with hydrogen emission H α are studied, and geomagnetic situation during proton aurora is investigated.

EURISGIC project: Geomagnetically induced currents in a power grid at the north-west of Russia

Ya. Sakharov¹, Yu. Katkalov¹, V. Selivanov², M. Barannik², A. Viljanen³

¹*Polar Geophysical Institute*

²*Centre for Physical and Technological Problems of Energy in Northern Areas*

³*Finnish Meteorological Institute*

In accordance with Work Package 8 of EURISGIC Project a special system for GIC recording was set at the Karelengo power grid. Original units were installed on the ground line of transformer station at five sites at Kola Peninsula and Karelia. The data are transmitted from the remote station to the data storage center every hour to provide near real time GIC records. Online access to Russian GIC records is available through eurisgic.org website as a public part of data services. Finnish archival GIC records and magnetic field derivations from Finnish stations are also available through website data services.

The research leading to these results has received funding from the European Community's Seventh Framework Programme (FP7/2007-2013) under grant agreement no 260330

Investigation of the energetic particle precipitation during the substorm explosive phase

S.A. Timofeeva, V.A. Sergeev (*Saint Petersburg State University, Physical Department, Saint Petersburg, Russia*)

During the substorm explosive phase the magnetic field configuration is changing. In this connection, conditions of particle scattering in loss-cone and structure of the auroral precipitation change also. Therefore interpreting the precipitation picture (regions of wave-induced precipitation and regions of non-adiabatic current-sheet precipitation) before and after the substorm onset we can obtain information about the magnetic field reconfiguration.

In this paper we study the energetic particle dynamics in the substorm, observed on April 19, 2009 at 02:32 in the Canadian sector. In this event three spacecraft pass through the auroral bulge: NOAA 17- 2 minutes before, Metop - 3 minutes after and NOAA 18- 5 minutes after the substorm onset.

Using energetic particle data from these low-altitude spacecraft, which crossed the auroral bulge, we compare precipitation structure before and after substorm onset to study their typical features. It is shown that after the onset, the increase in the fluxes of energetic particles and isotropic boundaries shifts for electrons and protons are observed. Also we can distinguish the areas of dipolarization, injections, and define the type of particle scattering producing energetic particle precipitation.

Global distribution of ionospheric conductivities and auroral luminosity inferred from the Auroral Precipitation Model

V.G. Vorobjev, O.I. Yagodkina, Yu.V. Katkalov, A.S. Kirillov (*Polar Geophysical Institute, Apatity, Murmansk region, 184200, Russia*)

Auroral Precipitation Model (APM) which is placed now on the PGI website <http://pgia.ru/lang/en/webapps/> was used to calculate the global distribution of integrated Hall and Pedersen ionospheric conductivities and auroral luminosity in visible and UVI spectral ranges. The model of global distribution of precipitating ions was developed to calculate ionospheric conductivities more exactly. Comparisons of electron and ion energy fluxes were carried out in different MLT sectors. It was shown that the ion deposit in the global precipitation power is more pronounced during magnetic quietness and in dusk sectors. Integral intensities of the N₂ LBH(L) band near 170.0 nm, 1NG N₂⁺ at 391.4 nm, (OI) 557.7 nm (the transition ¹S→¹D in atomic oxygen), and the 1PG N₂ band near 669.0 nm have

been calculated. To calculate (OI) 557.7 nm intensity the production of O(¹S) in the electron energy transfer process N₂(A³Σ_u⁺) + O(³P), the dissociative recombination, auroral electron impact and the production of electronically excited N₂ by auroral electron impact were taken into account. A good agreement was revealed by comparison of the LBH(L) global distribution observed by the IMAGE spacecraft and calculated from APM.

Monitoring of ionospheric and magnetospheric conditions from the Auroral Precipitation Model and dayside aurora observations

V.G. Vorobjev, O.I. Yagodkina, Yu.V. Katkalov, A.S. Kirillov (*Polar Geophysical Institute, Apatity, Murmansk region, 184200, Russia*)

The close connection of dayside precipitation with magnetic activity and interplanetary medium characteristics opens an opportunity of continuous monitoring of ionospheric and magnetospheric conditions by using of dayside aurora observations as the entrance parameter of the Auroral Precipitation Model (<http://pgia.ru/lang/en/webapps/>). In the ionosphere these are global distribution of auroral precipitation as well as global distribution of integrated ionospheric conductivities and auroral luminosity in various emissions and bands. Latitudinal positions of plasmapause and isotropy boundary, position and the size of the polar cap, value of the magnetic flux transferred from the dayside magnetosphere into the tail, and global precipitation power and so on can be attributed to the magnetospheric condition. Two time intervals on Dec. 27, 2000 and Dec. 12, 2004 of dayside aurora observations with meridian scanning photometer at Barentsburg observatory were used for the definition of magnetospheric variables. Satisfactory conformity of AL index values calculated from APM on the base of optical observations and published by WDC was found. It was discovered that, at least in two above events, the AL index value in the magnetic bay maximum was proportional to tail lobe magnetic flux rate ($\Delta F/\Delta t$) during the substorm growth phase.

Dynamics of the localized precipitation of energetic protons during geomagnetic storm

T.A. Yahnina and A.G. Yahnin (*Polar Geophysical Institute, Apatity, Russia*)

Localized precipitation of energetic (E>30 keV) protons (LPEP), which is observed equatorward of isotropy boundary, is the result of interaction between ring current protons and ion-cyclotron waves, and mark the field lines where the interaction exists. The ion-cyclotron waves also precipitate relativistic electrons from the radiation belt. Thus, LPEPs can be used for monitoring and investigation of the ring current / radiation belt losses. Using data from three low-orbiting NOAA POES satellites we considered the dynamics of LPEPs during a strong magnetic storm (Dst = -472 nT at 19 UT on 20 November 2003). The highest proton flux was observed during the main and early recovery phases. The flux decreased monotonically in a course of the recovery phase. During the main phase and half a day after the Dst minimum, LPEPs of type 2 (those associated with low energy (E<20 keV) proton precipitation) were generally observed. They occupied almost all MLTs and were located at low latitudes. Distinct transition from LPEPs of type 2 to LPEPs of type 1 (containing only >30 keV protons) appeared in a day after Dst minimum. During the early recovery phase LPEPs were concentrated in the morning and day sectors of MLT. Later, they were observed mainly around noon and shifted to higher latitudes. We modeled plasmapause position at different stages of the storm and found that most LPEPs tend to locate in the vicinity of plasmapause. However, at the end of the recovery phase some LPEPs appeared on the dayside at high latitudes well outside the plasmapause. We conclude that the intense cyclotron interaction of waves and particles during magnetic storm occurs at the cold plasma gradients. At later stage of the storm recovery the interaction seems to be not related with plasmapause. Probably, it is due to increased transversal anisotropy of hot protons at higher latitudes on the dayside, which results from drift shell splitting of particles having different pitch -angles and drifting from night side to dayside in the non-dipole magnetic field.

Geomagnetic storms and substorms

Геомагнитная активность в полярной шапке при значительной северной вертикальной компоненте ММП

А.Е. Левитин, Л.И. Громова, С.В. Громов, Л.А. Дремухина (*Институт земного магнетизма, ионосферы и распространения радиоволн им. Н.В.Пушкина РАН (ИЗМИРАН), Троицк, Московская обл., Россия*)

На основе данных магнитных обсерваторий северной полярной шапки исследуются геомагнитные возмущения, возникающие в этой области высокоширотного пространства в периоды взаимодействия с магнитосферой межпланетного магнитного поля (ММП), вектор которого имеет высокоамплитудную северную вертикальную компоненту ($Bz \gg 1$). Эти возмущения можно рассматривать как суббури и бури в полярной шапке, которые генерируются проникающим в неё в течение нескольких часов подряд (от 2-3 часов до >10 часов) электрическим полем солнечного ветра при $Bz \gg 1$. Такие возмущения присущи только полярной шапке, и при их возникновении значительного усиления токовых систем в области авроральной зоны не происходит. Высокоамплитудное северное межпланетное поле одновременно с северным полем содержит в магнитном облаке, взаимодействующим с магнитосферой. Поэтому одно и тоже магнитное облако может вызывать разные по интенсивности классические магнитные бури или не вызвать их в зависимости от траектории прохождения Земли через это облако. Как показывает годовая статистика регистрации магнитных облаков, вероятность прохождения магнитосферы через области магнитного облака, где присутствует наиболее геоэффективная южная компонента вектора ММП ($Bz \ll -1$) равна вероятности её прохождения через области, где присутствует значительная северная компонента ММП ($Bz \gg 1$ нТл). В докладе приводится анализ ситуаций, когда магнитные облака создают как классические магнитные бури (Bz -компоненты ММП длительное время сохраняют большое отрицательное значение), так и магнитные бури только в области полярной шапки (Bz -компоненты ММП длительное время сохраняют большое положительное значение).

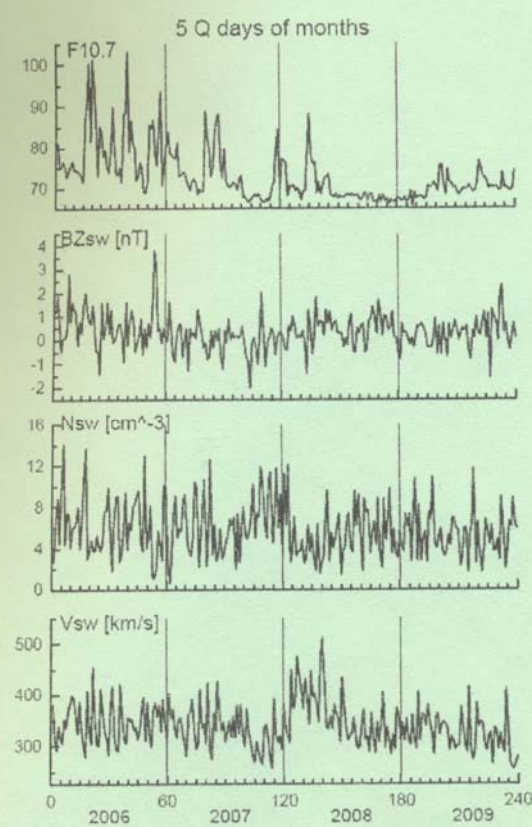
Работа выполнена при финансовой поддержке гранта РФФИ №11-0500306.

Супербурия 06.04.2000: определение скрытых зависимостей магнитного потока долей хвоста от значений динамического давления и электрического поля солнечного ветра

А.А. Шаповалова, Ю.А. Караваев, В.В. Мишин, и В.М. Мишин (*ИСЗФ СО РАН, Иркутск*)

Вопрос о линейной, или нелинейной зависимости магнитного потока долей хвоста Ψ от параметров солнечного ветра активно обсуждается в литературе (например, Shuktina et al., 2004, 2005; Lopez et al., 2009). Мы использовали данные WIND, и получили временные ряды изменений Ψ в ходе супербури 06.04.2000, коррелированные с изменениями параметров СВ: электрическим полем E_{sw} и динамическим давлением Pd . Использовался также разработанный в СибиЗмире вариант техники инверсии магнитограмм (ТИМ) для обработки измерений 120 наземных магнитометров. Получены карты распределения в полярной ионосфере плотности продольных токов, по которым определены временные ряды Ψ . По этим данным, на основе оригинального итерационного метода уменьшающихся вкладов, получены графики изменения в ходе супербури производных $\delta\Psi/\delta E_{sw}$ и $\delta\Psi/\delta Pd$, и графики скрытых зависимостей этих производных от параметров E_{sw} и Pd . Описаны результаты, существенно отличные от ранее известных. Отмечены ясно выраженные признаки насыщения Ψ с ростом E_{sw} .

Fields, Currents, Particles in the magnetosphere



Wavelet component manifestation of Solar Wind parameter disturbances which corresponding to the plasma flows at the dynamics of magnetic disturbance spectrums along the geomagnetic meridian

N.A. Barkhatov, S.E. Revunov, D.V. Shadrukov (*Nizhny Novgorod State Pedagogical University*)

At intervals of different strength of geomagnetic storms a comparison of the wavelet components in the form of local maxima of the spectrum (skeletons), the horizontal component of the geomagnetic field disturbances in the range of Pc4-5 along the meridional chain of stations and disturbances of Solar Wind parameters was made. In the framework the algorithm quantifying the consistency of analyzed skeletons is developed. This approach allows evaluating by latitude distributed response of the magnetosphere as geomagnetic field disturbances on the disturbed parameters of the Solar flow. It in turn specifies type of a geoeffectiveness flow with which occurrence of a geomagnetic storm is connected. As a result of the executed research following laws have been noted.

1) Before storm time response of the magnetosphere as geomagnetic field disturbances to the disturbed Solar flow parameters is its quick response in high latitudes (an average of 5 min.) and delayed in the subauroral zone (an average of 11 min.). This means that the area of the polar cap and fragmentary area of auroral oval directly exposed to Solar Wind wave disturbance of advanced flow and sub-auroral region have wave effect like as inner magnetosphere source.

2) Reaction time of the magnetosphere in geomagnetic field disturbances at the initial phase of the storm at all latitudes considered equally small (an average of 5 min.). This means that the total compression of the magnetosphere, caused by increase pressure of the Solar flow, facilitates the synchronization of disturbances along the meridian taken. Probably that all stations of reception of the analyzed data, in this case, get to area of a polar cap.

3) At the main phase of storms under the influence of flow of type CIR magnetosphere reaction as geomagnetic field disturbances at the disturbed Solar flow parameters by rapid response at high latitudes (an average of 4 min.) and delayed in the subauroral zone (an average of 12 min.) is characterized. Under the influence of flow of type magnetic cloud with the sheath and/or with shock wave reaction time at all latitudes equally and an average of 5 minutes considered. Perhaps this difference is caused by different geometry of curving power lines of the magnetosphere under the influence of different flows, which leads to different moments of synchronization of fluctuations at different latitudes.

Thus, it is shown how the dynamics of the spectrum components for disturbances of Solar Wind parameters corresponding to the plasma flow, in the spectrums of observatories magnetograms are appears. This is especially noticeable at the main phase of the storm: the disturbances of horizontal component of the geomagnetic field in the range of Pc4-5 analyzed along the meridional chain of stations information about the type of approaching to the magnetosphere disturbed Solar Wind flow is contain. Is also noted a decrease in the number of skeletons in the Solar Wind parameters at the initial phase of geomagnetic storms. This indicates about increase in overall stability of the frequency mode in the "Solar Wind-Magnetosphere" system on a time interval of Solar flow contact with the Earth's magnetosphere.

Ions heating on the polar border of the aurora

D.V. Chugunin, M.M. Mogilevsky, I.L. Moiseenko, T.V. Romantsova (*IKI RAN, Moscow, Russian Federation, dimokch@iki.rssi.ru*)

Data of plasma and electromagnetic fields on auroral polar border measured by Interball-2 (Auroral Probe) satellite is presented during geomagnetic disturbances. It was shown that near midnight during auroral polar border crossing ionospheric ions H⁺ and O⁺ with energy up to several keV were detected. At the same region AKR generation at the satellite altitude was observed. On the aurora border ions have pitch-angle close to 90 degrees, i.e. local ions heating occurs. From analysis it has been conclude that ions were heated up to 300 eV/s.

Response of the magnetosphere to an impulse of solar wind density at southward IMF in the dynamics of aurorae near the plasmapause

I.B. Ievenko (*Yu. G. Shafer Institute of Cosmophysical Research and Aeronomy, Yakutsk, Russia*)

A close connection of geomagnetic and auroral activity with the southward IMF B_z and solar wind (SW) speed is well-known. The dawn-dusk SW electric field $-V_x B_z$ causes a growth of magnetospheric convection. Recently Boudouridis et al. (2005, 2008) have shown that the increase of dynamic pressure owing to a fast growth of SW density at southward B_z immediately strengthens the convection electric field in the magnetosphere.

Fields, currents, particles in the magnetosphere

In this work we analyze manifestations of impulse increase of SW density at southward IMF in the dynamics of SAR arc and aurorae in 427.8 (N_2^+), 557.7 and 630.0 [OI] nm emissions at the Yakutsk meridian (130°E) by data of the meridian scanning and zenith photometers for the isolated event of December 28, 2010. It is generally accepted that the observation of diffuse aurora (DA) and SAR arcs is an informative research technique of magnetospheric processes in a vicinity of plasmapause. DA is caused by precipitations of low-energy electrons from a plasma sheet. SAR arcs are a consequence of interaction of the outer plasmasphere with ring current energetic ions. During substorms there is an increase of DA intensity and its equatorward extension up to a plasmapause projection which is mapped by the SAR arc appearing at this time (Ievenko, 1999, 2008).

The main development features of the phenomena of December 28, 2010. After a fast southward turn of IMF B_z there is a slow depression of the Earth's magnetic field at low latitudes with the ASYM-H / SYM-H = 3-4 ratio. The velocity of decay of H-component increases as southward B_z decreases up to -10 nT at low SW speed of 300-330 km/s. From 12 UT the growth of magnetospheric convection is observed in the equatorward extension of DA at the Yakutsk meridian in the evening sector of MLT.

A sudden pulse of SW density up to $\sim 70 \text{ sm}^{-3}$ with a duration of ~ 10 minutes is observed in SI at low latitudes at 1340 UT and causes: 1) the impulse intensification of the westward electrojet at auroral latitudes at midnight sector of MLT with a duration of SI and also the increase of ASYM-H up to $\sim 100 \text{ nT}$; 2) the sharp brightening of auroral arc at the geomagnetic latitude $\sim 61\text{--}62^\circ\text{N}$ and DA at lower latitudes; 3) the appearance of intense SAR arc in the equatorial region of DA and its southward movement with velocity of $\sim 70 \text{ m/s}$ till 1630 UT.

Subsequent sudden changes of the SW density up to $\sim 30 \text{ sm}^{-3}$ cause DCF magnetic field variations at low latitudes in the midday and midnight sectors of MLT and are well manifested in the brightening of auroral arc, DA and SAR arc during ~ 4 hours of observations. Magnetic and auroral activities promptly damp at 1730-1800 UT after the sharp northward turn of IMF B_z . We assume that the observed dynamics of aurorae and SAR arc in this event is caused by the fast intensification of convection and asymmetric ring current in the magnetosphere as consequences of the impulse increase of SW density at southward IMF.

Fine space-time structure of fields and particle fluxes measured by THEMIS

I.A. Kornilov, T.A. Kornilova (*Polar Geophysical Institute, Apatity, Russia. kornilova@pgia.ru*)

Well-known CLUSTER mission found many new phenomena in magnetosphere (flapping waves, for example). In 2010-2011 some THEMIS spacecraft were moving along almost the same orbits with a small space separation as well. Two probes were in the solar wind at the distances about 50-60 Re above magnetosphere subsolar point, and three others flew mostly inside magnetosphere at the different distances from the planet. In compare with CLUSTER experiment, THEMIS probes precisely measured electric and magnetic field in a very broad dynamic range, and large square ion and electron detectors had extremely good statistical accuracy, high angular and energy resolution, allowing construction of particle fluxes energy spectra with an excellent quality. Unique ballistic and equipment properties of THEMIS probes give a possibility to investigate fine structures in solar wind (shock waves, reconnection exhausts, etc), and in magnetosphere (radiation belts and plasmasphere irregularities, depolarization and particle injection front details and many other things). In this report we present some initial results of cross correlation and differential analyzes of E, B fields and energetic spectra of electrons and protons in the range about 0.1-200 keV.

Investigation of fractal properties of geophysical data by two-dimensional wavelet analysis

V.A. Ljubchich (*Polar Geophysical Institute, Murmansk, Russia*)

Many physical systems have hierarchical structure, for example plasma turbulence or distribution of ore bodies. Therefore physical fields observed on these systems have fractal properties. The wavelet analysis is useful tool for investigation of fractal properties of two-dimensional arrays of geophysical data. The wavelet transformation is decomposition of signal in term of wavelet basis functions. Local signal singularities, that defined by Holder exponent α , are investigated successfully by the wavelet analysis due to high time-frequency resolution and self-similarity property of wavelet basis functions. Signal features information is concentrated in skeleton of wavelet transformation. The skeleton of wavelet transformation is a set of local maximum points of wavelet transformation. The skeleton of wavelet transformation has tree-like structure for fractal arrays of geophysical data. The fractal dimension d_f and singularity spectrum $f(\alpha)$ of data array may be calculated from the skeleton of wavelet transformation.

This report deals with two-dimensional wavelet analysis of magnetic data observed in the Pechenga ore region. Main part of intensive local maximums of wavelet transformation is concentrated within productive ore layer of the

Pechenga geological structure. Most singular Holder exponents α correspond to deposits of solid and breccioso copper-nickel ore. The fractal dimension calculated from rate of skeleton ridge branching is equal $d_f=1.60$. Thus, we may conclude, that the two-dimensional wavelet analysis is useful method for investigation of fractal properties of geophysical data arrays, allowed to quantitatively estimate the degree of physical systems heterogeneity.

Numerical modeling of non-linear interactions of small-scale field-aligned current filaments by the macroparticle method

M.N. Melnik, O.V. Mingalev, I.V. Golovchanskaya (*Polar Geophysical Institute, Apatity, Russia*)

Algorithm for 2D numerical modeling of the time evolution of field-aligned current filaments interacting non-linearly under the action of Ampere's force is presented. From the form of the governing equations it follows that the macroparticle method can be applied for their solution, the macroparticle being a field-aligned current of a given value. The macroparticles are moving and interacting in the self-consistent magnetic field, which is calculated at each time step by solving the Poisson type equation for the vector potential over 1024×1024 grid with the periodic boundary conditions imposed. The details of the simulation such as a numerical scheme, code parallelization, and others are discussed.

Influence of the external magnetic field component B_y on the thin current sheet configuration

O.V. Mingalev¹, I.V. Mingalev¹, M.N. Melnik¹, H.V. Malova^{2,3}, L.M. Zelenyi², A.V. Artemyev²

¹ *Polar Geophysical Institute, Apatity, Russia*

² *Space Research Institute, Moscow, Russia*

³ *Institute of Nuclear Physics, Moscow State University, Moscow, Russia*

Numerical self-consistent model of high-temperature collisionless magnetotail thin current sheets (TCSs) based on macro-particle method has been used for investigation of the influence of the external magnetic field component B_y^E on the TCS configurations with constant external B_z and two self-consistent components of the magnetic field ($B_x(z)$, $B_y(z)$) and current ($j_x(z)$, $j_y(z)$) in *GSM* coordinate system.

Magnetic field parameters near the subsolar magnetopause in accordance with THEMIS data

M.S. Pulinet¹, M. Riazantseva^{1,2}, E.E. Antonova^{1,2}, I.P. Kirpichev^{2,1}

¹ *Skobeltsyn Institute of Nuclear Physics, Lomonosov Moscow State University, Moscow, Russia*

² *Space Research Institute RAS, Moscow, Russia*

We analyze the crossings of the magnetopause near the subsolar point using FGM and ESA devices of THEMIS mission. The aim of the research was the understanding of the applicability of the frozen in conditions to the processes of plasma flow in the magnetosheath. Variations of the magnetic field near magnetopause measured by one of THEMIS satellites are compared with simultaneous measurements in the solar wind by another THEMIS satellite. 30 and 90 s averaging of magnetic field in the magnetosheath is produced. The results of averaging are compared with the results of measurement just after the magnetopause crossing. It is shown, that B_x component of the magnetic field near magnetopause is near to zero, which supports the possibility to consider the magnetopause as the tangential discontinuity. Comparatively good correlation of B_y component in the solar wind and near the magnetopause is observed. The correlation of B_z component near the magnetopause and IMF is practically absent. It is shown, that in many cases the sign of the B_z component of magnetic field near the subsolar point does not coincide with the sign of IMF B_z component. The results of the analysis create definite difficulties to simplified theories of magnetic reconnection of solar wind magnetic field at the magnetopause.

Study of magnetic field intensity in the magnetic barrier near the subsolar point of the Earth's magnetosphere in dependence on IMF

K.Yu. Slivka, N.P. Dmitrieva, and V.S. Semenov (*Department of Geophysics, Faculty of Physics, Saint-Petersburg State University, Saint-Petersburg*)

The magnetic barrier is the region with enhanced magnitude of magnetic field. It is formed in the inner magnetosheath layer adjacent to the dayside magnetopause.

There is a general point of view now that a magnetic barrier can persist only for the northward direction of IMF while it is absent for the southward direction. We make a special study to check appearance of magnetic barrier for different directions of IMF. To this end a data base consisting 149 events of low-latitude dayside magnetopause crossings by the Themis satellites with signatures of magnetic barrier, was created and analyzed. It turns out that the magnetic barrier is the most pronounced for the northward IMF, the magnetic field intensity corresponds to the Erkaev analytical estimation [Erkaev et al., 1992] in this case. For the southward IMF we still were able to find signatures of magnetic barrier although it was highly disturbed by the reconnection.

The influence of the tailward magnetic field lines on the formation of the currents within the Harang discontinuity

M.A. Volkov (*Murmansk State Technical University, 13 Sportivnaya Str., Murmansk, 183010, e-mail: volkovma@mstu.edu.ru*)

This work is focused on the formation of the electric fields and currents in the Harang discontinuity. The charge separation in this region of the magnetosphere is the result of various protons and electrons drift in the inhomogeneous magnetic field. The cold electrons move with velocity of the electric drift, while the hot ions move with velocity of electric and gradient drift. The gradient drift is directed along the lines of the equal magnetic field. Within the research the magnetic field model with the tailward magnetic fields lines has been used. In the magnetosphere model the hot ions have velocity component directed away from Earth to the evening sector of the magnetosphere at the distance of~10 Re. As the result, the negative charge, electric fields and currents have been appearing in this region with the typical distribution of these electric fields and currents for the Harang discontinuity.

Mapping the sub-oval proton aurora spots relatively plasmapause

A.G. Yahnin and T.A. Yahnina (*Polar Geophysical Institute, Apatity, Russia*)

Proton aurora spots are sometimes observed equatorward of the main proton aurora oval. The spots are long-lasting phenomena occurring during recovery phase of geomagnetic storms; they co-rotate with the Earth remaining at (approximately) the same latitude. They associate with quasi-monochromatic pulsations Pc1. The latest means that proton precipitation responsible for these auroras relates to the ion-cyclotron instability. To understand where the instability develops we mapped proton aurora spots onto the equatorial plane and compared the mapping results with the plasmapause model introduced by Viviane Pierrard and colleagues. The model is based on the quasi-interchange mechanism of the plasmapause formation and depends on the history of magnetospheric electric field variations. At all, 13 proton aurora spots were considered. In 11 events we found that mapped spots are in a close vicinity of the modeled plasmapause. In one of the two remaining events the proton aurora spot was mapped well inside the modeled plasmapause. This event had been already considered in the literature (Frey et al., 2004). Combining the data from FUV and EUV imagers onboard the IMAGE spacecraft, these authors showed that the spot projection falls onto the cold plasma gradient inside the plasmapause. Thus, 12 of 13 events confirm the suggestion that ion-cyclotron instability producing Pc1 and proton aurora spots develops in the vicinity of the cold plasma gradient (plasmapause). In the latter event the spot projection was well outside the plasmapause. One may suggest that this event relates to the cold plasma structure detached from plasmapause. We conclude that observations of proton aurora spots and related localized precipitation of energetic protons can be used as indicator of plasmapause or gradient of the cold plasma in the equatorial plane.

Unusual sub-oval proton aurora occurred on 10 and 11 November 2004: Image of plasmapause

T.A. Yahnina¹, A.G. Yahnin¹, F.Soraas²

¹ *Polar Geophysical Institute, Apatity, Russia*

² *University of Bergen, Norway*

During interval of 01-03 UT on 10 November 2004 an unusual “proton aurora” (emission of the excited hydrogen atoms generated by precipitating magnetospheric protons after charge-exchange with atmospheric constituents) was observed from the IMAGE spacecraft well equatorward of the auroral oval. This was a narrow arc of “proton” luminosity situated at $L = 2.5$ and $MLT = 23 - 06$. Localized precipitation of energetic ($E > 30$ keV) protons was observed by the NOAA POES satellite above the arc. At the end of considered interval the arc broke into separate spots. For this case the plasmapause position was found using the model, which is based on the quasi-interchange mechanism of the plasmapause formation and depends on the history of magnetospheric electric field variations. This position fairly well agrees with the location of the proton arc. During interval of 06-09 UT on 11 November 2004 an arc-like structure formed from several proton aurora spots was also observed. In the morning sector this structure was at $L=2.5$, and it jumps to $L=4$ in the pre-noon sector. This agrees with the form of the modeled plasmapause, which exhibits a pre-noon “shoulder”. As known, sub-oval proton auroras are the result of interaction of the ring current protons with ion-cyclotron waves. Relationship between the arc-like proton aurora structures and plasmapause agrees with suggestion that favorable conditions for the ion-cyclotron instability occur at the cold plasma gradient (plasmapause). This means that observation of sub-oval proton auroras can be used for monitoring the plasmapause.

Авроральное километровое излучение как индикатор образования каверны Кальверта

И.Л. Моисеенко¹, М.М. Могилевский¹, Т.В. Романцова¹, Д.В. Чугунин¹, Я. Ханаш²

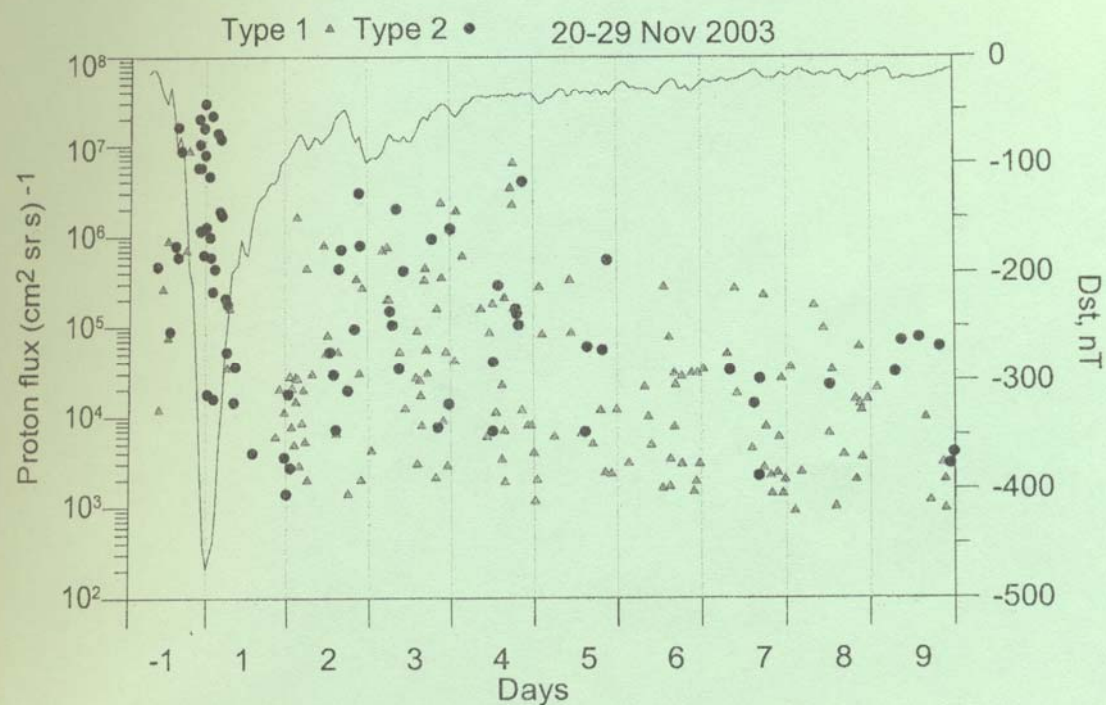
¹ *Институт космических исследований РАН, Россия*

² *Центр космических исследований ПАН, Польша*

Авроральное Километровое Радиоизлучение (АКР), впервые обнаруженное в 1965 году на спутнике «Электрон», представляет собой интенсивное излучение магнитосферы Земли на частотах 30-800 кГц. Общепризнанным механизмом генерации АКР является циклотронная мазерная неустойчивость, развивающаяся в авроральной области, в т.н. кавернах Кальверта с пониженной плотностью плазмы, где выполняется условие $f_{pe}/f_{ce} \ll 1$ (f_{pe} и f_{ce} – плазменная и циклотронная частоты электронов). Источники АКР расположены над авроральной ионосферой на высотах 2-10 тыс. км, на инвариантных широтах $\sim 65^\circ - 70^\circ$. На основе прямых измерений электромагнитного излучения в диапазоне частот 4 кГц – 1 МГц, сделанных на борту спутника ИНТЕРБОЛ-2 при помощи прибора ПОЛЬРАД, рассматриваются вопросы генерации низкочастотного аврорального километрового излучения (АКР) в пространственно ограниченном источнике. Особенностью орбиты спутника ИНТЕРБОЛ-2 является длительное движение вдоль магнитной оболочки ($L = \text{const}$) в авроральной области магнитосферы, что позволяет в этой области разделить пространственные и временные изменения параметров излучения.

Обнаруженное в эксперименте увеличение интенсивности АКР вблизи локальной гирочастоты электронов, интерпретируется нами как наблюдение медленных волноводных мод внутри источника. «Классическое» АКР, представляющее собой R-X-моду электромагнитного излучения, является результатом трансформации волноводных мод на границе источника. Из сравнительного анализа измерений электромагнитного поля и параметров плазмы делается заключение, что на полярной границе авроральной области, во время геомагнитных возмущений образуется область с пониженной плотностью фоновой плазмы – каверна Кальверта. В этой области развивается циклотронная мазерная неустойчивость, результатом чего является наблюдавшееся излучение. Особенности изменения максимума спектра излучения позволяют оценить характерные продольные размеры источника.

Waves, Wave-Particle Interaction



The morning auroral arcs associated with *Pc5* geomagnetic pulsations

V.B. Belakhovsky¹, A.E. Kozlovsky², V.A. Pilipenko³

¹ *Polar Geophysical Institute, Apatity, Russia*

² *Sodankyla Geophysical Observatory of the University of Oulu, Finland*

³ *Institute of the Earth Physics, Moscow, Russia*

We study the event of *Pc5* geomagnetic pulsations observed in the morning sector on 18 December 2001 at the stations of *IMAGE* magnetometer network. The pulsations were observed in the wide range of latitudes from 58° to 76° MLAT. Geomagnetic *Pc5* pulsations exhibit signatures of the filed-line resonance (FLR), namely, the decrease of the frequency with increase of the latitude, change of the ellipse during the propagation thought the resonance region, and phase propagation from low to high latitudes.

Corresponding variations of the ionosphere plasma velocity were seen by the *VHF EISCAT* radar, which beam was pointed to north at low elevation (30°) to the horizon. The frequency of pulsations in the ionosphere plasma velocity decreases with latitude. Signatures of the *Pc5* pulsations were also seen in the data of ionosphere plasma velocity, density, and ion temperature obtained from the *EISCAT* Svalbard radar.

The cosmic noise absorption did not demonstrate significant signatures of *Pc5* pulsations in the data of riometers in *KIL* (*IRIS*) and *HOR* (Spitsbergen). At the same time the *Pc5* pulsations in aurora intensity in 630.0, 557.7 nm emissions were observed by meridian scanning photometer in Barentsburg (Spitsbergen). The frequency of auroral *Pc5* pulsations and geomagnetic *Pc5* pulsations seen on *LYR* stations are coincide. During this time auroral arcs were observed by the all-sky TV camera in Barentsburg. We suppose that *Pc5* geomagnetic pulsations generated by FLR modulate the intensity of morning auroral arcs.

Poloidal geomagnetic *Pc5* pulsations and pulsations in the fluxes of energetic particles

V.B. Belakhovsky¹, V.A. Pilipenko²

¹ *Polar Geophysical Institute, Apatity, Russia, e-mail: belakhov@mail.ru*

² *Institute of the Earth Physics, Moscow, Russia*

The event of 9 May 2003 when the poloidal geomagnetic *Pc5* pulsations were observed at geostationary orbit on *GOES-10* spacecraft was considered. The radial *he*-component of the geomagnetic field on *GOES-10* exceeds the azimuthal *hn*-component. It is also seen the strong *Pc5* pulsations in the module of the geomagnetic field. It confirms that the observed *Pc5* pulsations are pulsations of the poloidal type. The *Dst*-index during this day has the minimum value -50 nT.

It is seen the cloud of protons on *LANL-1991* satellite before the appearance of the poloidal geomagnetic *Pc5* pulsations. Obviously this cloud is the source of the observed poloidal geomagnetic *Pc5* pulsations due to development of kinetic instabilities. The poloidal geomagnetic *Pc5* pulsations at *GOES-10* spacecraft were accompanied by the pulsations in the fluxes of protons with energies 50-75 keV at *LANL-1991* spacecraft.

The geomagnetic *Pc5* pulsations at geostationary orbit were accompanied by the *Pc5* pulsations in fluxes of energetic electrons at *LANL-1991* spacecraft and in cosmic noise absorption (*CNA*) at *MCM* station with the same frequency. The *MCM* station is located near the conjugate point according to the *GOES-10* satellite. The coherency between the geomagnetic field variations and variations of the fluxes of energetic electrons is 0.92, while the coherency between the geomagnetic field variations and variations of *CNA* is 0.85 at the frequency of the maximum power spectrum. The poloidal geomagnetic *Pc5* pulsations were not well seen on the ground magnetometers due to shielding effect of the ionosphere.

The important parameter of the pulsations is modulation depth. The depth of modulation for the *Pc5* pulsations in *CNA* reaches the value 85%.

So in our work we firstly show that the poloidal geomagnetic *Pc5* pulsations observed on the geostationary orbit were accompanied by the corresponding *Pc5* pulsations in *CNA* near the conjugate point. Thus it is shown that the poloidal geomagnetic *Pc5* pulsations were accompanied by the pulsations of precipitated energetic electrons.

Saturation of amplitude of whistler-mode waves generated in a nonuniform magnetic field and possible consequences for the parameters of VLF chorus emissions

A.G. Demekhov (*Institute of Applied Physics, Nizhny Novgorod, Russia*)

We study numerically the wave amplitude saturation upon the generation of VLF chorus emissions in the Earth's magnetosphere. The dependence of the characteristic amplitude of whistler-mode waves at the nonlinear stage on the linear-instability growth rate is one of key relationships in the chorus generation theory which determines the relation between the frequency drift rate and the linear growth rate. The latter relation based on analytical formula for the saturated wave amplitude in a uniform medium (Trakhtengerts, 1984) has been employed when studying the observational data on VLF chorus detected by Cluster spacecraft in the equatorial magnetosphere (Macusova et al., 2010; Titova et al., 2011). In this paper we verify the analytical relationship obtained by Trakhtengerts (1984) and update it for the nonuniform medium characteristic for the near-equatorial magnetospheric region. For that we use the numerical model of self-consistent nonlinear resonant interactions between energetic electrons and whistler-mode waves (Demekhov and Trakhtengerts, 2005). The implications for the estimates of electron-distribution parameters based on the parameters of observed VLF chorus elements will be discussed. We also consider the effects of the chorus generation on the electron velocity distribution and possible consequences for chorus generation conditions.

Broadband electrostatic noise associated with Alfvénic turbulence in the topside ionosphere

I.V. Golovchanskaya, O.V. Mingalev, B.V. Kozelov, M.N. Melnik, and I.V. Despirak (*Polar Geophysical Institute, Apatity, Russia*)

One phenomenon accompanying the Alfvénic turbulence in the high-latitude topside ionosphere is a broadband electrostatic noise seen in the electric field spectra at frequencies from about 10-20 Hz up to 1-3 kHz. The nature of this perturbation is not quite understood. We report two observational features that could, to a certain extent, shed light on its generation mechanism: (i) the broadband electrostatic noise always develops in the non-uniform background, i.e. in the presence of external gradients; (ii) it exhibits a clear seasonal variation, the intensity of the noise being, at least, factor 3-4 higher in winter than in summer. The second feature is especially intriguing because this perturbation lacks field-aligned currents, whose closure via poorly conductive winter ionosphere could require stronger electric fields in winter season. We discuss different mechanisms of broadband electrostatic noise generation and suggest that the inhomogeneous energy-density-driven instability (IEDDI) associated with localized electric fields of the Alfvénic turbulence can produce a perturbation consistent with the reported features.

Geomagnetic pulsations associated with substorm

N.G. Kleimenova (*Institute of the Earth Physics RAS, Moscow, Russia*)

Different wave generation is a fundamental behavior of the magnetospheric plasma which is represented the interrelated system of resonators and waveguides with a distinguished feature of the field line resonances. A most part of the generated in the magnetosphere waves could be observed at the Earth surface as a wide range of geomagnetic pulsations (or ULF waves), which are defined as fine indicators of a different plasma instabilities development. The history of the pulsation discovery, their classification and the first pioneer results are presented. Some forgotten and seldom referred evidences of the relationship between Pi2 geomagnetic pulsations and visible auroras are shown. The substorm associated geomagnetic pulsations, exhibited the traditional substorm feature are discussed. The high- and low-latitudes Pi2 pulsations, directly driven by compressional pulses during a substorm onset and their possible effects at the day side magnetosphere are given. It is shown that the simultaneity of the Pi1B, Pi2, and Pi3 pulsations burst exiting demonstrates their common nature at a substorm onset. Despite of the well documented facts of the relationship between the morning Pc5 pulsations and substorm development, the role of substorm in the generation of the magnetosphere field line resonances is still unknown.

Spatio-temporal features of pulsating aurora: New observations and approaches

B.V. Kozelov, E.E. Titova, V.E. Yurov, L.P. Borovkov, S.V. Pilgaev (*Polar Geophysical Institute, Apatity, Murmansk region, 184209 Russia*)

Optical observations with a new system of auroral cameras (MAIN - Multiscale Aurora Imaging Network) have been analyzed to deduce spatio-temporal features of pulsating aurora. The observational system consists of 5 cameras which were installed at Kola Peninsula for observations of auroral structures at different scales: from fine structured near magnetic zenith to all-sky luminosity. We discuss the traditional features of the pulsating aurora (periods, spatial size, altitude), as well as new approaches: number of degrees of freedom, coherency, spatial modes, etc. Comparison with previous experimental and theoretical results is presented.

Kink and sausage modes of the flapping oscillations in the magnetotail current sheet

D.I. Kubyshkina, D.A. Sormakov, V.S. Semenov, V.A. Sergeev (*Institute of Physics, State University, St. Petersburg, Russia*)

Flapping oscillations observed in the current sheet of the Earth's magnetotail, represent rather slow waves propagating from the center to the flanks with a typical speed \sim 20-60 km/s, amplitude \sim 1-2R_e and quasiperiod \sim 2-10 minutes. The relevant model is based on double gradient of magnetic field: gradient of tangential (B_x) component along the normal (z) direction and normal component (B_z) along the x-direction. Calculations were made for two different variants of initial disturbance.

In the framework of this model the rotation of the vector of magnetic field in the plane Z-Y as well as vector of plasma velocity is investigated to find differences between kink and sausage modes of the flapping oscillations. Were observed that rotation of the vectors don't depend from type of initial disturbance and it is also shown that the speed of the rotation of the vector (v or B) gives the fundamental parameters of the model including double gradient frequency.

The theoretical results are compared to the flapping oscillations observed by space mission Themis on 03.05.2008 in the morning sector of the magnetotail. The observed rotation of the velocity vector simultaneously on two spacecrafts of Themis mission corresponds to the kink mode of the flapping oscillations.

The results obtained show that data on rotation of v and B vectors can give important information about modes and characteristics of the flapping waves.

Temporal change of the VLF hiss polarization: Case study of the event on 12 April 2011

J. Manninen¹, N.G. Kleimenova², O.V. Kozyreva²

¹ *Sodankyla Geophysical Observatory, Finland*

² *Institute of the Earth Physics RAS, Moscow, Russia*

VLF hiss burst was observed on 12 April 2011 at 04-06 UT in Northern Finland at the temporal station Kannuslehto (L=5.3), which is located near Sodankyla at the auroral latitude. The event occurred at the end of the initial phase of the small magnetic storm. Initial phase of the storm was distinguished by very high solar wind dynamic pressure (up to 14 nPa) on 11 April 2011 at \sim 16 UT, which resulted a significant squeezing of the dayside magnetosphere. Because of that the plasmapause could be shifted to L-shells less than 5.3. A few hours later, on 12 April 2011, in the morning sector, an intense VLF hiss burst at 1.5-4.0 kHz was recorded at Kannuslehto. The VLF burst can be attributed to the typical plasmaspheric hiss. A temporal dynamic change of the signal polarization properties was found. At the beginning, the polarization of VLF hiss was left-handed, which can be interpreted by long distance propagation in the Earth-ionosphere wave-guide. Mostly waves arrived from the north-south direction, probably from lower latitudes. After one hour the wave polarization gradually turned to a strong right-hand polarization, which can indicate that the ionospheric exit point of wave moved nearly overhead. Before the appearance of VLF hiss burst, the solar wind dynamic pressure fell down to 1 nPa and the magnetosphere (and the plasmapause) began to extend to its ordinary state. The plasmapause could be mapped near Kannuslehto station. The VLF waves arrived from the north-south direction as well, but the intensity of northern and southern signals became comparable. We suppose, that such dynamic change of wave polarization can be explained by the temporal dynamics of the plasmapause due to VLF wave guiding effect along the plasmapause.

The VLF hiss was modulated by simultaneously observed geomagnetic pulsations of the Pc4 range. The Pc4 spectral maxima changed with time from higher frequency to lower that can be interpreted as a latitude shift of the

Waves, wave-particle interaction

resonant field lines. Thus, the temporal dynamics of the polarization of the VLF hiss as well as the change of the resonant geomagnetic pulsations spectra may demonstrate the temporal dynamics of the plasmapause location.

Simultaneous observations of correlated quasi-periodic ELF/VLF wave emissions and energetic-electron precipitation by DEMETER

D. Pasmanik¹, M. Hayosh², A. Demekhov¹, O. Santolík², E. Titova³, and M. Parrot⁴

¹ *Institute of Applied Physics RAS, Nizhny Novgorod, Russia*

² *Institute of Atmospheric Physics, Prague, Czech Republic*

³ *Polar Geophysical Institute RAS, Apatity, Russia*

⁴ *LPC2E/CNRS, 3A Avenue de la Recherche Scientifique, Orléans, 45071, France*

One of the proposed explanations of the quasi-periodic (QP) VLF waves observed in the ionosphere is based on their generation by energetic electrons in the equatorial region of the magnetosphere. These electrons then precipitate into the ionosphere and their flux should be modulated with the same period as the QP emissions. The main attention in our study is paid to the correlation between both features. We use the DEMETER spacecraft data for this purpose. We have analyzed more than two hundred events of the QP wave measurements by DEMETER. In this large data set, we have found several cases where precipitated electrons are highly correlated with the QP wave bursts. To our knowledge, such observations made onboard satellites have not been reported earlier. We have found the cases at both low ($L < 4$) and high ($L > 4$) McIlwain parameter, however characteristics of the QP emissions (the frequencies, the dynamic spectrums, the periods) differ for different latitudes. Energetic particle data from the DEMETER satellite are supplemented by data from the NOAA-17 satellite. The orbit of this spacecraft is very similar to the orbit of DEMETER. We discuss mechanisms of removal of energetic electrons from a generation region and we compare the parameters of the observed events with the cyclotron maser model of the QP emissions.

Pc1-2 auroral pulsations

V.C. Roldugin, AV. Roldugin and S.V. Pilgaev (*Polar Geophysical Institute, Apatity, Russia*)

There are regular optical observations of aurora in Lovozerovo ($\phi=68.0^\circ$ N, $\lambda=35.0^\circ$ E, $\Phi=64.4^\circ$, $\Lambda=114.3^\circ$) by all sky camera "Spica". This camera consists of «fish-eye» lens of model FE-0.8-MAO(4.2) manufactured by Main Astronomical Observatory UAS, and CCD F-046 Stingray. The frame rate is one per second, the resolution is 360 x 360 pixels with two bytes per pixel.

The event of 2 February 2011 morning is considered. During recovery phase of negative bay about of 40 nT between 0200 and 0400 UT some trains of geomagnetic pulsations $Pc2$ with 7.5 sec period and about of 0.04 nT intensity appeared. Near the northern horizon a homogeneous arc was observed, and to the South from it weak auroras with indistinct form were situated. We discriminate 11 circles in field of view: 3 near zenith and 8 along azimuth every 45°, and determine averaged light intensity in each circle. Thus obtained variations of luminosity with 1 sec resolution in different circles are compared with magnetic pulsations with 0.1 sec resolution.

It is found that in the circles with aurora the luminosity variations correlate well with the geomagnetic $Pc2$ pulsations. The "pearl" structure is observed both in magnetic and auroral oscillations. The luminosity bursts are accompanied by positive half-periods in Z -component, by negative ones in D -component, and the positive peaks in H lag with the luminous peaks about of $\pi/2$.

Methods of fractal analysis of the high-latitude ULF emissions to study magnetosphere dynamics and monitor the space weather

N.A. Smirnova¹, A.A. Isavnin¹, T.V. Bondareva¹, A.N. Vasilev², Yu.V. Katkalov²

¹ Institute of Physics, St.-Petersburg State University, St.-Petersburg, Russia

² Polar Geophysical Institute, Apatity, Russia

Now it is recognized that the Earth's magnetosphere exhibit the properties of the SOC (self-organizes critical) systems. The main feature of the SOC state is fractal organization (power-law distributions) of the output parameters in both space and time domains (scale-invariant structures and fractal noise or 1/f fluctuations). Hence we can use fractal methods to study scaling properties of the magnetospheric emissions in different frequency ranges and thus trace multi-scale magnetospheric processes.

Here we apply fractal methods to the high-latitude ULF emissions registered at Barentsburg ($\Phi_m = 76^\circ\text{N}$) and Lovozero ($\Phi_m = 64^\circ\text{N}$) during one year period of 2008. The advanced equipment used at those stations and rather high resolution of 10 Hz allow us to analyze appropriately fractal properties of the ground-observed magnetic fluctuations in the wide frequency range from DC up to 3-5 Hz. We restrict our analysis to ULF range of $f = 0.002 - 2$ Hz since it is the principal range of magnetospheric ULF waves, which play an important role in multi-scale magnetosphere dynamics.

Three methods of fractal analysis are considered: 1) PSD (Power spectral density) method (Feder 1989, Turcotte 1997); 2) Burlaga-Klein method (Burlaga and Klein 1986); 3) Higuchi method (Higuchi 1988, 1990). Some interesting peculiarities in dynamics of the ULF fractal characteristics have been detected and discussed on the basis of the SOC consideration. The most interesting peculiarity revealed is the kink on the fractal curve at the time scale near 0.5 sec. A similar kink was theoretically predicted by Milovanov and Zelenyi in 1996 on the basis of the Geotail data analysis (Hoshino et al., 1994). We discuss such a correspondence and validate, that fractal characteristics of the high-latitude ULF emissions can be used to study magnetosphere SOC dynamics and monitor some plasma parameters related to the space weather.

Using VLF chorus elements observed by CLUSTER satellites for study of the backward wave oscillator in the magnetosphere

E. Titova¹, B. Kozelov¹, A. Demekhov², O. Santolik³, E. Macusova³, J.-L. Rauch⁴, J.-G. Trotignon⁴, D. Gurnett⁵, and J. Pickett⁵

¹ Polar Geophysical Institute, Fersmana 14, 184209, Apatity, Russia

² Institute of Applied Physics, Ulyanov 46, 603950, Nizhny Novgorod, Russia,

³ IAP/CAS, Bocni II/1401, 14131 Prague, Czech Republic,

⁴ LPCE/CNRS, 45071, Orleans, France,

⁵ University of Iowa, Iowa City, IA, 52242, USA

A generation mechanism for VLF chorus was suggested by Trakhtengerts [1995, 1999] on the basis of the backward wave oscillator (BWO) regime of magnetospheric cyclotron maser. According to the BWO model, a sharp gradient (or step-like deformation) on the electron distribution function is the most important factor of chorus generation, but such a feature is very difficult to observe directly. The properties of the step in the BWO model determine the dimensionless parameter q quantifying the excess of the energetic electron flux above the absolute-instability threshold. This parameter, in turn, is related to the frequency sweep rate of chorus elements, which we obtained by using the data from WBD instrument onboard CLUSTER satellites in the equatorial region for more than 7000 chorus elements. Then using the CLUSTER data for the plasma density and magnetic field we calculated q and found that the q values depend only weakly on the density; the average values of $q \approx 7$ for the lower band chorus ($f / fH < 0.5$) and $q \approx 13$ for the upper band ($f / fH > 0.5$). Such a large excess over the generation threshold obtained from observations is consistent with the results of numerical simulation of discrete elements with rising frequency (Demekhov and Trakhtengerts, 2008). Another important feature of the q parameter is significant scatter of its values during each Cluster passage of the generation region. Using the obtained q values we estimate the relative height of the step on electron distribution function to lie in the range from 0.01 to 0.3. The spread in q values indicates the importance of the fluctuations of the distribution function in the formation of chorus elements.

Модель поля среднеширотных Pi2 пульсаций на ионосферных высотах

Е.Н. Федоров¹, В.А. Пилипенко^{1,2}, Б. Хэйлиг³, П. Сатклиф⁴, Х.Л. Люор⁵

¹ ИФЗ РАН, Москва (enfedorov1@yandex.ru)

² ИКИ РАН, Москва

³ Геофизический Институт им. Лорана, Будапешт, Венгрия

⁴ Магнитная обсерватория Германус, Германус, ЮАР

⁵ Национальный Научный центр наук о Земле, Потсдам, Германия

Поле среднеширотных Pi2 пульсаций на ионосферных высотах представлено в виде суммы парциальных альфеновской и БМЗ волн. Предложена модель распределения поля пульсаций с учетом сферичности Земли. Модель применима для периодов $T > 50$ с. Предложен метод оценки амплитуд парциальных волн. Интерпретируются одновременные наблюдения Pi2 на спутнике CHAMP ($h \sim 350$ km) и на двух наземных сопряженных станциях.

Геомагнитные пульсации диапазона Pc2-3 на Земле, в верхней ионосфере и в магнитосфере

Н.В. Ягова¹, Б. Хэйлиг², Е.Н. Федоров¹, П. Ковач³

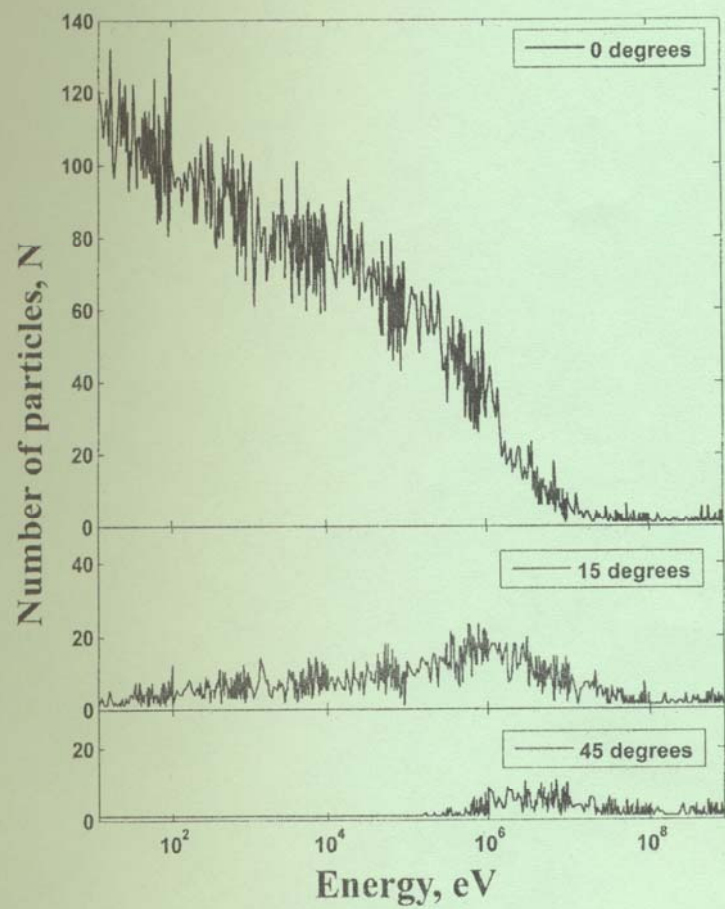
¹ ИФЗ РАН, Москва, nyagova@yandex.ru

² Геофизическая обсерватория Тихани, п. Тихани, Венгрия

³ Геофизический институт им. Лорана, Будапешт, Венгрия

Рассматриваются пульсации диапазона Pc2-3 (80-250 мГц) на земной поверхности, в F-слое ионосферы и в магнитосфере. В случаях, когда сигнал наблюдается одновременно на Земле и в ионосфере, амплитуда сигнала на поверхности Земли в среднем на порядок ниже измеренного в ионосфере, а частота несколько выше, что приводит к оценке пространственного масштаба в несколько десятков километров. Поляризация пульсаций соответствует альфеновской моде. Морфологические свойства и зависимость параметров рассматриваемых Pc2-3 пульсаций от факторов космической погоды существенно отличаются от соответствующих параметров среднеширотных Pc3 пульсаций.

The Sun, Solar Wind, Cosmic Ray



Observing of atmospheric hadronic shower on the Barentsburg neutron monitor

Yu.V. Balabin, A.V. Germanenko, E.V. Vashenyuk, B.B. Gvozdevsky (*Polar Geophysical Institute, Russian Academy of Sci., Apatity, Russia*)

The Barentsburg 18-NM-64 neutron monitor (NM) has a notable feature. It consists of three sections 6-NM-64, which have spaced at about 5 m. Due to the new recording system with 1 mcs time resolution between pulses one can study such fast and transient phenomenon like multiplicity. A multiplicity event is an isolated sequence of pulses into a data set with short time intervals between them. In the present work a two-section multiplicity was studied i.e. a multiplicity event, which is formed by pulses appearing simultaneously at two different sections. We select only such two-section multiplicities in which each section must put more than 4 pulses into an event. In this case a probability of a random coincidence of pulses in the data set is around 10^{-8} . It means one event in the NM data per 5-10 days. But number of such events is 20-30 per a day really. We consider this to be the effect of atmospheric hadronic shower on the NM. Cross-section size of such shower is estimated to be about 10 m. There is no doubt of reality of the multiplicity, because other characteristics of two-section multiplicity events (like total time duration, time profile etc.) are near to the same values of one section multiplicity.

Geomagnetic efficiency of Solar ejection depended on relative orientation of Sun and Earth rotation axes

N.A. Barkhatov¹, E.A. Revunova¹, A.E. Levitin²

¹ *Nizhniy Novgorod State Pedagogical University, Nizhniy Novgorod, Russia*

² *Pushkov Institute of Terrestrial Magnetism, Ionosphere and Radio Wave Propagation, Troitsk, Russia*

Seasonal variations of geomagnetic activity have two peaks which fit to spring and autumn equinoxes periods. Analyzing such pattern it has been assumed that reason of these peaks is formation of active Sun areas which are grouped in zones from 10 to 30 degrees northern and southern heliographic latitudes [Cortie, 1912]. Therefore during the equinoxes periods when the Earth's latitude helioprojection has maximum the most probable collision of the Earth with Solar streams from active areas promotes. With time researchers began to consider geomagnetic dipole inclination to ecliptic plane and effect of occurrence of these two peaks has connected with the following situation. The interplanetary magnetic field (IMF) usually considered in Solar-ecliptic coordinate system whereas its influence on geomagnetic activity depends on sign and amplitude vertical Bz vector IMF component in solar-magnetospheric coordinate system when this field is brought to magnetosphere by Solar wind. Seasonal effect described by Kp-index according to Russell and McPherron consist geomagnetic activity dependence on vector IMF components. Positive polarity of this components IMF is the most geoeffective in the autumn and negative polarity – in the spring [Russell and McPherron, 1973]. There is also representation about a direct connection between this activity and relative orientation of electric field vector E of Solar wind and geomagnetic moment vector M [Kuznetsova et al, 2006, and references]. However, as the electric field contains Bz component of IMF vector, it is possible that the relationship Kp index with the angle between M and E vectors is due simply dependent cosine of this angle of IMF Bz component in the Solar-magnetospheric coordinate system. In this connection, in [Barkhatov et al, 2008] the estimation of relationship between Kp index with Solar wind electric field and with projection of this field on the geomagnetic dipole has been executed. Method for calculating Solar wind electric field, showing its greatest geoeffectiveness in form of correlation with an index of global geomagnetic activity Kp is developed.

Another cause of the greater number of magnetic storms and storms with strong intensity during spring and autumn equinoxes may be seasonal dynamics of the Coronal Mass Ejections (CME) parameters like magnetic clouds reached the Earth's magnetosphere. Due to changing of Sun rotation axis inclination to ecliptic plane during the year the interaction probability of Earth with ejections from the “royal zones” increases during the equinoxes. Accordingly, the generation probability of intensive magnetic storms increases also. This is possible because the strong magnetic field, which is responsible for the magnetic storms intensity, is observed on the axis CME and Earth will pass through center of CME during the equinox.

Establishing the influence of the Sun axis rotation orientation on the geomagnetic activity in the statistical analysis of the seasonal distribution of CME Solar source locations causing geomagnetic storms was carried out. For this purpose data of Solar catalogues for a complete Solar cycle 23 (1996-2006) has been involved. The carried out analysis has shown that during the autumn/spring equinox Solar sources of geoeffective position CME source mainly located above/below the Solar equator while during the periods of solstice coordinates are approximately symmetrical distribution concerning equator. This effect is more pronounced during Solar minimum.

Oscillations of a thin flux tube inside polytropic star

R.O. Bortnikov, V.S. Semenov (*Saint-Petersburg State University*)

According to the model of Babcock (1961), during the minimum of the solar cycle initially poloidal field receives increasing toroidal term due to differential rotation below the convective zone. The stability of such toroidal fields is considered. Toroidal field is modeled by a single thin flux tube, for which action integral was formulated by Erkaev (1989) and Achterberg (1996). The equations of motion has been derived from action integral and in 1-dimensional case of axisymmetric tube in equatorial plane effective potential was derived. It is shown that such tube may have two regimes of motion: nonlinear oscillations in equatorial plane and emergence to the Sun's surface. Dependence of the regime of motion on the initial field strength in the tube has been studied.

Simulation analysis of galactic cosmic ray transport through the atmosphere

E.A. Maurechev, Yu.V. Balabin, E.V. Vashenyuk, B.B. Gvozdevsky (*Polar Geophysical Institute, Russian Academy of Sci., Apatity, Russia*)

Using the PLANETOCOSMICS simulation framework we simulated the galactic cosmic ray transport through the Earth's atmosphere and estimated energy distributions of secondaries (protons, electrons, positrons, muons, photons and neutrons) at various atmospheric levels. As the source spectrum of galactic protons at the boundary of atmosphere the spectrum according to the standard 25645.122-85 has been used. In addition as a result of simulation the histogram of energy deposited by cosmic ray showers in the atmosphere in function of altitude has been obtained.

Gamma-ray spectrometers developed for problems of radiation monitoring: comparison of simulations with experimental data

E.A. Maurechev, A.V. Germanenko, Yu.V. Balabin, E.V. Vashenyuk (*Polar Geophysical Institute, Russian Academy of Sci., Apatity, Russia*)

For the solution of the wide range of radiation monitoring problems we use scintillation detectors NaI (Tl). In the present work we have carried out simulations of scintillators of different geometry with GEANT4 toolkit to improve the accuracy of the experimental data. As a model particle source the point source with a spectrum corresponding to the ^{137}Cs and ^{241}Am has been used. In addition a gamma-ray registration efficiency in function of a scintillator thickness has been obtained. The simulation results are in good agreement with experimental data.

Modeling of ground level X-ray radiation increases during atmosphere precipitations

E.A. Maurechev, A.V. Germanenko, Yu.V. Balabin, E.V. Vashenyuk (*Polar Geophysical Institute, Russian Academy of Sci., Apatity, Russia*)

A X-ray monitoring at ground level showed systematic radiation increases during the precipitations (rain, snowfall). At present time the measurements are performed with different spectrometers registering X-rays in a range from 20 keV to 4 MeV. In this work we modeled the process of X-ray origin in the atmosphere during precipitations using simulation toolkit GEANT4. The computational model includes electric fields in nimbostratus clouds which accelerates the electrons creating the bremsstrahlung X-rays. We also modeled the responses of the scintillation gamma-spectrometers in use. Simulation results were compared with the experimental data.

MHD simulation of solar flare - determination mechanism of the phenomenon or hypothesis testing

A. I. Podgorny¹, I. M. Podgorny²

¹ *Lebedev Physical Institute RAS, Moscow, Russia, podgorny@fian.fian.su*

² *Institute for Astronomy RAS, Moscow, Russia, podgorny@inasan.ru*

Currently, the different solar flare scenarios are discussed by several authors. Among them: the destruction of the current sheet above the active region, the generation of the linear current along an arched magnetic line (a current source located below the photosphere), magnetic rope ejection that penetrate a magnetic arch, MHD instability of a magnetic rope producing the a coronal mass ejection, dissipation of the magnetic helicity ejecting from the active region, and other. Independently of the fact, which the physical mechanism is responsible for flare creation, the numerical simulation of flare phenomena should be executed under the initial and boundary conditions taken from observations of a real active region before this flare. The mechanism of occurrence of a flare should be shown by results of numerical simulation, instead of its artificially introducing in the initial or boundary conditions. The main goal of solar flare numerical simulation is finding-out of the physical mechanism responsible for energy $\sim 10^{32}$ erg accumulation over an active region before the flare. Using the measurements of the photosphere dynamics of the before a flare the 3D MHD simulation performed without introducing any assumptions about the mechanism of solar flares. It is shown that in the preflare state the current sheet appears in the corona above the active region. The energy accumulated in the current sheet magnetic field is dissipated during the flare. The main problem of such simulation is calculation of flare development in the real time.

The active region magnetic field association with solar flares

I. M. Podgorny¹, and A. I. Podgorny²

¹ *Institute for Astronomy RAS, Moscow, Russia, podgorny@inasan.ru*

² *Lebedev Physical Institute RAS, Moscow, Russia*

At the active region NOAA 11158 traveling across the solar disk the magnetic field continuous evolution takes place. The behavior of weak active regions appearing on the eastern limb of the Sun is considered, which become stronger and stronger traveling across the solar disk. When the magnetic flux of the active region reaches the critical value of $\sim 10^{22}$ Mx, the powerful (X2.2) flare is produced. The development of the active region is investigated in the preflare time and during the flare. For performance the work the HMI SDO data were used with time resolution 45 s. However, the HMI SDO measures the component of the magnetic field along the line of sight, which strongly depends on the position of the active region on the disk. To eliminate this dependence, the normal component of the magnetic field is obtained by solution of the Laplace equation with boundary conditions in the form of the oblique derivative of the magnetic potential. The comparison with the not flare productive active regions shows that the increased flux is not a sufficient condition for the occurrence of a flare. The powerful active region with the dipole distribution of the magnetic dipole type field does not produce flares. For flare appearance the magnetic field distribution in the active region should not have a regular character – the magnetic field sources must be intruded in the area of the field of the opposite sign. Only such photospheric field can form singular magnetic field lines in the corona, around which the flare productive current sheets can be formed. No strong change of magnetic field is observed during a flare. The observed weak localized change of the line-of-sight magnetic field component does not produce appreciable influence on magnetic field distribution in the active region during a flare.

The interhemispheric asymmetry of the parameters of midday recovery (MDR) effect during PCA events

V.A. Uljev¹, M.I. Tyasto², O.A. Danilova², O.I. Shumilov³

¹ *Arctic and Antarctic Research Institute (AARI, St. Petersburg) vauljev@yandex.ru*

² *St-Petersburg Filial of Institute of Terrestrial Magnetism, Ionosphere and Radiowave Propagation of RAN (SPbF IZMIRAN) marta@mt4697.spb.edu*

³ *Institute of North Industrial Ecology Problems, Kola Science Center RAS oleg@aprec.ru*

During PCA events at the stations of the auroral zone at midday, a decrease of the absorption, which is called the effect of the midday recovery (MDR), is often occurred. Parameters of MDR (amplitude and frequency of

The Sun, solar wind, cosmic rays

occurrence of this effect) at the stations of the Northern and Southern hemispheres are compared. It is established that the amplitude and frequency of occurrence of MDR are higher in the southern hemisphere than in the northern one. It is suggested that the asymmetry of MDR parameters is due to interhemispheric differences of geomagnetic cutoff rigidity and the temperature of the upper mesosphere at auroral zone. The calculations confirm this assumption.

Study of the MHD discontinuities inside the reconnection exhausts in the solar wind

J.O. Vinnikova, Yu.L. Sasunov, V.S. Semenov (*Institute of Physics, University of St-Petersburg, St-Petersburg, Russia*)

Magnetic reconnection is a fundamental plasma process, which is responsible for transformation of magnetic energy to kinetic and internal plasma energy.

Data base of J.Gosling consisting of 102 magnetic reconnection events in the solar wind simultaneously detected by ACE and Wind spacecraft over a period from 1998 to 2005 was used for our study. For every event profiles of magnetic field components, magnetic field rotation angle, velocity components, proton temperature, concentration as well as total (magnetic plus proton) pressure. Entropy is one of the most significant characteristics of dissipative processes on slow shock waves and therefore it was investigated in details. The analysis of ACE and Wind data show

Entropy increase is observed in 72 reconnection events (50 events of magnetic reconnection were detected by Wind spacecraft and 22 by ACE). Consequently, there is a process of plasma heating and accelerating on slow shock waves during the switch on phase of magnetic reconnection, which is in agreement with Petschek type reconnection model.

It was determined that an angle between discontinuities bounded the exhaust regions varies from 6^0 to 23^0 , which corresponds to the reconnection rate $0.1 - 0.4$.

Electron temperature is nearly constant inside the exhaust region in contrast to the proton temperature which noticeably increases, which means that protons are heated at the slow shocks whereas electrons do not.

The separation of Alfvén discontinuity and slow shock wave was detected by Wind only once on 1998 – 03 – 25 according. For the rest of 101 events Alfvén discontinuity features (field rotation) happen simultaneously with slow shock wave features (increase of temperature, concentration and entropy and magnetic field intensity decrease). This means that the exhaust region is bounded not only by Alfvénic and slow mode waves but also, to a large extent, by tangential discontinuities.

Impulses of sunspot activity and surges of magnetic field to the solar poles

N.V. Zolotova, D.I. Ponyavin (*St-Petersburg State University, St-Petersburg, Russia*)

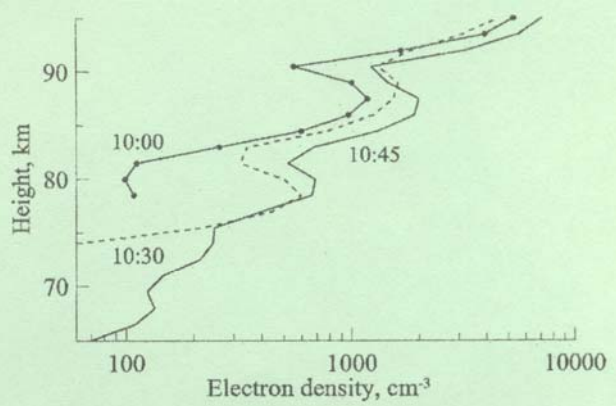
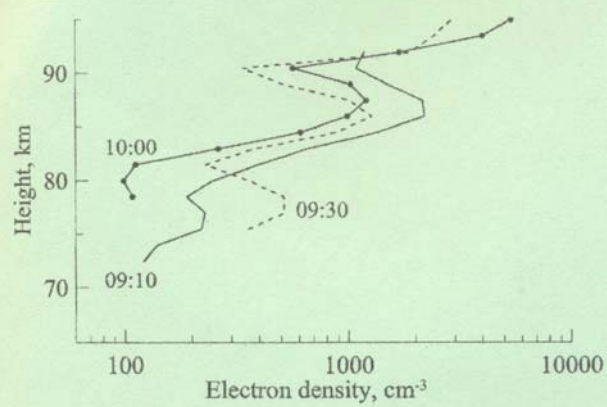
The time-latitude diagram of the photospheric magnetic field of the Sun during 1975-2011 (Kitt Peak NSO, SOLIS NSO, SOHO MDI data) is analyzed using Gnevyshev idea on impulsive structure of sunspot cycle and a flux transport concept. We perform reconstruction of magnetic field surges from sunspot impulses without diffusion assignment. Using the meridional flow and latitudinal segregation between the leading and trailing sunspot distributions, it was shown that each sunspot impulse produces a poleward wave of new (trailing) polarity of unbalanced magnetic flux. Old (leading) polarities do not annihilate across the equator, but are also transported to the poles.

Применение теории распознавания образов для решения задачи отбора требуемых событий в базах данных мировой сети нейтронных мониторов и результатов измерений параметров межпланетной среды на космических аппаратах

В.В. Пчелкин (*Полярный геофизический институт КНЦ РАН*)

В работе рассматривается проблема автоматизации поиска в данных мировой сети нейтронных мониторов и в спутниковых данных событий, удовлетворяющих заданным требованиям. Предлагаются и обсуждаются дескрипторы, позволяющие количественно описывать принципиальные особенности требуемых фрагментов экспериментальных рядов. Разработанные алгоритмы применены для решения задач автоматизированного отбора солнечных протонных событий и Форбуш - понижений различных типов.

Ionosphere and Upper Atmosphere



The display of heliogeophysical disturbance in midlatitude ionospheric activity index (IAI)

O.M. Barkhatova^{1,2}, I.A. Dodonova¹, N.V. Kosolapova²

¹ *Nizhniy Novgorod State University of Architecture and Civil Engineering, Nizhniy Novgorod, Russia*

² *Nizhniy Novgorod State Pedagogical University, Nizhniy Novgorod, Russia*

The estimation of influence degree of the Solar-Magnetospheric parameters for the ionospheric activity index IAI [Barkhatova et al., 2011] computed at the station Moscow (55° N, 37° E) for 1986 was carried out. Such the parameters were considered: the intensity of the auroral electrojets (index AE), geomagnetic field horizontal component and intensity of long-wavelength X-ray (1-8 Å) [Barkhatova et al., 2009]. To establish the relationship of considered parameter with index IAI, the original values of all these parameters have been also indexed. In order to eliminate the effect of regular events on the sought relationship index IAI has been preliminary cleaned. Any long-period variation, diurnal variation, the 27-day cycle, as well as the phenomena associated with the terminator passage were removed.

The influence observed Solar-Magnetospheric parameters on index IAI variation was revealed due to comparing the index IAI values to each of parameters. The estimation of contribution degree of each parameter to the index was executed. The results showed that the contribution degree of auroral disturbances in the IAI index gives a value of about 10%. The value of geomagnetic disturbance contribution to IAI is about 20%. The contribution degree of the long-wavelength X-rays to the IAI index is about 10%. Thus, the total contribution of auroral disturbances, geomagnetic disturbances and disturbances caused by long-wavelength X-ray emission effect to ionospheric disturbance is about 40%.

Obtained result was used to recover the value of IAI index by the method of artificial neural networks. The best result was achieved using a feed forward neural network. Input feed of each of additional parameters increases the recovery efficiency on average at 6-7%. The maximum efficiency of 75% achieved by using such parameters combinations: the geomagnetic field horizontal component plus index AE or geomagnetic field horizontal component plus long-wavelength X-rays intensity.

Application of nonlinear dynamics methods to study the auroral region

A.A. Chernyshov¹, M.M. Mogilevsky¹, B.V. Kozelov²

¹ *Space Research Institute of the Russian Academy of Science, Moscow, Russia*

² *Polar Geophysical Institute of the Russian Academy of Science, Apatity, Russia*

Most of the processes taking place in the auroral region of Earth's magnetosphere are reflected in a variety of dynamic forms of the aurora borealis. In order to study these processes it is necessary to consider temporary and spatial variations of the characteristics of the auroral zone. Most traditional methods of classical physics are applicable mainly for stationary or quasi-stationary phenomena, but dynamic regimes, transients, fluctuations, self-similar scaling could be considered using the methods of nonlinear dynamics. Therefore, development of methods for studies of characteristics of nonlinear processes in open dissipative systems is now actual problem, in particular, to study the auroral region of Earth's magnetosphere. Special interest is the development of the methods for describing the spatial structure and the temporal dynamics of the auroral zone based on the ideas of percolation theory and fractal geometry. The fractal characteristics (the Hausdorff fractal dimension and the index of connectivity) of Hall and Pedersen conductivities are used to the description of fractal patterns in the ionosphere. To obtain the self-consistent estimates of the parameters the Hausdorff fractal dimension and the index of connectivity in the auroral zone, an additional relation describing universal behavior of the fractal geometry of percolation at the critical threshold is applied.

Diurnal dynamics of the broadband spectral maximum in the ULF background noise.

E.N. Ermakova¹, A.V. Pershin¹, T. Bosinger², Q. Zhou³

¹ Radiophysical Research Institute, Nizhnii Novgorod, Russia

² Department of Physical Sciences, University of Oulu, Oulu, Finland

³ Electrical and Computer Engineering Department, Miami University, Oxford, Ohio, USA

The diurnal dynamics of a broadband spectral maximum (BSM) in the background magnetic noise at frequencies between two and seven Hz is investigated. In previous studies the diurnal behavior of BSM at mid latitudes was described as a shift of the central frequency towards higher frequencies from sunset towards local midnight accompanied with a gradual broadening of the maximum [Belyaev et al., 2002; Ermakova et al., 2007]; the BSM is an entire nighttime phenomenon. At low latitudes (Crete) the phenomenon is more of a sporadic nature and manifests itself as quasi-periodic oscillations in the polarization parameter epsilon (degree of polarization in the background noise) rather than a spectral maximum [Bösinger et al., 2009]. Here we give some more details in the nighttime behavior of BSM for the past two years of rising solar activity in 2009-2011. A more sporadic nature of BSM became evident now also for the mid latitude observation at "New Life" (56 N, 46 E). We focused particular the frequency at which the polarization parameter epsilon changes sign from negative to positive values (right-handed to left-handed circular polarization). Analyses of ionosonde data showed that such changes in the nighttime behavior can be linked to variations of foF2. This is in accord with the conjecture that the lower boundary of the F layer forms the upper boundary of the sub-IAR cavity. A sporadic jump of the central frequency of BSM to lower values often around local midnight was also noticed. It was not accompanied with a change in foF2. Thus it may indicate a redistribution of the electron density in the E layer Valley (hinting some connection to sporadic E formation). Based on observations in "New Life" we examined also the occurrence rate of BSM on season and solar activity.

Numerical calculations using IRI-2007 for the polarization parameter of the magnetic field components cannot explain such sporadic changes of the BSM central frequency. We had also the possibility to use actual measured electron density height profiles obtained from Arecibo. The calculated spectra confirm the sporadic occurrence of BSM at these low latitudes; their appearance sometimes coincided with the formation of an Es - layer around 100 km. Using Arecibo data we did also some efforts to access the occurrence rate of BSM at periods of solar activity minimum and maximum.

A new multichannel analog-to-digital converter synchronizing data with GPS clock

M.V. Filatov, S.V. Pilgaev, A.V. Larchenko and Yu.V. Fedorenko (Polar Geophysical Institute, Apatity, Russia)

At present, an obsolete data acquisition system is used in a network of geophysical stations of the Polar Geophysical Institute, Kola Research Center, Russian Academy of Sciences, to investigate geophysical signals in a frequency band from hundredths portions up to 200 Hz. The system contains a recorder, 22-bit analog-to-digital converter (ADC), and synchronizer, which ensures an accuracy of synchronizing to the real-time clock (UTC) with a root-mean-square error of no more than 1 μ . The drawbacks of the ADC of this system are the nonlinearity of the amplitude-frequency response (AFR), absence of an antialias filter, and a low conversion frequency. A new unit was designed to extend the input signal frequency range to 16 kHz, increase the ADC bit capacity to 24, and obtain the linear AFR. Depending on the target system can be equipped with up to eight channels of analog input. The data exchange with a recorder is carried out via the Ethernet interface.

The calculation of rate coefficients for the interaction of vibrationally excited singlet and triplet molecular oxygen in the active medium of chemical oxygen-iodine laser

A.S. Kirillov (Polar Geophysical Institute, RAS, Apatity, Murmansk region, Russia)

Singlet (electronically excited $a^1\Delta_g$ and $b^1\Sigma_g^+$ states) and triplet (ground $X^3\Sigma_g^-$ state) oxygen molecules play an important role in radiational balance of auroral ionosphere, in the emitting of Atmospheric and Infrared Atmospheric band at the altitudes of the nightglow, in chemical kinetics of the O₂-I₂-I mixture in the active medium of chemical oxygen-iodine laser (COIL). Using available in scientific literature experimental data on values of quenching rate coefficients of O₂($b^1\Sigma_g^+$, $v=1-3$) by molecular oxygen at different temperatures we estimate parameters for analytic formulas allowing calculate quenching constants of singlet oxygen. The calculated quenching constants for O₂($b^1\Sigma_g^+$, $v=1-15$) and O₂($a^1\Delta_g$, $v=1-20$) by unexcited oxygen molecule at temperatures $T=300$ and 155 K show good

agreement with experimental data. Main channels of $O_2(a^1\Delta_g, v=0-20)$ and $O_2(b^1\Sigma_g^+, v=0-15)$ quenching by vibrationally excited oxygen molecule $O_2(X^3\Sigma_g^-, v=1-4)$ are investigated. The calculated coefficients can be applied in a modeling of vibrational populations of singlet and triplet oxygen molecules in the active medium of COIL.

The study of the influence of intermolecular electron energy transfer processes on vibrational populations of $N_2(a^1\Pi_g)$ and $N_2(A^3\Sigma_u^+)$ molecules in the mixture of N_2 and O_2 molecules

A.S. Kirillov (*Polar Geophysical Institute, RAS, Apatity, Murmansk region, Russia*)

Total quenching rate coefficients of three singlet and three triplet states of molecular nitrogen in the collisions with O_2 molecules are calculated on the basis of quantum-chemical approximations. The calculated rate coefficients of electronic quenching of N_2^* molecules are compared with available experimental data. An influence of collisional processes on vibrational populations of electronically excited $N_2(a^1\Pi_g)$ and $N_2(A^3\Sigma_u^+)$ molecules is studied for conditions of laboratory discharge in N_2 and O_2 at admixtures of molecular oxygen 0–20% for the pressures 1–1000 Pa. It is indicated that molecular collisions cause changes in relative populations of vibrational levels of these states and intensity relations of ultraviolet bands of N_2 with the rise in the pressure and O_2 admixture.

High- and mid-latitude ionospheric disturbances during geomagnetic storms

M.V. Klimenko, V.V. Klimenko (*West Department of Pushkov IZMIRAN RAS, Kaliningrad, Russia, e-mail: maksim.klimenko@mail.ru*)

In this study, we use the modified GSM TIP model to explore how the thermosphere–ionosphere system responded to the two geomagnetic storm events. Comparison of modeling results with experimental data at different high- and mid-latitude stations has shown a good agreement of ionospheric disturbances. We examine in detail the formation mechanisms of these disturbances and describe some of the important physical processes affecting the behavior of the F -region. Above high- and mid-latitude stations during storm-time, we clearly see the G condition, when $F2$ -layer critical frequency becomes smaller than $F1$ -layer critical frequency (sometimes even $F2$ -layer maximum disappears) and $F1$ -layer becomes the main maximum of ionospheric F -region. In addition the molecular ion density during storm-time becomes particularly significant. The F -layer maximum height can increase up to 500 km during storm-time due to the formation of maximum in molecular ions at this height because of non-uniform in height ionization processes near solar terminator. We also considered the propagation of thermospheric wind surge forming during geomagnetic storms.

Various magnetospheric inputs to the GSM TIP model for investigation of ionospheric response to geomagnetic storm events on May 2010

V.V. Klimenko¹, M.V. Klimenko¹, V.G. Vorobjev², O.I. Yagodkina²

¹ *West Department of Pushkov IZMIRAN RAS, Kaliningrad, Russia, e-mail: vvk_48@mail.ru*

² *Polar Geophysical Institute KSC RAS, Apatity, Russia*

Recent modifications to the Global Self-Consistent Model of the Thermosphere, Ionosphere and Protonosphere (GSM TIP) include adding the empirical model for high-energy electron precipitation and introducing a high-resolution (1-min) calculation of cross-polar cap potential and region 2 field aligned currents (R2 FAC). We take into account the 30 min time delay of R2 FAC variations with respect to the variations of cross-polar cap potential. These modifications resulted in better representation of such effects as prompt penetration of magnetospheric convection electric field to the lower latitudes and overshielding. This study presents the GSM TIP numerical simulations of the ionospheric response to the two geomagnetic storm events on May 2010. We try to investigate the problem of the model input parameters setting at the simulations of geomagnetic storms. In numerical experiments such model input parameters as cross-polar cap potential and R2 FAC were set as function of different indices of geomagnetic activity, Solar wind parameters and Interplanetary Magnetic Field. Current simulation uses two different empirical models for high-energy particle precipitation – the model by Zhang and Paxton developed in Johns Hopkins University Applied Physics Laboratory, Laurel, USA and Auroral Precipitation model developed in Polar Geophysical Institute, Apatity, Russia. Our results shows a difference between both these two models of particle precipitation and between the ionospheric effects of geomagnetic storm events on May 2010 obtained with their use in the model GSM TIP.

Background ionization calculation in the auroral ionospheric model

S.K. Kondratiev^{1,2}, V.D. Nikolaeva^{1,3}, L.N. Makarova¹, A.V. Shirochkov¹, V.N. Morozov²

¹ *Arctic and Antarctic Research Institute (AARI), St. Petersburg, Russia*

² *Main Geophysical Observatory (MGO), St. Petersburg, Russia*

³ *Saint-Petersburg University (SPbU), St. Petersburg, Russia*

The auroral ionospheric model is currently developed in AARI, including all basic processes responsible for ionosphere formation. Main attention should be paid to the description of auroral particles precipitation processes. The correct description of the background ionization, including solar radiation ionization and ion generation and dissipation in chemical reactions should be the first and the basic step in such model developing. Ionization function calculation was made taking into account the photon flux density dependence on $F_{10.7}$ index and solar activity cycle position. In addition to ionization functions, background ionization block includes more than 70 chemical ion generation and dissipation equations. Neutral NO concentration is time-dependent and is also calculated using these equations. Other neutral components concentrations are obtained by NRLMSISE00 model. Calculation results were compared with data obtained by Tromso ionosonde in quiet conditions, depending on solar activity cycle position, for different months and different time of day.

Modeling of the thermosphere-ionosphere system response to the high-latitude Sudden Stratospheric Warming events

Yu.N. Korenkov, M.V. Klimenko, V.V. Klimenko, F.S. Bessarab, I.V. Karpov (*West Department of Pushkov Institute of Terrestrial Magnetism, Ionosphere and Radio Wave Propagation RAS, Pobedy Av., 41, Kaliningrad, 236017, Russia*)

This report presents an investigation of thermospheric and ionospheric response to the sudden stratospheric warming (SSW) events, which took place in January 2008 and 2009. These periods were characterized by low solar and geomagnetic activity. Analysis was carried out within the Global Self-consistent Model of Thermosphere, Ionosphere and Protonosphere (GSM TIP). SSW events were modeled by specifying the temperature and density perturbations at the lower boundary of the GSM TIP model (80 km altitude). It was shown that when specifying disturbances in the form of a stationary planetary perturbation $s = 1$ at the lower boundary of the thermosphere, one could reproduce the negative electron density disturbances in the F region of ionosphere during SSW events. The analysis of observation data showed that the neutral temperature perturbations in the mesosphere and lower thermosphere region during 2009 and 2008 SSW events was quite different, although the helio-geophysical conditions during these periods were similar. Our scenario for the 2008 and 2009 SSW event in the GSM TIP allowed to obtain results which are in a satisfactory agreement with the observation data.

On triangulation by auroral cameras

B.V. Kozelov, S.V. Pilgaev, L.P. Borovkov, V.E. Yurov (*Polar Geophysical Institute, Apatity, Murmansk region, 184209 Russia*)

The data of the MAIN (Multiscale Aurora Imaging Network) auroral cameras located in Apatity and all-sky camera in Lovozero observatory have been used to triangulate auroral structures. Two pairs of cameras were employed i) narrow (18°) field-of-view cameras with ~ 4 km distance between them and ii) two all-sky cameras which were ~ 86 km spaced. Triangulation abilities and discrepancies are tested by events of satellite flashes and meteor tracks. The results are compared with previous results and theoretical estimations.

Calibration of an induction magnetometer and a vertical electric field antenna

A.V. Larchenko, O.M. Lebed, R. Zubov, M. Shkarbalyuk, M. Filatov and Yu.V. Fedorenko (*Polar Geophysical Institute, Apatity, Russia*)

Observations of natural and artificial electromagnetic fields in ELF frequency range typically aim to acquire spectral and temporal behavior of field components. To evaluate power spectra, amplitudes and phases one have to know transfer function of a data acquisition system. Although this transfer function may be theoretically calculated from sensor parameters and sensor preamplifier circuitry, a common practice is to obtain it by calibration procedure. The main difficulties arise from the fact that it is not possible to screen the sensor under calibration from external electromagnetic noise. It places a limit to calibration accuracy, especially at lower frequencies below 1-2 Hz where geomagnetic pulsations sometimes are so strong that make calibration if not impossible but unacceptably long to reach desired accuracy by averaging. In the frequency range 50-300 Hz most of interference comes from impulsive electromagnetic signals (atmospherics) produced by thunderstorms around the World.

In this work, we present a calibration procedure used in PGI to evaluate transfer functions of data acquisition system that comprises three-component induction magnetometer and vertical electric field antenna. Sinusoidal signal from oscillator is applied to calibration coil via resistor thus generating calibrating magnetic field with amplitude given while the same signal goes to vertical electric field antenna through small capacitor creating a calibrating signal with arbitrary amplitude but a phase coinciding with calibration magnetic field phase. Voltage of oscillator output is measured by the same AD converter. Atmospherics impulsive noise in the frequency range 50-300 Hz is suppressed by median filter. In contrast to conventional method which includes estimation of amplitudes and phases at number of frequencies considering them as an independent samples we make use of an a-priory information that the transfer function of any sensor with preamplifier is a rational function of $j\omega$. Transfer function may be expressed in terms of several zeros and poles of rational function. We calculate zeros and poles using numerical optimization, and weight of each sample is not the same because noise influence is altered with frequency. Our method has better accuracy against conventional one and more convenient in use because it utilizes a-priory information of the transfer function form and expresses it in a small number of poles and zeros.

Velocity of atmospherics along Lovozero – Barentsburg propagation path

O.M. Lebed, S.V. Pilgaev, Yu.V. Fedorenko (*Polar Geophysical Institute KSC RAS, Apatity, Russia*)

It is a well-established fact that electromagnetic field structure and group velocity of impulsive signals (atmospherics) propagating in Earth-ionosphere waveguide depend on ionosphere profile. Propagation models predict different values of local group velocities defined by day and night ionosphere while Schumann resonance frequencies represent mean velocity. A comparison of measured local velocity obtained from time delay between atmospheric's arrivals to stations separated by about thousand kilometers and averaged velocity acquired from Schumann resonance may help to verify propagation model and assess influence of ionosphere profile to group velocity. We investigate group velocities of atmospherics using their arrival time to Lovozero (68°00'N, 35°03'E) and Barentsburg (78°04'N 14°13'E) along about 1200 km propagation path and compare them to simultaneously measured mean velocities acquired from Schumann resonance frequencies. In this study, we present velocity, and source azimuth estimation approaches including calibration of equipment and power line noise suppression method and preliminary results of atmospheric velocity comparisons during December 2011 – January 2012.

Ionospheric TEC variations before three recent strong earthquakes: A comparative study

A.A. Namgaladze¹, O.V. Zolotov¹, B.E. Prokhorov^{2,3}

¹ Murmansk State Technical University, 183010 Murmansk, Russia

² Helmholtz Centre Potsdam, GFZ German Research Centre for Geosciences, Telegrafenberg, 14473 Potsdam, Germany

³ University Potsdam, Applied Mathematics, Interdisciplinary Center for Dynamics of Complex Systems (DYCOS), 14476 Potsdam, Germany

Relative ionospheric TEC (Total Electron Content) disturbances obtained from the GPS satellite data during March 8-11, 2011 and Oct. 20-23, 2011 (see <http://goo.gl/zRW9H>) periods were investigated for Japan M9.0, March 11, 2011 and Turkey Van M7.1, Oct. 23, 2011 earthquakes, respectively, and they were compared with the results of our earlier investigations for the Haiti Jan. 12, 2010 EQ. The effects that could be considered as possible earthquake

Ionosphere and upper atmosphere

precursors for all three events were revealed.

All three cases had persistent features: living (lasting ~6-8 hrs.) relative TEC disturbances (30-60% background values) near the epicenter and magnetically conjugated areas ($\sim 15^\circ \times \sim 30^\circ$ via latitude \times longitude) affected by the terminator and subsolar point (they disappeared at the near-midday time).

We investigated as well how the results depend on the quiet background TEC choice. The quiet background values were calculated as centered medians using from 3 to 27 days grouped by UT moments. It was shown that sliding window width (SWW, see <http://goo.gl/hllIV>) increase generally led to disturbances' magnitude increase but the isolines' form being kept rather stable.

We discuss these TEC anomalies in terms of the electromagnetic lithosphere-ionosphere coupling mechanism and interpret the disturbances as a result of the seismically induced electromagnetic [E \times B] drift of the ionospheric F2-layer plasma.

Study of fine structure of ionospheric current with the conjugate DMSP and EISCAT measurements

V.D. Nikolaeva^{1,2}, A.L. Kotikov^{2,3}, T.I. Sergienko⁴, S.K. Kondratiev^{1,5}

¹ *Arctic and Antarctic Research Institute (AARI)*

² *Saint-Petersburg University (SPbU)*

³ *SPbF IZMIRAN*

⁴ *Swedish Institute of Space Physics (IRF)*

⁵ *A.I. Voeikov Main Geophysical Observatory (MGO)*

The purpose of this paper is to compare the results ionospheric conductivity calculations based on measurements of fluxes of precipitating electrons measured on DMSP satellites and direct measurements of electron density from incoherent scatter EISCAT radar.

To calculate the conductivity in real ionosphere conditions it is necessary to know the composition of the neutral atmosphere, ion, neutral and electron temperatures, and the concentration of ions and electrons. The parameters of the neutral atmosphere were obtained from NRLMSISE-00 model.

Electron concentration can be calculated from satellite DMSP data, measuring the flow of electrons precipitation in various parts of the energy spectrum along the satellite trajectory.

Also, for conductivity calculations we used radar EISCAT data (Tromso), working in CP3 program (sounding not only with the height, but also by latitude).

4 cases of synchronous operations of the radar EISCAT CP3 program and the satellite DMSP-13 and DMSP-14 over the auroral oval (from 6 to 8 December 2004) were selected.

Based on the analysis of ionospheric conductivities obtained in two different ways it become possible to restore the real distribution of the ionosphere and the field-aligned currents for the different phases of a substorm.

Absorption of high frequency waves in a heated ionosphere region

A.B. Pashin, A.A. Mochalov (*Polar Geophysical Institute, Apatity, Russia*)

Numerical modeling has been used for study of absorption of high frequency waves in ionosphere modified by powerful ground-based HF transmitter. The ionosphere electron heating is accompanied by a growth of the HF wave absorption in lower ionosphere. The additional absorption is great enough to be measured, and it is possible to use the absorption for diagnostics of disturbed parameters of the ionosphere. Increasing of the diagnostic HF wave frequency leads to absorption decreasing, so optimal frequencies belong to a range from 30 to 40 MHz. These frequencies are usually used for cosmic noise absorption observations. Increasing of the diagnostic wave frequency requires high stability of the wave power. This makes cosmic radio noise useless for the diagnostics. Manmade source of the HF diagnostic wave is needed for this purpose.

The event of riometer absorption on 5 May 2011 may be caused by auroral protons?

V.C. Roldugin and M.E. Shkarbalyuk (*Polar Geophysical Institute, Apatity, Russia*)

There are regular riometer observations in Lovozero ($\Phi=64.4^\circ$, $\Lambda=114.3^\circ$) with 30 MHz frequency. The event of 5 May 2011 is considered. During small positive bay about of 40 nT in Lovozero and close Scandinavian stations in evening time between 1630 and 1700 UT an absorption of cosmic noise about of 1.5 db occurred. A west auroral electrojet may be situated this time at more high latitude, and the small positive bay can not be caused by its spreading currents. During this absorption time $Pc1$ and $Pc5$ pulsations took place in Lovozero and in Scandinavia. We hypothesize on the base of these facts that this riometer absorption was induced by energetic proton precipitation.

Is the F2-layer Summer Nighttime Anomaly Midlatitudinal or Subauroral: an investigation by means of global numerical modeling

Yu.V. Romanovskaya, A.A. Namgaladze (*Murmansk State Technical University, Murmansk, Russia*, y-romanovskaya@yandex.ru)

Midlatitude Summer Nighttime Anomaly (MSNA) is an inverted diurnal variation of the F2-layer electron density with maximal values at midnight hours and minimal values at day ones. The anomaly was detected both in the Southern and Northern Hemispheres under undisturbed summer solstice conditions. The most well-known sample of the MSNA is the Weddell Sea Anomaly in the Antarctic region with the maximal effect from 255° to 315° in geodetic longitude and from 60°S to 70°S in geodetic latitude. In the Northern Hemisphere the inverted electron density variations are observed at the meridians of 120 - 140° in longitude and from 40°N to 60°N in latitude. We investigate physical mechanism of the MSNA using the global 3D numerical Upper Atmosphere Model and the empirical IRI model. The relative roles of the thermospheric winds, plasmaspheric fluxes, magnetospheric convection and energetic electron precipitations are considered. The calculation results are compared with ionosonde data in order to obtain both qualitative and quantitative agreement with them. We conclude that MSNA is rather subauroral than midlatitude F2-layer anomaly or at least both midlatitudinal and subauroral physical processes participate in its forming.

Ionospheric fluctuations over high latitude using Greenland GPS network and aurora

I. Shagimuratov¹, S. Chernouss², Y. Cherniak¹, I. Ephishov¹

¹ *IZMIRAN, Kaliningrad, Russia*

² *PGI KSC RAS, Apatity, Russia*

Comparison of the oval of TEC fluctuation activity with the auroral oval was done. GPS measurements of Greenland network were used to study the occurrence of TEC fluctuations at the northern high latitude ionosphere during period of solar minimum activity. GPS stations with geomagnetic coordinates higher than 55°N and different longitudes were involved in this investigation. Dual-frequency GPS measurements for individual satellite passes served as raw data. Standard GPS observations with 30 sec sampling interval provide information about occurrence of middle- and large-scale ionospheric irregularities. As a measure of fluctuation activity the rate of TEC (ROT) was used and fluctuation intensity was evaluated by using ROTI index calculated with 10 min resolution. In the report occurrence GPS TEC fluctuations occurrence over Greenland during January- December 2007 are discussed. The statistic of number and intensity TEC fluctuations over polar ionosphere for quiet and disturbed geophysical conditions are presented. During a storm the intensity of TEC fluctuations essentially increased at subauroral, auroral ionosphere and polar cap. Maximal intensity may observed during moderate conditions in polar cap and cusp regions. Using the daily GPS measurements from stations, located over 60 - 87°CGL near the images of spatial and temporal behavior of TEC fluctuations were formed (in Corrected Geomagnetic Coordinates - CGC and geomagnetic local time - GLT). Similarly to the auroral oval, these images demonstrate the irregularity oval. The occurrence of the irregularity oval relates with auroral oval, cusp and polar cap. It was revealed that for quiet conditions location of the equatorward edge of the irregularity oval at magnetic midnight was 65 - 68°CGL , for day-side – higher than 70°CGL . The irregularity oval expands equatorward with increase of the magnetic activity. Taking account permanent increasing number GPS stations in Greenland may more detaille picture irregularity oval obtain. From the point of view we will show structure and dynamics oval also for September 2011 during high activity. The study showed that the operating high-latitudes GPS stations can provide a permanent monitoring tool

Ionosphere and upper atmosphere

for the irregularity oval in near real-time. The results demonstrated that dynamics and structure of irregularity ovals and auroral ovals well are matched.

Schumann resonance in the vertical magnetic field observed near geological faults

E.D. Tereshchenko, A.E. Sidorenko (*Polar Geophysical Institute, Murmansk, Russia*)

Measurements of extremely low frequency (ELF) magnetic background noise have been taken along the 30 km length line crossing the geological fault. Schumann resonance effect was observed in both horizontal and vertical field. The power spectral density of vertical component H_z within the frequency range 0-30 Hz was significantly increased close to the fault line. In such area vertical magnetic field of Schumann resonance was higher than horizontal one. At the fault nearest point four Schumann resonances in H_z were distinctly observed but only one first resonance was observed at other points with the same signal processing parameters. Thus the typical transverse electromagnetic field polarization in ELF range violates near geological faults. In particular, relatively high vertical magnetic field strength is a consequence of electrical currents excitation inside an extended circuit of the geological faults having raised conductivity. These currents excited by the natural electromagnetic ELF wave penetrated the Earth's crust from the Earth-ionosphere cavity. The considered anomalous increasing of vertical magnetic field can be used to locate the conducting Earth's crust faults and in Schumann resonance research as well.

An underwater explosion and its acoustic effects on the D region of the polar ionosphere

V.D. Tereshchenko, S.M. Cherniakov, V.A. Tereshchenko, O.F. Ogloblina

Polar Geophysical Institute KSC RAS, Murmansk, 183010
E-mail: vladter@pgi.ru

Results of experimental researches of acoustic influence of the underwater explosion equivalent to 3-7 tons of trinitrotoluene on the polar lower ionosphere by the method of partial reflections of radio waves are submitted. It was shown, that passage of an air-blast wave caused quasi-periodic disturbances of total electron content in the D region of the ionosphere with the periods of infrasonic (2-4 minutes) and internal gravity waves (6, 8 and 16 minutes). Duration of observable disturbances was about 20 minutes; the phase speed of registered waves was close to the speed of sound in the lower ionosphere.

Experimental researches of wave disturbances in the polar lower ionosphere during the partial solar eclipse on 1 June 2011

V.D. Tereshchenko, V.A. Tereshchenko, S.M. Cherniakov, O.F. Ogloblina

Polar Geophysical Institute KSC RAS, Murmansk, 183010
E-mail: vladter@pgi.ru

Ionospheric effects of a partial solar eclipse in conditions of a polar day under large zenith angles were investigated by the methods of partial reflections and riometric absorption. Synchronous reduction of electron concentration in 3-4 times at the heights of 85-90 km and increase of virtual heights of the reflecting layer approximately by 10 km were shown. The feature of the parameters was presence of wave variations with the periods of 13-20 minutes. It made difficulties for more exact definition of these parameters because of absorption had sharp changes at that period.

Despite of the large zenith angles of the Sun ($\chi = 88^\circ$ at the place of observation and $\chi = 78-80^\circ$ at the heights of 70-120 km), effects of the eclipse were showed at all heights in the lower ionosphere and also in the magnetic field of the Earth. It was marked, that observable fluctuations of ionospheric parameters arose because of influence of the internal gravity waves generated by imbalance of heat at the shaded part of the atmosphere and supersonic movement of the lunar shadow.

Characteristics of the anomalous heat structures within dusty auroral dynamo layer

E.E. Timofeev¹, S.L. Shalimov^{2,3}, O.G. Chkhetiani³, M.K. Vallinkoski⁴, J. Kangas⁴

¹ *Admiral Makarov State Maritime Academy, St-Peterburg, Russia*

² *Institute of Physics of the Earth, Russian Academy of Sciences, Moscow, Russia*

³ *Space Research Institute, Russian Academy of Sciences, Moscow, Russia*

⁴ *Space Physics Department of the University of Oulu, Oulu, Finland*

In the present paper we analyze spatial and temporal variations of the ion (T_i) and electron (T_e) temperatures measured by the EISCAT facility within the dark dynamo layer over Tromsø during two auroral substorms: March 15 and 23, 1988. High-frequency fluctuations of the temperatures are smoothed by sliding average method. Smoothed temperatures are studied as functions of the ionospheric electric field strength (E) and electron density(N_e). It is found that: 1) On time scales from 7 to 15 minutes, the temperature of ions and electrons vary in antiphase: Ion heating is accompanied by cooling of the electrons. 2) The time scales of about 30 to 45 minutes revealed wavy anti-phase variations of T_e and N_e . 3). The value of the temperature anomaly ($T_i - T_e$) increases with decreasing strength of the E -field and the increase in electron density at the maximum reaching of about 120 K. The scale of the electron cooling, on average, about twice the size of ion heating. 4) For the values of the E -field above the threshold of the FB-instability of and low N_e -level the temperature anomaly is replaced by classical picture of overheating of the electrons ($T_e - T_i = \sim 50$ K), typical of dust-free plasma dynamo layer. The experimental results are compared with models of spatial patterns of dusty plasma, corresponding to a typical scale of wind and gravity waves.

Numerical study of atmospherics EM field structure near day-night transition

R.A. Zubov, O.M. Lebed, Yu.V. Fedorenko (*Polar Geophysical Institute KSC RAS, Apatity, Russia*)

The electromagnetic field structure of impulsive signals (atmospherics) propagating in Earth-ionosphere waveguide depends on conductivity profile and can be used to detect its inhomogeneities. The E_z/H ratio is one of the interesting parameters of this structure. Data from Lovozerovo station shows diurnal variations of this quantity that cannot be explained using classical mode theory of wave propagation. In this work we develop 3d numerical code that model EM field of atmospherics in arbitrary isotropic media at local distances. This model gives qualitative agreement with experimental data. It also predicts considerable growth of H_z component under strong ionosphere inhomogeneities, in the first place under transition region between day and night.

Моделирование взаимосвязи нижней и верхней атмосферы

К.Е. Белоушко (*Мурманск, МГТУ, кафедра физики, beloushko@mail.ru*)

Рассматривается проблема создания единой численной модели атмосферы Земли. Проанализированы существующие модели верхней и нижней атмосферы и осуществлён выбор конкретных моделей для дальнейшего использования в качестве частей будущей метамодели атмосферы Земли, предлагается общий алгоритм объединения этих моделей посредством обмена граничными условиями.

Исследуются такие вопросы, как сезонная и суточная изменчивость в ионосфере и термосфере, управляемая метеорологическими процессами; отклик экваториальной ионосферы на внезапные разогревы в зимней полярной стратосфере; температурная инверсия в мезосфере.

Представлены результаты некоторых совместных расчётов на основе модели верхней атмосферы UAM и модели общей циркуляции ИВМ РАН.

Исследование вариаций собственных частот ионосферного альвеновского резонатора на средних широтах

Е.Н. Ермакова, С.В. Поляков, А.В. Першин (*Научно-исследовательский радиофизический институт, Н. Новгород, Россия*)

Известно, что собственные частоты ионосферного альвеновского резонатора (ИАР) определяются показателем преломления альвеновских волн на высотах максимума F-слоя, а, следовательно, зависят от величины электронной концентрации на этих высотах. При вариациях концентрации, обусловленной наличием ионосферных возмущений и ВГВ, возможны вариации гармоник традиционной РСС с теми же временными периодами.

На основе построения и анализа суточных спектрограмм магнитных компонент фонового шума С-Ю & В-З, измеренных на среднеширотном пункте “Новая Жизнь” (Нижегородская область, Россия), обнаружены периоды с регистрацией крупномасштабных вариаций (от 2 до 6 часов) основных частотных гармоник традиционной резонансной структуры. Наиболее сильные вариации были зарегистрированы около полуночи в декабре 2009-2010 гг. Абсолютная глубина вариации увеличивалась с ростом номера гармоники и могла достигать 0.5-1.5 Гц. Изменения собственных частот ИАР связаны, по-видимому, с наличием крупномасштабных волновых возмущений в ионосфере. Был проведен анализ одновременных с регистрацией вариаций собственных частот ИАР записей ионозонда на ближайшей к приемным низкочастотным пунктам станции и анализ суточного хода f0F2. Обнаружены вариации электронной концентрации на высотах максимума F- слоя, совпадающие по времени с вариациями, обнаруженными в гармониках РСС. По абсолютным величинам вариации гармоник были сделаны оценки относительных изменений электронной концентрации в F –слое. Полученные значения изменений концентрации, как правило, соответствовали данным ионозондовых наблюдений. При анализе вариаций собственных частот ИАР по измерениям в двух разнесенных пунктах (“Новая Жизнь” и “Старая Пустынь” – расположены на расстоянии 135 км от первого) обнаружена разница в величине амплитуды вариаций основных гармоник.

Наблюдаемые «резонансные» структуры и спектры ИАР

А.Ю. Щекотов, Е.Н. Федоров

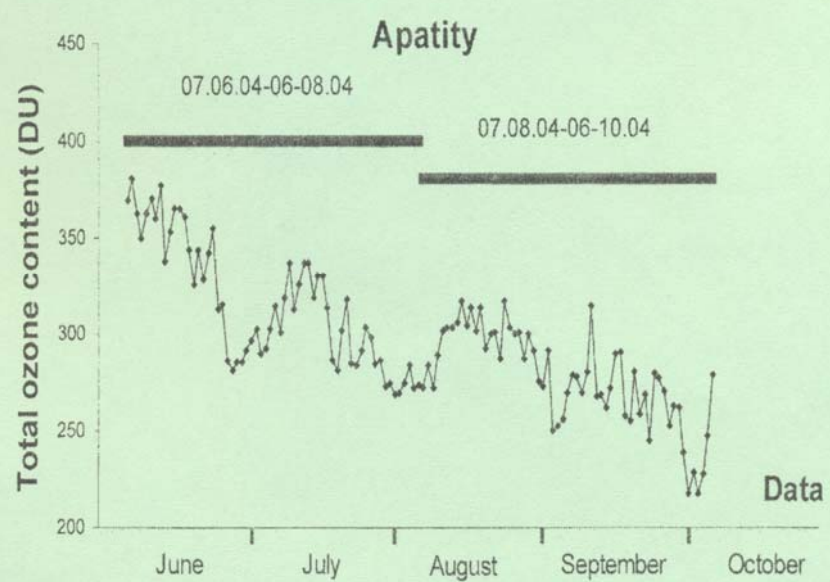
В докладе приводятся результаты анализа магнитных полей в диапазоне 0.1-4 Гц. Использованы данные семи индукционных магнитометров полярной сети STEP, расположенных на территории США и Канады. Показано, что гребенчатые спектры в диапазоне первых герц, обычно ассоциируемые с ионосферным альвеновским резонатором, могут вызываться двумя последовательными импульсами. Первый импульс приходит в точку наблюдения по волноводу Земля-нижняя ионосфера, второй, с противоположной полярностью – отразившись от верхней границы F-слоя. Время задержки совпадает с обратной частотой фундаментальной гармоники ИАР. Таким образом, наблюдаемые гребенчатые спектры в диапазоне первых герц не всегда являются спектрами ИАР.

Сейсмо-ионосферная депрессия в окрестности мощных землетрясений

А.Ю. Щекотов, Е.Н. Федоров, М. Хаякава

Сейсмо-ионосферная депрессия – это уменьшение флюктуаций УНЧ поля за несколько дней перед землетрясением. В докладе приводятся примеры этого явления в окрестности мощных землетрясений с магнитудой более 8, которые произошли в 2006-2011 годах в Японии и на Курилах. Использованы данные трёх японских феррозондовых магнитометров, установленных на станциях Мемамбетсу (Хоккайдо), Какиока (Хонсю) и Канойя (Кюсю). Их взаимные расстояния примерно 700 и 900 км. Депрессия максимальна в частотном диапазоне 0.02 – 0.05 Гц. Эффект устойчиво регистрируется на расстояниях до 1000 км от эпицентра.

Low Atmosphere, Ozone



Anisotropy variation of low energy neutron background in the atmosphere

Yu.V. Balabin, E.A. Maurehev (*Polar Geophysical Institute KSC of RAS, Apatity, Russia*)

A low energy (up to 1 eV) neutron detector with fan acceptance diagram was processed in Polar Geophysical Institute. The detector is set on a neutron background monitoring. Short- and long-term variations were found. A long-term variation is seasonal. There are short-term variations, which are connected to precipitations. It is suggested that an excess of hydrogen atoms into the environment (wet soil and drops into the atmosphere in summer, snow blanket in winter) is caused of it. Hydrogen atoms are more effective to reduce and scatter energetic neutrons and make neutron flux more isotropic.

Total ozone content over the Kola Peninsula: 1973-2011

V.I. Demin¹, G.P. Beloglazova¹, A.M. Zvyagintsev²

¹ *Polar Geophysical Institute, Apatity, Russia*

² *Central Aerological Observatory, Moscow, Russia*

During 2011 year the total ozone content over the Kola Peninsula was less than normal values. Abnormal low ozone contents were measured in the region during March 27 – April 2, 2011 when negative anomalies were reaching 35-42% from typical seasonal values. This episode was caused by extended the arctic air masses with very low ozone concentration from the North Pole to southern Scandinavia.

Although the total amount of Arctic ozone measured was much more than typically seen in an Antarctic spring, the amount destroyed was comparable to that in some previous Antarctic ozone holes for the first time. Previously the phenomenon of a similar duration, ozone depletion and spread area, in the Arctic was not observed. It is suggested that unprecedented depletion of ozone layer above the Arctic last winter and spring caused by an unusually prolonged period of extremely low temperatures in the stratosphere. The appearance of similar Arctic ozone hole in the future is open to question.

During the two last decades the total ozone content over the Kola Peninsula was less than mean values over the period of 1973-1990 years and less than mean for the period of 1950-1972 years which were calculated using ozone measurements in Tromsø. No significant negative ozone trend is seen for the latter period.

Atmospheric circulations epoch and long-range total ozone variations

V.I. Demin¹, A.M. Zvyagintsev²

¹ *Polar Geophysical Institute, Apatity, Russia*

² *Central Aerological Observatory, Moscow, Russia*

Using ozone measurement series from Arosa to illustrate (the series from Arosa is the longest in the world (since 1926) we show that long-range total ozone variations can be clearly explained on the basis of hypothesis about circulation epochs. During each circulation epoch the definite circulation patterns in the atmosphere is observed more frequently in comparison with its climatic normal values.

According G.Vangengeim classification there are three so-called circulation forms – one zonal (W) and two meridional circulation forms (E and C). Ozone contents were calculated for main circulation forms. Statistically significant difference between total ozone contents in various circulation forms allows long-ranges ozone changes to be forecasted as the circulation epoch can last for decade or more years.

A model study of how solar activity affects the global circulation of the middle atmosphere for January conditions

I.V. Mingalev, G.I. Mingaleva, V.S. Mingalev (*Polar Geophysical Institute, Apatity, Russia*)

To investigate how solar activity affects the formation of the global circulation of the middle atmosphere, a mathematical model of the global neutral wind system of the Earth's atmosphere, developed earlier in the Polar Geophysical Institute, is applied. The applied model produces three-dimensional global distributions of the zonal, meridional, and vertical components of the neutral wind and neutral gas density. The peculiarity of the utilized

Low atmosphere, ozone

model consists in that the internal energy equation for the neutral gas is not solved in the model calculations. Instead, the global temperature field is assumed to be a given distribution, i.e. the input parameter of the model, and obtained from the NRLMSISE-00 empirical model. Moreover, in the model calculations, not only the horizontal components but also the vertical component of the neutral wind velocity is obtained by means of a numerical solution of a generalized Navier-Stokes equation for compressible gas, so the hydrostatic equation is not applied. Simulations are performed for the winter period in the northern hemisphere (16 January) and for two distinct values of solar activity ($F_{10.7}=101$ and 230). The simulation results indicate that solar activity ought to influence considerably on the formation of global neutral wind system in the middle atmosphere and lower thermosphere. The influence is conditioned by the vertical transport of air from the lower thermosphere to the mesosphere and stratosphere. This transport may be rather different under distinct solar activity conditions.

This work was partly supported by the RFBR grant 10-01-00451.

The increase of NO_x content in the polar middle atmosphere during intensive solar proton events

L.I. Miroshnichenko¹, A.S. Kirillov², R. Werner³, V. Guineva³

¹ IZMIRAN, Troitsk, Moscow Region, Russia

² Polar Geophysical Institute, RAS, Apatity, Murmansk region, Russia

³ Space and Solar-Terrestrial Research Institute, BAS, Stara Zagora, Bulgaria

In this study we investigate periods of enhanced production of NO_x in the middle atmosphere during intensive solar proton events (SPE), especially due to invasion of intensive fluxes of high-energy solar cosmic rays (SCR). One-dimensional non-stationary model of a chemical composition of the middle atmosphere is applied. Our study is based on the model of upper limit spectrum (ULS) for SCR. Energy distribution of solar cosmic rays is suggested to be a power-law function with a changing spectral index up to maximum expected energies of 10 GeV. Model calculations of enhanced NO_x concentrations in the middle atmosphere are made for different periods of time in the course of the events for three energy intervals: 10 MeV – 100 MeV, 100 MeV - 1 GeV, 1 GeV - 10 GeV. Possible influence of the enhanced NO₂ and NO₃ concentrations on the atmospheric transparencies in visible region of the solar spectrum is discussed.

Stratospheric NO₂ long time trends obtained at the Stara Zagora station and some NDACC stations

R. Werner¹, D. Valev¹, At. Atanasov¹, V. Guineva¹, I. Kostadinov², G. Giovanelli², A. Petritoli², F. Ravegnani², S. Masieri², A. Kirillov³

¹ Space Research&Technologies Institute (SR&TI), BAS, Stara Zagora Department, Stara Zagora, Bulgaria

² Institute of Atmospheric Science and Climate (ISAC), Bologna, CNR, Italy

³ Polar Geophysical Institute, RAS, Apatity, Russia

Increase or decrease of stratospheric NO₂ density can change the ozone concentration, which act on the radiative balance in the stratosphere and troposphere. Therefore the NO₂ trend analysis is very important for the global climate change study. Daily time series of the NO₂ slant column amounts obtained by the GASCOD-BG instrument at Stara Zagora and of European NDACC stations near 40°N and two subtropical stations are analysed. Extreme values, which can be a result of tropospheric pollutions or of strong lightning processes, are removed. Monthly averages are determined by means of the remaining values. The series are homogenized based on linear regression between neighbour stations using Ordinary Least Squares, by interpolation and by filling of data gapes using seasonal means. To determine the linear trend a multiple linear regression model, including different impact factors is used. The influence of the solar activity and the aerosol loading are tested. The QBO effect on the NO₂ variation is checked. The significances of the impacts are tested, taking into account the auto-correlation of the NO₂ residuals.

Differences between Antarctic and Arctic spring ozone losses

A.M. Zvyagintsev (*Central Aerological Observatory, Dolgoprudny, Russia*)

This work surveys the depth and character of ozone losses in the Antarctic and Arctic using available long balloon-borne and ground-based records that cover multiple decades from ground-based sites. Such data reveal changes in the range of ozone values including the extremes observed as polar air passes over the stations. Antarctic ozone observations reveal widespread and massive local losses in the heart of the ozone “hole” region near 18 km, frequently exceeding 99 % in ozone mixing ratio. Although some ozone losses are apparent in the Arctic during particular years (the strongest losses were observed in 1997 and 2011), the depth of the ozone losses in the Arctic are considerably smaller, and their occurrence is far less frequent. Many Antarctic total integrated column ozone observations in spring since approximately the 1980s show values considerably below those ever observed in earlier decades. For the Arctic, there is evidence of some spring season depletion of total ozone at particular stations, but the changes are much less pronounced compared with the range of past data. Minimal column ozone values in Antarctic holes are below 100 D.u. and minimal spring Arctic column ozone values exceed 230 D.u. Thus, we confirm S. Solomon et al. affirmation (2007) that the observations demonstrate that the widespread and deep ozone depletion that characterizes the Antarctic ozone hole is a unique feature on the planet. In order to Arctic spring ozone losses would become comparable with Antarctic ones meteorological conditions (in the first place, temperature and stability of polar vortex) have to become similar, too.

Вариации спектров гамма-излучения во время осадков

Ю.В. Балабин, А.В. Германенко, Б.Б. Гвоздевский, Э.В. Ващенюк (*Полярный геофизический институт, Апатиты, Россия*)

В настоящей работе продолжается исследование возрастаний естественного рентгеновского фона во время осадков, регистрируемых на станциях космических лучей в Апатитах и Баренцбурге. На основе данных многолетних наблюдений и обработки сотен событий возрастаний выявлены некоторые закономерности. Во-первых, наблюдается линейная связь между показателем спектра рентгеновского излучения и амплитудой возрастания. Во-вторых, имеется временной сдвиг (20-30 минут) между средним профилем возрастания рентгеновского излучения и скоростью выпадения осадков. Предложена модель, основанная на ускорении зараженных частиц в электрических полях в облаках, которая удовлетворительно описывает наблюдаемый эффект.

Непрерывная регистрация спектров гамма-излучения в широком диапазоне энергий во время атмосферных осадков

Ю.В. Балабин, А.В. Германенко, Б.Б. Гвоздевский, Э.В. Ващенюк (*Полярный геофизический институт, Апатиты, Россия*)

На станции космических лучей ПГИ в Апатитах создан прибор для непрерывной регистрации спектров гамма-излучения. Использован спектрометр БДЭГ2-39, имеющий размеры сцинтилляционного кристалла (150x100мм). Регистрация спектров гамма-излучения производится с высоким разрешением при помощи 4096-канального амплитудного анализатора в диапазоне энергий от 100 кэВ до 4 МэВ.

В результате обработки энергетических спектров, полученных во время возрастаний (и выпадения осадков), и сравнения их со спектрами, полученными в ясную погоду, найдено, что собственно возрастание вызывается дополнительным потоком излучения с экспоненциальным энергетическим спектром. Значение характеристической энергии составляет около 300 кэВ. Каких-либо линий, связанных с радионуклидами, не обнаружено. Наблюдается четкий верхний энергетический предел излучения, сопровождающего осадки, который составляет 1.6 МэВ.

Вариации естественного рентгеновского излучения в приземной атмосфере на различных широтах

Ю.В. Балабин¹, Н.М. Салихов², О.Н Крякунова², Г.Д. Пак², А.Л. Щепетов³, А.В. Германенко¹, Э.В. Вашенюк¹

¹Полярный геофизический институт КНЦ РАН, Апатиты, Россия.

²ДТОО "Институт ионосферы" АО "Национальный центр космических исследований и технологий", Алматы, Казахстан.

³ФИАН, Москва, Россия.

Исследованы вариации естественного рентгеновского фона в приземном слое атмосферы в энергетическом диапазоне от 20 кэВ до сотен кэВ с разбиением на 2 поддиапазона. Измерения рентгеновского фона выполнены на трех станциях: г. Апатиты (Мурманская обл.), п. Баренцбург (арх. Шпицберген) и г. Алматы (Казахстан) с помощью сцинтилляционных детекторов. Обнаружена устойчивая связь возрастаний рентгеновского фона с выпадением осадков. Профили возрастаний на всех станциях имеют одинаковую форму.

Определены вариации показателя энергетического спектра рентгеновского излучения во время возрастаний. Найдено, что во время возрастаний происходит ужесточение спектра (показатель уменьшается), кроме того, наблюдается линейная связь между амплитудой возрастания и относительной вариацией показателя: большей амплитуде возрастания соответствует более жесткий спектр.

Исследование амплитудного распределения потока атмосфериков в УНЧ-ОНЧ диапазонах при двухкомпонентной регистрации.

В.И. Кириллов, А.А. Галахов, М.И. Белоглазов, В.В. Пчелкин, О.И. Ахметов (Полярный Геофизический Институт, Апатиты, Россия.)

В работе анализируются результаты измерений двух горизонтальных компонент магнитной составляющей импульсного естественного шумового электромагнитного поля на частотах 0.6 кГц и 6 кГц, проведенных в течение ноября 2011 года. Регистрация сфериков выполнялась с помощью комплекса аппаратуры, который был разработан в Полярном геофизическом институте КНЦ РАН и установлен на архипелаге Шпицберген. Оптимизационными методами были найдены параметры функции распределения амплитуд потока атмосфериков. Исследована суточная вариация числа регистрируемых атмосфериков в единицу времени. Проведено сравнение статистических характеристик потока атмосфериков регистрируемых на архипелаге Шпицберген с аналогичными характеристиками, полученными в обсерватории «Ловозеро».

Влияние геометрии течения воздушных масс в области внутритропической зоны конвергенции на процесс формирования циклонических вихрей

И.В.Мингалев¹, Н.М.Астафьева², К.Г.Орлов¹, В.С.Мингалев¹, О.В.Мингалев¹, В.М. Чечеткин³

¹Полярный геофизический институт Кольского научного центра РАН, Россия

²Институт космических исследований РАН, Россия

³Институт прикладной математики им. М.В.Келдыша РАН, Россия

В данной работе при помощи численного моделирования исследуется влияние геометрической конфигурации течения воздушных масс в области внутритропической зоны конвергенции на процесс формирования циклонических вихрей в этой области при появлении различных возмущений течения. Проводится сравнение полученных результатов моделирования с данными микроволнового спутникового мониторинга глобальных радиотепловых полей Земли из электронной коллекции GLOBAL-Field. Как показывают данные наблюдений, в периоды активного образования тропических циклонов направление центрального течения во внутритропической зоне конвергенции может отклоняться от направления с запада на восток на 10-20 градусов, причем в этом течении могут появляться один или несколько искривленных участков, что может приводить к образованию одного, двух, трех и более циклонических вихрей. Работа выполнена при финансовой поддержке гранта РФФИ № 10-01-00451.

Отражение суточного перемещения долготного максимума глобальной грозовой активности в угловых распределениях шумовых электромагнитных сигналов диапазона частот первого шумановского резонанса

В.В. Пчелкин (*Полярный геофизический институт КНЦ РАН*)

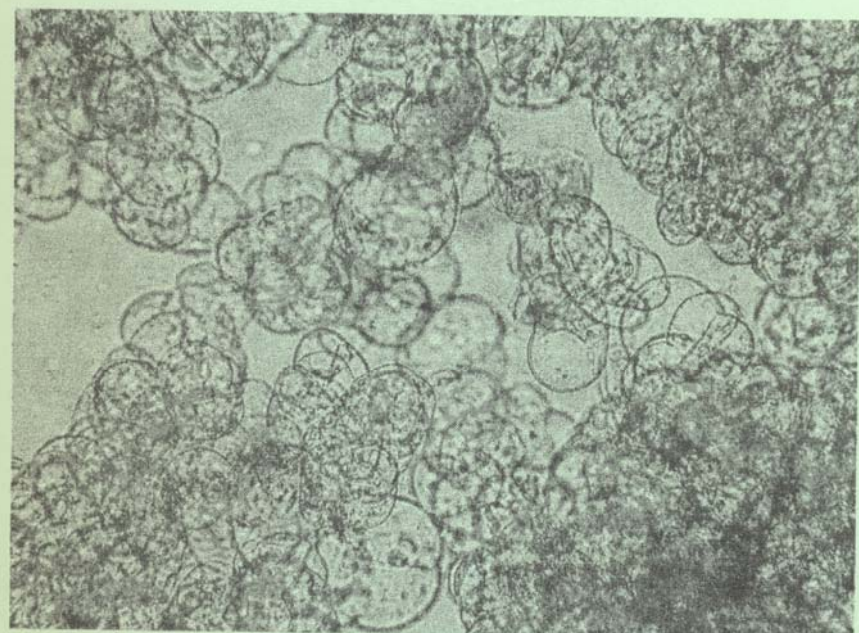
Анализируются вопросы связи угловых распределений электромагнитных шумовых сигналов диапазона частот 6-11 Гц с пространственным распределением гроз по поверхности земли. Показан отклик суточных вариаций доминирующих направлений прихода шумовых сигналов на смещение долготного максимума в пространственном распределении грозовой активности, связанное с вращением Земли. Установлено ослабление выраженности этого отклика в зимний сезон, объясняемое уменьшением площадей очагов мировых центров гроз зимой.

Связь сезонных изменений глобальной грозовой активности с сезонными вариациями амплитудных характеристик шумового электромагнитного поля диапазона частот 6-11 Гц.

В.В. Пчёлкин (*Полярный геофизический институт КНЦ РАН*)

В работе проведено сопоставление результатов измерений шумового электромагнитного поля на частотах района первого шумановского резонанса, проведенных в течение 2006-2009 годов в обсерватории «Ловозеро», с данными спутниковых наблюдений за числом молниевых разрядов и наземными наблюдениями за числом гроз. Показано увеличение среднего уровня шумов при увеличении числа молниевых ударов, определяемом по наблюдениям на спутнике, летом по отношению к зиме (сезоны северного полушария). Показан аналогичный сезонный положительный тренд зависимости амплитуды шумов от суммарной площади, охваченной грозами.

Heliosphere



On correlation between superweak radiation readings and cosmophysical factors

E.S. Gorshkov, V.V. Ivanov (*St. Petersburg Branch of the Institute of Terrestrial Magnetism, Ionosphere and Radio Wave Propagation of The RAS*)

The available findings on cosmobiological correlations with vital processes in living organisms raise an issue of whether cosmophysical factors (CPF) can influence the inner elements of devices registering various physical fields and, consequently, their readings. In order to obtain direct evidence of the influence, we used a supersensitive sensor for superweak radiation (SSR) in the longitudinal study during the 46th Russian Antarctic Expedition at the Antarctic station Vostok Apr 20 – Dec 21, 2001. The output variable, which is a function of internal resistance of SSR forming elements, was registered. The reason to choose the sensor was its successful application for the intervals including instants of the Moon and Sun meridian and horizon transits. These astronomic phenomena, in certain cases, provoked substantial changes in its conductivity.

In our study, the meridian-oriented sensor was placed inside a customized metal screen covered with a heating cable and foam enclosure for temperature stabilization. The thermometer was positioned so that its head was 2-3 cm away from the sensor. The SSR output signal was being recorded to PC (using DIGISCOP software) via multi-meter with a sampling period of 5 minutes. Temperature and sensor's readings correlated at -0.7.

To completely eliminate the influence of temperature on the analyzed data, we used new information-bearing characteristics of SSR, which were conventionally named density (absolute deviation of current multi-meter readings from the model curve - dDB) and reliability (number of intersections with the curve during the day - f). Here the model curve was defined on the basis of the most appropriate description of the linear relationship between two parameters within each current 5-day interval: $Dbmod = A - B\cdot T$, where T is current temperature, Dbmod – prototype curve values, A and B – coefficients. Estimate values of dDB and f averaged over 9 spots were used for studying the correlations of their fluctuations with CPF variations.

The obtained results bring the following facts to our attention:

The oscillatory nature of dDB and f fluctuations manifested itself clearly with the period of appr. 18-21 days). For both indices, the amplitude of oscillation is $\pm 30\text{-}40\%$ from the average values. The relative changes of dDB and f are opposing ($r = -0.69$). Changes of f retarded in phase for 2 days from changes of dDB ($r = -0.71$ at the inversed juxtaposition of curves). In addition, readings of the sensor practically did not correlate with temperature (correlation coefficients between T and dDB and f are 0.08 and -0.08, respectively). The changes in daily average values apparently correspond with such seasonal factors as Polar day-night alternations. Particularly, during a polar night dDB decreases to the minimum, while f raises to the maximum.

Matching polynomial trends (fifth-order polynomials) for dDB and f with the equation of time (ET) and the equation of equinoxes (EE) revealed significant correlations of ET and EE variations with f (direct correlation at $r = 0.53$, $r = 0.83$) and dDB (inverse correlation at $r = -0.25$, $r = -0.64$). The polynomial trends for readings correlated at $r = -0.84$. At the same time, short-period fluctuations of dDB and f corresponded with sign reversal for the sector structure of the interplanetary magnetic field (IMF). The correlations between them are 0.52 and -0.46, respectively. Additionally, the changes of readings are indirectly (via affecting IMF) influenced by the Moon orbital position (phase) and its orbital velocity. There are no sufficient evidences of solar radio intensity (SRI, 10.7 cm) and basic solar disturbances (λ in the equation of lunar motion) influencing dDB and f.

Spectral analysis of the variations in the sensor's density and reliability values revealed periods which are similar to the periods of SRI variations (51.2, 25.6, 28.44 days), λ -15.06 days and IMF (25.6, 28.44 and 15.06 days).

Therefore, the similarity of the above-mentioned periods and the presence of correlations between dDB and f variations and variations in gravitational indices of the Sun, the Earth, the Moon and IMF confirm the correspondence of the internal processes in supersensitive sensor with the influence from cosmophysical factors. Here the relatively high correlation of SRI value variations and IMF variations can be attributed to the impact of a gravity-determined IMF-relevant factor onto the screened sensor. In case of the positive IMF sector structure this factor causes increasing of the sensor's density, which contributes into measuring error.

Characteristics of changes in length of subjective minute at different space-and-time conditions

V.V. Ivanov, E.S. Gorshkov (*St. Petersburg Branch of the Institute of Terrestrial Magnetism, Ionosphere and Radio Wave Propagation of The RAS*)

Length of subjective minute (LSM) is a psychophysical index and an important component of the general process of space and time perception in humans. To estimate LSM we used the well-known test, which was performed in the following way: test person turned on the stopwatch, evenly, calmly, without pauses counted to 121-180 and then documented the completion time.

Heliosphere

The study of LSM registered in one individual during February 2001 – January 2002 (7-8 times a day, at an average) at the polar station Vostok (Antarctica) demonstrated that the values vary in a wide range between 36 and 88 sec (daily average values- between 45 and 62 sec). The values distribution is normal. The variations of LSM during a day correspond to the day-night alternation: the highest values were registered from 3 to 7 a.m. (56-63 sec), while during the day they did not exceed 54-55 sec. Three local minimums (50-52 sec) were found - at 9 a.m., 1-3 p.m. and 7-9 p.m. The changes in daily average LSM values (averaged over 5 spots) well agree with such seasonal factors as alternation of polar day and night. Within the period including the polar night divide, LSM first grows from 47 to 55 sec and then decreases to 52-53 sec. As the Sun rises over the horizon and the polar day begins, LSM reaches its highest point of 59 sec. Matching the daily average values of LSM and heart rate, LSM and respiration rate showed inverted correlations between them at $r = -0.43$ and $r = -0.52$, respectively.

As we know, timing characteristics of all processes in human body are interdependent and synchronized. In this context, we would like to consider the relation between two biological rhythms – LSM and length of R-R intervals in electrocardiogram (RR, sec). We valued LSM and RR (by defining shares of their components in total sums during the whole year analyzed) and compared them. The analysis of daily average difference (%) between RR and LSM reveals a linear trend gradually transiting from the negative to the positive value area. It means that there are certain values of LSM and RR (heart rate) at which these biological rhythms are synchronized. The values are: HR = 63.3 ± 0.7 beat/min, RespR = 9.2 ± 0.4 respiratory cycles/min, LSM = 53.5 ± 0.5 sec. It should be mentioned that the obtained values of HR and RespR relate to the optimal cardiac functioning.

The further study of LSM was performed in 2002-2008 to estimate the influence of such astronomic phenomena as new moon (NM), full moon (FM), solar and lunar eclipses (SE, LE) onto LSM variations. Over 20 sets of registering LSM during 6 to 12 hours were done. In each case the variations of LSM were similar: within 2-2.5 hours it increased to the maximum, exceeding 1.5-1.8 times the background level (at the moment of the Sun, the Earth and the Moon's collinear positioning), and then decreased within appr. 2 hours. The average values of LSM peaks are: 86.3 sec at FM, 99.5 sec at LE, 85 sec for NM, 90.3 sec for SE and 65 sec for “background” intervals. The pattern of LSM peaks distribution during a day was defined. According to it, LSM extreme values are located within the interval of 4-6 hours, which clearly agrees with its daily distribution.

We also estimated the possible influence on LSM from a rare planetary phenomenon (previously observed in 1882), connected with the Venus transiting across the disk of the Sun on June 6, 2004 (from 9.13 a.m. till 3.16 p.m.), by analyzing the registered LSM variations from 6 a.m. till 6 p.m. We found that the LSM variations during the outer intervals (approaching the solar disk and moving away from it) and during NM (FM, SE, LE) are similar. LSM raises dramatically (from 67 to 79 sec) about 2 hours prior to the planet starting moving across the disk. After that it drops down to the background level, noticeably dips with the beginning of the eclipse and keeps decreasing more intensely down to the minimum (52 sec) as the planet reaches the point equidistant to the limb of the Sun. Then LSM increases to 74-76 sec (during the time interval of the eclipse ending), which is followed with a sharp decline to 55-57 sec in the next 3 hours.

Similar changes of LSM were registered during the Mercury transiting across the disk of the Sun on November 8-9, 2006 (the phenomenon previously observed in 1886).

We studied the dynamics of LSM for each case: in the Antarctic, at NM (FM, SE, LE), at the Mercury and Venus transiting across the disk of the Sun. LSM varies in an evidently similar manner. The only difference is duration of the eclipse phase: from several minutes for NM (FM, SE, LE) to about 6 hours for the Mercury and Venus transiting across the solar disk and over 4 months for the polar night. Such a pattern of LSM changes in various situations reflects the similarity of the processes, related either to the fact of three celestial bodies conjunction: Sun-Earth-Moon (Mercury, Venus) or to the solar “eclipse” akin to the polar night.

The findings confirm the direct relation of the phenomena in question to the dynamics of biospheric processes.

Solar activity and life expectancy of patients in the mental boarding

R.E. Mihaylov¹, H.K Belisheva¹, R.G. Novoseltsev², S.D. Cherney², A.N. Vinogradov¹

¹ Kola Science Centre of the Russian Academy of Sciences

² State regional stationary establishment of social service of system of social protection of the population, the Apatity Psychoneurological Internat

In this study we examine the dependence of the life expectancy of patients psychoneurological internat of the level of solar activity (SA) in the year they were born. The material of study were health-statistics on the dates of birth and death in patients of internat in 1984 - 2009 year (total 967 cases). Years of birth of people investigated include the period from 1895 to 1984 years. As an indicator of the CA used the Wolf numbers. Statistical comparison of samples of patients born during the high and low SA was conducted by using the methods of Mann-Whitney and

Wald-Wolfowitz at a significance level of $p < 0.05$. We have shown that the average lifespan of people born in years of low SA at 8.4 years later. Also shown is the high sensitivity of males to these influences.

Cytogenotoxic effects of the ionizing radiation in the miners buccal cells

D.A. Petrushova, N.K. Belisheva (*Kola science centre of the Russian academy of science, Apatity, e-mail: petrushova@admksc.apatity.ru*)

Deep-mined output containing naturally occurring radionuclides such as uranium, thorium and radium is dangerous to the health of miners due to irradiation of different kinds of mixed ionizing radiation: inhalation / ingestion of dust particles containing radium, radon inhalation, and its decay products, external irradiation of the body, inhalation of dust particles mixed radioisotopes. The objective of this study was to evaluate the cyto- and genotoxic effects of natural ionizing radiation on buccal cells of the underground miners working in the ionizing radiation terms.

Material studies were samples of buccal cells of the miners working in the loparite ore output (Lovozero district, Murmansk reg.) and the control group of the healthy men living in the Apatity. The test groups consisted of 10 and 8 male smokers, respectively, at the age of 25 to 40 years.

It was established the binucleated cells frequency in the miners group to be 26.2 times more than in the control group. The micronuclei cell frequencies were not significantly different in the both groups ($p = 0.37$). The cell death by necrosis type occurs 1.9 times more often in the miners group than in the control group (66.9% vs. 35.2%, $p=0.0001$), with the cell death by apoptosis type occurring in the 1.8 times more in control group than in the miners group (5.9% vs. 3.3%, $p=0.0771$).

Thus, the cytogenetic effects of the natural mixed ionizing radiation in the miners buccal cells are manifested in the reducing of the normal cell frequency, in the increasing of the necrotic cells and in the increasing of the binucleated cells in 26 times in compare with the control group.

The binuclear cell frequency increasing in the miners group in compare with the control group may indicate the influence of the ionizing radiation on the cytogenesis. The cell culture studies showed the multinucleated cells frequency to increase synchronously with the increasing of the neutron component intensity by Earth surface (Belisheva et al., 2012). It is possible that the neutron component contributes to irradiation of the natural ionizing radiation through interacting of the alphas with atmosphere molecules. This contribution may appear in the increasing of the multinucleated cells frequency in the miners buccal cells.

The increasing of the binucleated cells frequency and the decrease of the apoptosis frequency in the miners buccal cells in comparison with control groups denotes low efficiency of the apoptosis mechanism. It is adverse prognostic appearance, to prove genotoxic high rate of the irradiation of mixed ionizing radiation in the deep-mined output conditions.

This study was supported by RFBR grant and administration of the Murmansk region, project number 10-04-98809-r_sever_a.

Физиологическая основа чувствительности организма к гелиогеофизическим агентам

Н.К. Белишева, Д.А. Петрушова, А.А. Мартынова, В.В. Пожарская, С.В. Пряничников

Научный отдел медико-биологических проблем адаптации человека в Арктике, КНЦ РАН, г.Апатиты

Цель работы состояла в выявление внутрисистемных связей в организме и возможных мишеней воздействия вариаций гелиогеофизических агентов. Исследования проводили на однородной по возрасту и полу группе испытуемых мужского пола (11 человек), у которых ежедневно на протяжении 20 дней оценивали физиологическое состояние организма (апрель, 2008 г.). Индикаторами физиологического состояния служили показатели функциональной активности периферической крови, сердечно-сосудистой системы, психофизиологические характеристики, отражающие регуляторные воздействия со стороны центральной и вегетативной нервной системы. О функциональной активности крови судили на основании клинического анализа и формулы белой крови; состояние сердечно-сосудистой системы детектировали с применением прибора АКР – артериокардиоритмографа, позволяющего регистрировать электрокардиограмму (ЭКГ) и пульсовую волну артериального давления (АД). Спектральная плотность мощности вариабельности сердечного ритма (ВСР), систолического и диастолического давления в различных спектральных диапазонах характеризует активность вегетативной нервной системы и другие показатели. Главные спектральные составляющие ВСР и вариабельности диастолического (ДАД) и систолического (САД) давления включают очень низкочастотный VLF (very low frequency < 0.04 Гц), низкочастотный LF (low frequency 0.04 – 0.15 Гц) и высокочастотный HF (high frequency 0.15 – 0.4 Гц) диапазоны колебаний.

Heliosphere

Психофизиологическое состояние оценивали по модифицированному тесту САН и длительности индивидуальной минуты (ДИМ). Анализ усредненных показателей, по ансамблю испытуемых, за каждый день исследования показал, что скорость оседания эритроцитов (СОЭ) является интегральным показателем состояния периферической крови, сердечнососудистой системы и психофизиологического состояния организма. Оказалось, что СОЭ имеет значимые ($p<0,05$) положительные корреляции с содержанием эритроцитов ($r=0,45$), тромбоцитов ($r=0,46$), сердечным ритмом (СР) ($r=0,47$), полным спектром мощности систолического (TPS), $r=0,53$ и диастолического (TPD), $r=0,54$, артериального давления. Отрицательные связи ($p<0,05$) были найдены между СОЭ и вариабельностью интервалов сердечного ритма (RR), $r=-0,44$, пульсом (Ps), $r=-0,49$ и настроением, $r=-0,44$. В свою очередь, настроение было позитивно связано с НF ($r=0,47$), как и самочувствие ($r=0,44$), и, негативно, с LF ($r=-0,50$) и TPD ($r=-0,48$). ДИМ была позитивно связана с САД ($r=0,45$), а ДАД - с САД ($r=0,80$) и моноцитами крови ($r=0,46$), при возрастании которых уменьшалось содержание палочкоядерных нейтрофилов ($r=-0,45$). Соотношение лимфоцитов и сегментоядерных нейтрофилов ($r=-0,87$) в крови является ведущим регулятором ее функционального состояния, от которого, наряду с моноцитами, зависит иммунорезистентность организма. Однако значимых связей между этими клетками крови и другими системами организма человека выявлено не было. Оценка связи между показателями физиологического состояния организма и вариациями гелиогеофизических агентов показала, что содержание сегментоядерных нейтрофилов возрастает при возрастании геомагнитной активности (ГМА), оцененной по Кр-индексу ($r=0,44$), а содержание лимфоцитов снижается при возрастании нуклонной компоненты вторичных космических лучей (КЛ) у поверхности Земли ($r=-0,44$), $p<0,05$. СОЭ возрастает при возрастании У-компоненты геомагнитного поля (ГМП) и плотности потоков КЛ в околоземном пространстве: коэффициенты корреляции с протонами с энергией >100 Мэв и скорректированной на давление скоростью счета нейтронного монитора $r=0,52$ и $r=0,50$, соответственно, при $p<0,05$. Значимые связи ($p<0,05$) потоков КЛ в околоземном пространстве, нуклонной компоненты КЛ у поверхности Земли с показателями физиологического состояния организма показывают, что за исследуемый период времени КЛ имели ведущее значение для состояние организма. Так, при возрастании интенсивности КЛ возрастало содержание в периферической крови лейкоцитов ($r=0,44$), палочкоядерных нейтрофилов ($r=0,61$), увеличивалась СОЭ ($r=0,52$), снижалось содержание тромбоцитов ($r=-0,45$) и лимфоцитов ($r=-0,44$). При этом возрастала скорость сердечного ритма ($r=0,66$), снижалась его вариабельность ($r=-0,64$), возрастала низкочастотная ($r=0,50$) и снижалась высокочастотная ($r=-0,53$) компоненты в спектре мощности сердечного ритма. Смысловое содержание таких связей показывает, что возрастание интенсивности КЛ приводит к напряжению адаптивных реакций организма, проявляющихся в снижении иммунорезистентности, напряжении центральной и вегетативной регуляции функций организма, включая сердечно-сосудистую систему, в ухудшении самочувствия, в снижении активности и настроения, что следует из анализа внутрисистемных связей. Механизм влияния вторичных компонент КЛ на организм человека связан с физико-химическими процессами радиационной природы, обусловленными воздействием низкоинтенсивного и плотноионизирующего излучения на клеточное и межклеточное вещество.

Вклад гелиогеофизических агентов в структуру заболеваемости населения Мурманской области

Н.К. Белишева¹, Л.В. Талыкова², Н.А. Мельник³

¹ Научный отдел медико-биологических проблем адаптации человека в Арктике, КНЦ РАН, г.Апатиты

² ФГУН Северо-западного научного центра гигиены и общественного здоровья Роспотребнадзора

³ Учреждение Российской академии наук Институт химии и технологии редких элементов и минерального сырья им. И.В. Тананаева КНЦ РАН

В работе выявлен вклад высокоширотных гелиогеофизических агентов в картину заболеваемости населения в Мурманской области. Было показано, что число значимых корреляций ($p<0,05$) между заболеваемостью у детей и гелиогеофизическими показателями в период с 1995 по 1999 г.г. больше, чем у взрослого населения, что свидетельствует о большей чувствительности детского организма к вариациям гелиогеофизических агентов. Выявлено, что общая заболеваемость, число случаев новообразований, болезни мочеполовой и костно-мышечной систем, как у детей, так и у взрослых имеют тенденцию возрастать при возрастании солнечной активности (СА), сопряженной с возрастанием интенсивности нуклонной компоненты солнечных космических лучей (КЛ) у поверхности Земли (GLE). Не исключено, что влияние на заболеваемость может вносить Be-7, генерация которого увеличивается в период солнечных протонных событий. Вместе с тем, такие нозологические формы как болезни нервной системы, болезни кожи и подкожной клетчатки (дерматиты, экземы и др.) имеют противоположные знаки корреляции у детей и взрослых, что, вероятно, отражает различную чувствительность детского и взрослого организма к

«дозовому» соотношению воздействий вариаций геомагнитного поля (ГМП) и КЛ. Было показано, что перинатальная смертность и мертворожденность альтернативно связаны с ГМА и вариациями интенсивности КЛ. После рождения характер связи заболеваемости у детей с гелиогеофизическими агентами меняется на противоположный: возрастание интенсивности КЛ сопряжено с увеличением заболеваемости детей до первого года жизни. Эта тенденция сохраняется и в дальнейшей жизни. Сопоставление случаев врожденных пороков развития (ВПР) у детей в Кандалакшском, Мончегорском и Ловозерском районах на 1000 рождений показало, что среднегодовое число случаев ВПР за 10 лет (с 1989 по 1998) в Ловозерском районе (92.0 ± 16.4) в 5.2 и в 3.6 раза превышает частоту случаев ВПР в Кандалакшском (17.6 ± 4.4) и Мончегорском (25.9 ± 3.2) районах, соответственно. Оказалось, что в Кандалакше и Мончегорске частота ВПР имеет прямую корреляцию с СА и GLE, а в Ловозерском р-не, напротив, частота ВПР снижается при возрастании СА. При этом, наиболее сильные связи ($p \leq 0.05$) частоты ВПР с гелиогеофизическими агентами характерны для Кандалакши и Ловозерского района. Оценка связи заболеваемости новорожденных в Кандалакше и Мончегорске с вариациями гелиогеофизических агентов показывает, что в Мончегорске заболеваемость новорожденных возрастает при возрастании интенсивности КЛ ($r=0.73$, $p \leq 0.05$), как и в целом по Мурманскому региону. Для Кандалакши значимые связи между заболеваемостью новорожденных и вариациями гелиогеофизических агентов не обнаружены. Проведенные исследования показали, что гелиогеофизические агенты существенно влияют на картину заболеваемости населения в Мурманской области. Заболеваемость детей и взрослых в Мурманском регионе в целом возрастает при возрастании интенсивности природных источников ионизирующего излучения. Это происходит в период минимума СА и во время солнечных протонных событий, сопровождающихся GLE, и, возможно, дополнительной генерацией в верхней атмосфере Be-7. Однако перинатальная смертность снижается при возрастании интенсивности КЛ и возрастает с увеличением ГМА.

Зависимость адаптации детей Заполярья к средним широтам от геомагнитных возмущений

А.А. Мартынова, С.В. Пряничников, Т.Б. Новикова, Н.К. Белишева

Научный отдел Медико-биологических проблем адаптации человека в Арктике, КНЦ РАН, г. Анадырь

Исследование было выполнено на базе оздоровительного комплекса «Эковит» КНЦ РАН с. Александровка-Донская Павловского района Воронежской области. Цель исследования состояла в оценке особенностей адаптации детей Заполярья (в возрасте от 10 до 18 лет) к условиям средних широт. Адаптационные возможности организма оценивали с помощью прибора «Омега-М», основанного на анализе биологических ритмов организма человека, выделяемых из электрокардиосигнала в широком диапазоне частот. Метод основан на новой информационной технологии анализа биоритмологических процессов «фрактальной нейродинамики». Системный анализ включал четыре режима: вариационный анализ ритмов сердца – оценка показателей вегетативной регуляции методами статистического, временного и спектрального анализа ритмов сердца; нейродинамический анализ – оценка показателей центральной регуляции и состояния эндокринной системы методами нейродинамического анализа биологических ритмов организма; картирование биоритмов мозга – оценка психофизиологического состояния пациента методами фазового анализа и картирования биоритмов мозга; фрактальный анализ – оценка степени гармонизации биоритмов организма и определение информационного показателя иммунного статуса методами фрактального анализа. Оценка среднего по выборке уровня адаптации детей показала, что адаптационный резерв колеблется от 49.6% до 74.6%, при норме выше 50%, и, у отдельных детей, он ниже нормы. Те же закономерности прослеживаются в вегетативной и центральной регуляции сердечного ритма, психоэмоциональном состоянии, а также в интегральном показателе психофизиологического состояния. Высокий уровень напряжения регуляторных систем организма у детей выразился в превышении средних значений по группе индекса вегетативного равновесия (171.35 ± 26.05), при норме 35-145 у.ед., и показателе адекватности процессов регуляции (51.15 ± 4.74), при норме 15-50 у.ед.. При этом, у отдельных испытуемых индекс вегетативного равновесия достигал значений 391.4, что свидетельствует о предболезненном состоянии организма. Анализ результатов показал, что по индексу напряжения (ИН) регуляторных систем организма, полноценной адаптации к смене широтного пояса у детей не происходит. Оценка связи средних значений по выборке показателей вегетативной регуляции с геомагнитной активностью (ГМА) показала, что в магнитовозмущенные дни, оцененные на основе вариации X-компоненты геомагнитного поля (ГМП), этот показатель возрастает ($r = -0.70$, $p \leq 0.05$). Таким образом, геомагнитные возмущения повышают уровень адаптации детей Заполярья в средних широтах. Полученные результаты показывают, что организм детей проживающих в высоких широтах, нуждается в определенной «дозе» раздражителя, которым в условиях Заполярья являются вариации ГМП.

AUTHOR INDEX

A

Akhmetov O.I.	62
Alexeyev V.N.	16
Angelopoulos V.	19
Antonova E.E.	13, 27
Artemyev A.V.	27
Astafieva N.M.	62
Atanasov At.	60

B

Balabin Yu.V.	41, 42, 59, 61, 62
Barannik M.	20
Barkhatov N.A.	25, 41
Barkhatova O.M.	47
Belakhovsky V.B.	33
Belisheva N.K.	68, 69, 70, 71
Beloglazov M.I.	62
Beloglazova G.P.	61
Beloushko K.E.	55
Bessarab F.S.	50
Bondareva T.V.	37
Borovkov L.P.	13, 35, 50
Bortnikov R.O.	42
Bosinger T.	48

C

Chechetkin V.M.	62
Cherney S.D.	68
Cherniak Y.	53
Cherniakov S.M.	54
Chernouss S.A.	13, 19, 53
Chernyaev I.A.	14
Chernyshov A.A.	47
Chkhetiani O.G.	55
Chugunin D.V.	25, 29

D

Danilova O.A.	43
Demekhov A.	34, 36, 37
Demin V.I.	59
Despirak I.V.	14, 34
Dmitrieva N.P.	15, 19, 28
Dodonova I.A.	47
Dremukhina L.A.	22
Dubyagin S.V.	14

E

Ephishov I.	53
Ermakova E.N.	48, 56

F

Fedorenko Yu.V.	48, 51, 55
Fedorov E.N.	38, 56
Filatov M.	48, 51

G

Galakhov A.A.	62
---------------	----

Germanenko A.V.	41, 42, 61, 62
Giovanelli G.	60
Golovchanskaya I.V.	18, 27, 34
Gordeev E.	15
Gorshkov E.S.	67
Gromov S.V.	22
Gromova L.I.	22
Guineva V.	60
Gurnett D.	37
Gvozdevsky B.B.	41, 42, 61

H

Hanash Ya.	29
Hayakawa M.	56
Hayosh M.	36
Heilig B.	38

I

Ievenko I.B.	16, 25
Isavnin A.A.	37
Ivanov V.V.	67

K

Kangas J.	55
Karavaev Yu.A.	22
Karpov I.V.	50
Katkalov Yu.	16, 20, 21, 37
Kirillov A.S.	20, 21, 48, 49, 60
Kirillov V.I.	62
Kirpichev I.P.	13, 27
Kleimenova N.G.	34, 35
Klimenko M.V.	49, 50
Klimenko V.V.	49, 50
Koleva R.	14
Kondratiev S.K.	50, 52
Korenkov Yu.N.	50
Kornilov I.A.	16, 17, 26
Kornilova T.A.	16, 17, 26
Kosolapova N.V.	47
Kostadinov I.	60
Kotikov A.L.	52
Kovacs P.	38
Kovalevsky J.	17
Kozelov B.V.	18, 34, 35, 37, 47, 50
Kozelova T.V.	18
Kozlovsky A.E.	33
Kozyreva O.V.	35
Krishtopov A.A.	19
Kryakunova O.N.	62
Kubyshkina D.I.	35

L

Larchenko A.V.	48, 51
Lebed O.M.	51, 55
Levitin A.E.	22, 41
Ljubchich V.A.	26
Lubchich A.A.	14
Lyur H.L.	38

M

Macusova E.....	37
Makarova L.N.....	50
Malova H.V.....	27
Manninen J.....	35
Martynova A.A.....	69, 71
Masieri S.....	60
Maurchev E.A.....	42, 59
Melnik M.N.....	27, 34
Melnik N.A.....	70
Mihaylov R.E.....	68
Mingalev I.V.....	27, 59, 62
Mingalev O.V.....	27, 34, 62
Mingalev V.S.....	61, 62
Mingaleva G.I.....	59
Miroshnichenko L.I.....	60
Mishin V.V.....	22
Mishin V.M.....	22
Miyashita Y.....	14
Mochalov A.A.....	52
Mogilevsky M.M.....	25, 29, 47
Moiseenko I.L.....	25, 29
Morozov V.N.....	50

N

Namgaladze A.A.....	51, 53
Nikolaev A.V.....	19
Nikolaeva V.D.....	50, 52
Novikova T.B.....	71
Novoseltsev R.G.....	68

O

Ogloblina O.F.....	54
Orlov K.G.....	62
Ovchinnikov I.L.....	13

P

Pak G.D.....	62
Palmroth M.....	15
Parnikov S.G.....	16
Parrot M.....	36
Pashin A.B.....	52
Pasmanik D.....	36
Pchelkin V.V.....	44, 62, 63
Pershin A.V.....	48, 56
Petrashova D.A.....	69
Petritoli A.....	60
Pickett J.....	37
Pilgaev S.V.....	20, 35, 36, 48, 51
Pilipenko V.A.....	33, 38
Platov Yu.V.....	19
Podgorny A.I.....	43
Podgorny I.M.....	43
Polyakov S.V.....	56
Ponyavin D.I.....	44
Pozharskaya V.V.....	69
Prokhorov B.E.....	51
Pryanichnikov S.V.....	69, 71
Pulinets M.S.....	13, 27
Pulkkinen T.I.....	15

R

Rauch J.-L.....	37
Ravegnani F.....	60
Revunov S.E.....	25
Revunova E.A.....	41
Riazantseva M.O.....	13, 27
Roldugin A.V.....	20, 36
Roldugin V.C.....	20, 36, 53
Romanovskaya Yu.V.....	53
Romantsova T.V.....	25, 29

S

Sakharov Ya.....	16, 20
Salihov N.M.....	62
Santolík O.....	36, 37
Sasunov Yu.L.....	44
Schekotov A.Yu.....	56
Schepetov A.L.....	62
Selivanov V.....	20
Semenov V.S.....	28, 35, 42, 44
Sergeev V.A.....	14, 15, 19, 20, 35
Sergienko T.I.....	52
Shadrukov D.V.....	25
Shagimuratov I.....	53
Shalimov S.L.....	55
Shapovalova A.A.....	22
Shirochkov A.V.....	50
Shkarbalyuk M.....	51, 53
Shumilov O.I.....	43
Sidorenko A.E.....	54
Singer H.....	19
Slivka K.Yu.....	28
Smirnova N.A.....	37
Soraas F.....	29
Sormakov D.A.....	35
Stepanova M.V.....	13
Sutcliffe P.....	38

T

Talykova L.V.....	70
Tereshchenko E.D.....	54
Tereshchenko V.A.....	54
Tereshchenko V.D.....	54
Timofeev E.E.....	55
Timofeeva S.A.....	20
Titova E.E.....	35, 36, 37
Trotignon J.-G.....	37
Tsyganenko N.A.....	19
Tyasto M.I.....	43

U

Uljev V.A.....	43
Uspensky M.V.....	19

V

Valev D.....	60
Vallinkoski M.K.....	55
Vashenyuk E.V.....	41, 42, 61, 62
Vasilev A.N.....	37

Viljanen A.	16, 20
Vinnikova J.O.	44
Vinogradov A.N.	68
Volkov M.A.	28
Vorobjev V.G.	20, 49
Vovchenko V.V.	13

W

Werner R.	60
----------------	----

Y

Yagodkina O.I.	20, 21, 49
Yagova N.V.	38
Yahnin A.G.	21, 28, 29
Yahnina T.A.	21, 28, 29
Yurov V.E.	35, 50

Z

Zelenyi L.M.	27
Zhou Q.	48
Znatkova S.S.	13
Zolotov O.V.	51
Zolotova N.V.	44
Zubov R.A.	51, 55
Zvyagintsev A.M.	59, 61